

UNCLASSIFIED

AD 263 472

*Reproduced
by the*

ARMED SERVICES TECHNICAL INFORMATION AGENCY
ARLINGTON HALL STATION
ARLINGTON 12, VIRGINIA



UNCLASSIFIED

NOTICE: When government or other drawings, specifications or other data are used for any purpose other than in connection with a definitely related government procurement operation, the U. S. Government thereby incurs no responsibility, nor any obligation whatsoever; and the fact that the Government may have formulated, furnished, or in any way supplied the said drawings, specifications, or other data is not to be regarded by implication or otherwise as in any manner licensing the holder or any other person or corporation, or conveying any rights or permission to manufacture, use or sell any patented invention that may in any way be related thereto.

263472

WADD TECHNICAL REPORT 60-857

16 2 60

LAUNCHING AND ALIGHTMENT SYSTEMS

FOR

AERO-SPACE VEHICLES

NELSON T. LEVINGS, JR.

CLEVELAND PNEUMATIC INDUSTRIES, INC.

197 650

MAY 1961



61-4-5
NOX

Best Available Copy

WRIGHT AIR DEVELOPMENT DIVISION

NOTICES

When Government drawings, specifications, or other data are used for any purpose other than in connection with a definitely related Government procurement operation, the United States Government thereby incurs no responsibility nor any obligation whatsoever; and the fact that the Government may have furnished, formulated, or in any way supplied the said drawings, specifications, or other data, is not to be regarded by implication or otherwise as in any manner licensing the holder or any other person or corporation, or conveying any rights or permission to manufacture, use, or sell any patented invention that may in any way be related thereto.

**

Qualified requesters may obtain copies of this report from the Armed Services Technical Information Agency, (ASTIA), Arlington Hall Station, Arlington 12, Virginia.

**

This report has been released to the Office of Technical Services, U. S. Department of Commerce, Washington 25, D. C., for sale to the general public.

**

Copies of WADD Technical Reports and Technical Notes should not be returned to the Wright Air Development Division unless return is required by security considerations, contractual obligations, or notice on a specific document.

AF-WP-B-MAY 60 1M

12

WADD TECHNICAL REPORT 60-857

LAUNCHING AND ALIGHTMENT SYSTEMS

FOR

AERO-SPACE VEHICLES

Nelson T. Levings, Jr.

Cleveland Pneumatic Industries, Inc.

May 1961

Flight Dynamics Laboratory
Contract No. AF33(616)-6572
Project No. 1369
Task No. 13529

Wright Air Development Division
Air Research and Development Command
United States Air Force
Wright-Patterson Air Force Base, Ohio

FOREWORD

The work described in this report was accomplished by the Instrumentation and Control Division of Cleveland Pneumatic Industries, Inc., under Contract No. AF 33(616)-6572, Project No. 1369, entitled, "Launching and Alightment Systems for Aero-Space Vehicles, Task No. 13529.

This project was administered under the direction of the Flight Dynamics Laboratory, Directorate of Advanced Systems Technology, Wright Air Development Division, with Mr. Wallace Buzzard as Military Project Engineer, having superseded Lt. Don Austin in January 1960.

This report covers work conducted from June 1959 to January 1961.

Mr. Nelson T. Levings, Jr., was Contractor Project Engineer, assisted by specialized engineering personnel from each Division of Cleveland Pneumatic Industries, Inc.

ABSTRACT

The purpose of this study was to investigate and derive concepts for alightment, attachment, and departure of advanced, extremely high-altitude flight vehicles.

The following report describes the investigatory work, problems encountered, methods by which concepts were selected, and results of preliminary design integrity testing as applicable to specifically selected concept models.

Results indicate that valuable data have been derived on the relative efficiency of the various types of shock mitigation systems as originally conceived through the efforts of this project.

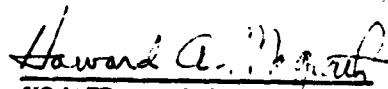
The basic framework for an evaluation technique by which the shock mitigation systems can be rated as to energy-absorbing capability and efficiency with regard to percentage of total mass of the system, has been provided.

Additionally, through precision application of the laws of similitude in developing models of the most promising concepts, evidence has been provided as to the value of utilizing dynamic scaling as an important adjunct to the analytical techniques for preliminary design.

PUBLICATION REVIEW

The publication of this report does not constitute approval by the Air Force of the findings or conclusions contained herein. It is published only for the exchange and stimulation of ideas.

FOR THE COMMANDER:


HOWARD A. MAGRATH
Technical Director
Flight Dynamics Laboratory

ACKNOWLEDGEMENTS

1. Brunswick Corporation
Muskegon, Michigan
2. Cleveland Pneumatic Industries, Inc.
All Divisions
3. Convair Astronautics Division
General Dynamics Corporation
San Diego, California
4. E. I. DuPont de Nemours & Company
Wilmington, Delaware
5. General Electric Company
Philadelphia, Pennsylvania
6. Goodyear Tire and Rubber Company
Akron, Ohio
7. Human Sciences Research, Incorporated
Arlington, Virginia
8. International Telephone and Telegraph Corporation
South Bend, Indiana
9. Jet Propulsion Laboratories
Pasadena, California
10. Lockheed Aircraft Corporation
Los Angeles, California
11. Lockheed Aircraft Corporation
Sunnyvale, California
12. National Aeronautics and Space Administration
Washington, D. C.
13. North American Aviation Corporation
Missile Division
Downey, California

15. North American Aviation Corporation
Los Angeles, California
16. Republic Aviation Corporation
Farmingdale L.I., New York
17. Wright Air Development Division
Wright-Patterson Air Force Base, Ohio
18. Dr. Waldo Kliever, Instrumentation Physicist
Cleveland, Ohio
19. Dr. Fred S. Singer, Radiation Physicist
University of Maryland

TABLE OF CONTENTS

<u>Paragraph</u>	<u>Description</u>	<u>Page</u>
1.	Introduction	1
2.	Framework for Concept Formulation	3
2.1	Extra-terrestrial Alightment	3
2.2	Extra-terrestrial Departure	5
2.3	Orbital Rendezvous	5
2.4	Earth Maneuvers	6
3.	Scope of Concepts	7
3.1	Concepts Submitted	7
3.2	Selection of Modeled Concepts	8
4.	Dynamic Scaling of Selected Concepts	10
4.1	Tri-Collapsible Outrigger	13
4.1.1	Frangible Ring Pogo	17
4.1.2	Departure Capability	20
4.2	Imbedment Anchor	22
4.3	Oleo Pogo	27
4.3.1	Departure Capability	27
4.4	Triple-Oleo Outrigger	27
4.5	Landing Pads	30
4.6	Concept Mass Ratios	30
5.	Structural and Human Factor Considerations	31
5.1	Structural Considerations	31

5.2	Human Factor Considerations	33
6.	Space Environment Effects on Materials	38
6.1	High-strength Materials	38
6.2	Thermal Shock	39
6.3	Radiation Effects	39
6.4	Lubricants	40
6.5	Fluids	41
6.6	Metal Coatings	41
6.7	Vacuum Effects	42
7.	Additional Project Phases	43
7.1	Test Apparatus	43
7.2	Staff Film	43
8.	Conclusions and Recommendations	46
8.1	Additional Study Required	46
8.2	Testing Media	47
APPENDIX		48
Class I	Pictorial Presentation of Earth Concepts	49
Class II	Pictorial Presentation of Orbital Concepts	62
Class III	Pictorial Presentation of Lunar Concepts	81

LIST OF ILLUSTRATIONS

<u>Figure</u>		<u>Page</u>
1	Tri-Collapsible Outrigger (Frangible Ring) Concept	14
2	Tri-Collapsible Outrigger (Exploded View)	15
3	Experimental Frangible Rings	16
4	Frangible Ring Pogo Concept	18
5	Pressure Vessel, Oleo Pogo, Collapsible Pogo Assemblies - Exploded View	19
6	Schematic of Anchor System	23
7	Imbedment Anchor Systems Mounted	24
8	Imbedment Anchor System, Exploded View	25
9	Basic Imbedment Anchor Design	26
10	Oleo Pogo Concept	28
11	Triple Oleo Outrigger Concept	29
12	Impact Sensitivities for Mice, Men, and Structures	35
13	Minimum Time vs. Velocity Change	36
14	Minimum Distance vs. Velocity Change	37
15	Test Bed Suspension and Brake Device	44
16	Adjustable Drop Platform with Test Bed Suspended Above	45

APPENDIX ILLUSTRATIONS

17	Concept E-1 (Departure) and E-2 (Rendezvous): Orbital Glide Vehicle and Supersonic Carrier	49
18	Attaching Boom for Tactical Vehicle for Concept E-1 and E-2	50

<u>Figure</u>	<u>Title</u>	<u>Page</u>
19	Pylon Pad for Tactical Vehicle for Concept E1 and E-2	51
20	Concept E-3: Parachute Alightment	52
21	Concept E-4: Balloon Departure	53
22	Concept E-5: Single Ski Alightment on Prepared Site	54
23	Concept E-6: Conventional Ski Alightment on Prepared Site	55
24	Ski Oleo System for Concepts E-5 and E-6	56
25	Concept E-7: Rendezvous by Drogue Capture - Low Altitude and Low Subsonic Speed	57
26	Boom Attachment used for Concept E-7	58
27	Pylon Pad for Concept E-7	59
28	Concept E-8: Alightment on Prepared Site with Tricycle Gear	60
29	Concept E-9: Alightment by Balloon Descent	61
30	Concept O-1: Attachment by Tail Hook Snag	62
31	Concept O-2: Attachment by Self-Guiding Probe Through Hoop	63
32	Concepts O-3 and O-4: Shock Mitigation between Two (2) Axially Aligned Vehicles	64
33	Arresting Gear for Storing Impact Energy for Subsequent Ejection Departure - Concepts O-3 and O-4	65
34	Concept O-5: Remotely Controlled Magnetic Contactor on Freely Swinging Cable	66
35	Concept O-6: Rendezvous by Utility Tug - Remotely Controlled	67

<u>Figure</u>	<u>Title</u>	<u>Page</u>
36	Concept O-7: Attachment by Mechanical Grappling Hook - Close Range	68
37	Thrust Compensator and Line Control for Concept O-7	69
38	Concept O-8: Orbital Attachment by Self-Guiding Probe	70
39	Concept O-9: Rendezvous by Manned Utility Tug	71
40	Concept O-10: Rendezvous by Simple, Remotely Controlled Tug	72
41	Concept O-11: Long Range Attachment by Probe and Drogue - Heat or Light Sensitive	73
42	Latch Coupling for Concept O-11	74
43	Mechanical Magnetic Ring Coupling for Concept O-11	75
44	Concept O-12: Rendezvous of Axially Aligned Vehicles by Penetration	76
45	Concept O-13: Rendezvous by Surface Contact	77
46	Concept O-14: Rendezvous in Matched Orbits by Man in Environmental Suit	78
47	Concept O-15: Attachment by Mechanical Parallelogram Grappler	79
48	Concept O-16: Attachment by Gas Actuated Parallelogram Grappler	80
49	Concept L-1: Lunar Alightment - Single Oleo Strut with Imbedment Anchors	81
50	Concept L-2: Lunar Departure Assist by Gas Fired Squib	82
51	Concept L-3: Alightment on Collapsible Strut - Payload Mounted Separately for Bandpass Shock Absorbtion	83

<u>Figure</u>	<u>Title</u>	<u>Page</u>
52	Collapsible Strut Sequence for Concept L-3	84
53	Design Concept of Collapsible Strut for Concept L-3	85
54	Concept L-4: Vehicle Erection on Lunar Surface	86
55	Concept L-5: Triple Oleo Outrigger for Alightment and Stabilization	87
56	Concept L-6: Secondary Propellant Tanks Serving as Energy Absorbers	88
57	Concept L-7: Inflatable Feet for Accommodating Soft Lunar Surface	89
58	Concept L-8: Alightment on Stabilizing Inflatable Torus Base	90
59	Concept L-9: Lunar Erection with Tri-Oleo Outriggers	91
60	Concept L-10: Lunar Erection using Imbedment Anchors and Outriggers	92
61	Concept L-11: Train Alightment - Payload Settled at Reduced Impact	93
62	Concept L-12: Double Bipod Strut System for Alightment with Anchor Stabilization	94
63	Double Bipod Strut for Concept L-12	95
64	Concept L-13: Departure from Double Bipod Strut Platform	96
65	Concept L-14: Rack and Pinion Cycling Spring for Mechanical Shock Absorbtion	97
66	Concept L-15: Rack and Pinion Disc Brake for Mechanical Shock Absorbtion	98
67	Concept L-16: Tension Spring Outrigger for Mechanical Shock Absorbtion	99

<u>Figure</u>	<u>Title</u>	<u>Page</u>
68	Concept L-17: Lunar Erection with Variable Pivot Axis, 4 Strut System	100
69	Variable Pivot Axis System for Concept L-17	101
70	Concept L-18: Impact Attenuation with Reel-out Shock Absorbers	102
71	Reel-out Shock Absorbers for Concept L-18	103
72	Concept L-19: Lunar Departure Assist from Tank Platform	104
73	Concept L-20: Torsion Spring Shock Absorber	105
74	Concept L-21: Mechanical Compression Bungee - Outrigger Energy Absorber	106
75	Concept L-22: Shock Absorption System for Large Horizontal Velocity Component - Separately Mounted Payload	107
76	Self-Centering Shock Mitigation Cylinder for Concept L-22	108
77	Concept L-23: Energy Absorption using Propellant Tanks as Vertical Telescoping Struts	109
78	Concept L-24: Departure Assist by Gas Fired Squibs in Telescoped Tanks (follows L-23)	110

1. INTRODUCTION

On 28 May 1959, a contract No. AF33(616)-6572, was undertaken by the Instrumentation and Control Division of Cleveland Pneumatic Industries, Inc., to investigate, formulate, and develop concepts for alightment, attachment, and departure of advanced, extremely high altitude vehicles, including those capable of maneuvers on extra-terrestrial surfaces.

Initially, concepts for attaching vehicles in orbit and alighting and departing from extra-terrestrial surfaces were derived and analyzed to varying degrees as to their basic feasibility and their value for use in the future in deriving design criteria.

Simultaneous with concept study, visits were made to a number of airframe manufacturers, universities, government agencies, and other research organizations to permit exchange of information on the problems of shock mitigation and the acquisition of data on contemplated spaceframes.

All divisions of Cleveland Pneumatic Industries, Inc., (CPI), made contributions in order to present the maximum number of concepts for consideration. Concepts initially considered numbered approximately 100; however, through cursory CPI and WADD analysis, 50 of the less promising concepts were eliminated.

After the 50 remaining concepts were submitted, a preliminary analysis was made to determine which of the 50 offered most promise.

At this point, WADD engineers selected the 16 most promising concepts, upon which a thorough analysis was made in order to determine next the 8 most promising, and then reducing to the 4 most promising, for which detailed design was initiated to show feasibility through the use of dynamic scaling model techniques. It was during this phase that precise mathematical models were derived.

In addition to concept formulation, CPI conducted a limited documentation study as pertaining to shock mitigation in order to determine (a) structural mass vs. descent velocity requirements, (b) shock mitigation aspects of the orbital rendezvous maneuver, (c) thermal and high-energy radiation effects on metals and non-metals, (d) ablation and welding effects of metals in vacuums, (e) lubricant and fluid behavior in space environments.

Manuscript released by the author 6 April 1961 for publication as a WADD Technical Report.

The modeling phase of the project consisted of selecting the proper dimensionless ratios and scale ratios to permit dynamic scaling of the concepts, design of the experimental equipment, design of a test bed model on which to test the concept models, and fabrication of the experimental equipment.

Following the experimental equipment construction phase, preliminary testing of the concept models was accomplished to establish basic design integrity. Included in this testing phase was the recording on high-speed film of the departure and alightment maneuvers for each concept.

Additionally, a study was made on the human factors aspects of landings. Decelerations, impact velocities, and their rates of application were studied to derive man's tolerance to these factors.

2. FRAMEWORK FOR CONCEPT FORMULATION

In order to formulate the alightment, attachment, and departure concepts, a basic framework of parameters, or limiting physical quantities, was required to establish a basis for comparison. In attempting to extrapolate from known shock mitigation performance levels, conventional aircraft operations were examined.

Landing gear of modern, land-based fighter, carrier-based fighter, and transport aircraft can withstand vertical impact velocities up to approximately 20, 26, and 14 ft/sec. respectively while their horizontal touchdown velocities range from 80 mph to over 160 mph. Vertical decelerations are accommodated up to approximately 12 "g's" and horizontal deceleration up to several "g's".

The vertical component of the landing impact force is traditionally mitigated by use of rigid air-oil ("oleo") struts, and the horizontal by aerodynamic drag, rolling friction, wheel brakes, drag chutes, etc.

2.1 LUNAR ALIGHTMENT

In studying lunar landing and departure maneuvers, it was obvious that existence of little or no atmosphere should be assumed, hence no reduction in vertical velocity by aerodynamic means. WADD established that the Contractor should not assume the availability of surface with sufficient smoothness and regularity to permit wheel landings, at least not for the initial manned flights.

WADD also directed that CPI should consider "manned" operations only; therefore, it was assumed that unmanned probes would provide data on space environments and extra-terrestrial surfaces before these "manned" maneuvers would be accomplished. Advanced vehicles, limited as to their minimum size and mass due to requirements for crew, were also assumed to have a return capability.

With regard to maximum anticipated deceleration rate, WADD instructed CPI to assume an impact of 4 g's* (4 x 32.2 or 128.8 ft/sec.²) as the safe maximum with an ultimate of 6 g's (193.2 ft/sec.²). Such levels were selected after completion of a survey of air-frame manufacturers and other space-oriented organizations during which each was requested to make their own estimate on minimum possible vertical settling rates and horizontal components which appeared feasible, based on extrapolation of current art in guidance and control.

* Earth g's; 1 g = 32.2 ft/sec.²

The estimates received varied greatly. Some organizations feared that exact control of attitude and retro-thrust would be very difficult; therefore, maximum settling rates were derived for this project by approaching the problem from the aspect of what would be the allowable mass for shock mitigation equipment.

Analysis in this area determined that a maximum settling rate of 30 to 50 ft/sec. could be decelerated without necessitating excessively heavy shock mitigation equipment.

Analysis with regard to control capability revealed that, if a control system were capable of taking a vehicle from an extra-terrestrial orbit and establishing and maintaining it in a proper descending attitude with respect to trajectory and local vertical, it should also be capable of bringing the system to an acceptably low velocity on approach to the surface of the extra-terrestrial body. Based on these facts and logical assumptions, it was agreed to assume a maximum vertical settling rate of 35 ft/sec. for purposes of this study.

With regard to the level of horizontal component to be assumed during landing, assistance was provided by the Flight Control Laboratory of WADD and, as a result of inter-laboratory discussion, values for horizontal velocity of 10% of the vertical component coupled with 10° out-of-parallelism between vehicle axis and local vertical were agreed upon.

Concerning surface, it was decided not to arbitrarily establish figures for maximum slope, compressibility, or regularity of the surface, as these quantities could vary widely and concepts would be classified as to their ability to cope with variations.

In summary, the criteria for concept formulation for alightment on extra-terrestrial surfaces was listed as:

- a. 4 "earth" g's max. safe deceleration.
- b. 1.5 safety factor applied to deceleration.
- c. System would include retro-thrust control capability sufficient to limit descent to 35 ft/sec. max. safe vertical impact velocity (42.8 ft/sec. ultimate).

- d. Horizontal velocity of 10% of vertical velocity.
- e. Vehicle axis 10° maximum out-of-parallelism with local vertical.
- f. System would be manned and would have a return capability.
- g. Based on "man-in-the-loop" and a return capability, it was assumed that a vehicle gross weight at impact would be on the order of 20 tons (earth weight).

2.2 EXTRA-TERRESTRIAL DEPARTURE

With regard to departure concepts, it was determined that if shock mitigation equipment could also assist a vehicle during its initial departure, departure aspects should be considered.

As a rocket ascends from its launching site, it uses less fuel proportionately at each successive instant. If a method could be derived to impart additional thrust on launch by utilizing other equipment in the vehicle, the net amount of fuel saved might be significant. During the study of alightment concepts, therefore, consideration was given to utilizing alightment equipment wherever possible as a means for improving launch capability with resultant fuel savings.

2.3 ORBITAL RENDEZVOUS

Work during this phase of the project was faced with many unknowns. Initially, a cursory study was made in the area of orbital mechanics to determine what precision was required from thrust control during orbital rendezvous and if there might be a mass trade-off between shock mitigation and thrust control equipment. Again, air-frame manufacturers and other agencies contributed to this effort. The findings are summarized below:

- a. The planes of the orbits of the target and intercept vehicles must be within minutes of arc.
- b. The orbits must be matched in shape, size, and orientation within minutes of arc and, at time and point of rendezvous, the vehicles come together within close proximity.

- c. The vehicles must be closely "in phase" to affect rendezvous.
- d. The vehicles, in the case of earth orbit rendezvous, should avoid lengthy exposure to the lower Van Allen radiation belt.
- e. To make a rendezvous possible, corrective vernier rockets will have to operate within extremely precise limitations of thrust and cut-off times to bring relative velocity within acceptable limits.
- f.* It was determined that, if each vehicle's velocity vector does not intercept the other's center of gravity on rendezvous, there may be a tumbling problem after contact.

To hold the mass of the shock mitigation equipment to an acceptable percentage of total mass, relative velocities were not to be considered over 35 ft/sec.

Parameters forming the framework for orbital attachment concepts include the same values applied in paragraph 2.1; therefore:

- a. 4 "earth" g's max. safe deceleration.
- b. 1.5 safety factor applied to deceleration.
- c. Vehicle gross weight approximately 20 tons (earth weight).

2.4 EARTH MANEUVERS

In this area, many concepts were submitted. However, since the problem of return to earth and landing are under detailed study in the Air Force as a portion of the Dyna-Soar development, no attempt was made to list a framework for concept formulation concerned with earth maneuvers.

* Any gravitational attraction between two bodies can be discounted with regard to bringing or holding them together. Eg: it takes only $2(10)^{-5}$ radians/sec. rotation about a common C.G. to make two bodies of 100 tons each (whose C.G.'s are 100 feet apart) to balance the gravitational force holding them together.

3. SCOPE OF CONCEPTS

As the project progressed, the concepts submitted were categorized as to earth alightment or departure, (labeled E-1, E-2, etc.), orbital attachment (O-1, O-2, etc.), and lunar alightment or departure (L-1, L-2, etc.). They were sub-categorized as logically as possible, as to their nature -- mechanical, electro-mechanical, multi-strut, etc.

3.1 CONCEPTS SUBMITTED

The appendix shows the concepts submitted in pictorial form. They are separated into the three major categories shown above. Class I illustrates earth alightment and departure, Class II orbital rendezvous, and Class III lunar alightment and departure.

The sixteen (16) most promising concepts as selected by WADD, are listed below:

Class I - Earth Concepts

1. E-1 Departure: Orbital glide vehicle and supersonic carrier.
2. E-2 Rendezvous: Orbital glide vehicle and supersonic carrier.

Class II - Orbital

3. O-1 Attachment by tail-hook snag.
4. O-2 Attachment by self-guiding probe through hoop.
5. O-7 Attachment by mechanical grappling hook -- close range.
6. O-8 Orbital attachment by self-guiding probe.
7. O-11 Long-range attachment by probe and drogue -- heat or light sensitive.
8. O-15 Attachment by mechanical parallelogram grapppler.

Class III - Lunar Concepts

9. L-1 - Lunar alightment - single oleo strut with imbedment anchors.
10. L-2 - Lunar Departure assist by gas-fired squib.
11. L-3 - Alightment on collapsible strut - payload mounted separately for bandpass shock absorption.
12. L-5 - Triple "oleo" outrigger for alightment and stabilization.
13. L-6 - Secondary propellant tanks serving as energy absorbers.
14. L-7 - Large area, inflatable feet for accommodating soft lunar surface.
15. L-23 - Energy absorption using propellant tanks as vertical telescoping struts.
16. L-24 - Departure assist by gas-fired squibs in telescoped tanks (follows L-23).

NOTE: The 34 concepts eliminated from further study by WADD were rejected on the basis of (a) insufficient anticipated reliability, (b) lack of confidence in state-of-the-art advances in that area and, (c) in the case of bags, balloons, and parachutes, cognizance by other WADD Laboratories.

3.2 SELECTION OF MODELED CONCEPTS

During January, 1960, CPI representatives attended an engineering conference at WADD to assist WADD engineers in reducing the sixteen (16) remaining concepts to eight (8). However, to allow more time for modeling, it was decided at that time by WADD to select the final four (4) concepts immediately, rather than narrow the sixteen down to eight and then to four. The four chosen for modeling included:

1. Imbedment anchor for stabilization of vehicle during and after alightment.
2. Oleo pogo for alightment and departure.

3. Triple vertical collapsing strut employing frangible rings for shock mitigation for alightment.
4. Triple-oleo outrigger for alightment.

Final selection of the four (4) concepts to be modeled was based on the belief that they represented those most promising as well as a cross-section of techniques from which valuable data could be derived relative to shock mitigation efficiency vs. mass.

4. DYNAMIC SCALING OF SELECTED CONCEPTS

The dynamic scale ratios and physical quantities describing the concepts and test bed vehicle were selected in concert with WADD engineers.

Essentially, the test bed model built by CPI represents a physical analog of an hypothetical full-size lunar prototype system.* Those physical quantities necessary were scaled to a convenient scale factor with economy and cost in mind. The test bed vehicle (designated the test bed model hereafter) was configured in such a manner that it could accommodate hardware for each of the selected concepts with only minor qualifications.

With regard to scaling of the test bed model, kinematic scaling was primarily employed. The configuration was arbitrarily selected by WADD and CPI with design and mass distribution derived from current state-of-the-art. Dimensions and overall radii of gyration were maintained in the selected length ratio of 10 to 1. Densities of materials were maintained in the ratio of .605 to 1, moduli 1 to 1, and centers of masses were kept proportional. Therefore, choice of materials remained nearly the same in the test bed model as in the prototype system.

The following table includes the pertinent quantities selected, as well as quantities relating to the modeled concepts.

The second table lists the dimensionless ratios that were involved. As a note of explanation, these were derived by dividing a prototype quantity by the corresponding model quantity; e.g., prototype mass by model mass. The upper case letters refer to prototype values, and the lower case to the model.

* For purposes of concept testing, a test bed system was constructed predicated on a structure/propellant ratio of 40/60 as based on required return capability and using liquid O₂ and H₂ of foreseeable reliable specific impulse of 300 lb.sec/sec. This 40-60% ratio was assumed to exist at time of touchdown. It was assumed the vehicle velocity would be brought to zero at 60 ± 55 ft. above the lunar surface and would free fall from this point to the surface. The tanks containing the propellant for dissipating the approach velocity toward the lunar surface were assumed to have been jettisoned at the point of zero velocity, thus their mass would not be included in the system's touchdown mass.

TABLE OF PROTOTYPE-MODEL QUANTITIES

	PROTOTYPE		MODEL	
1. Length (approx.)	L	42 ft. 6 in.	l	4 ft. 3 in.
2. Earth weight	W	45,375 lb.	w	75 lb.
3. Mass	M	1407 slugs	m	2.33 slugs
4. Gravity acceleration	G	5.32 ft/sec ²	g	32.2 ft/sec ²
5. Max. safe impact velocity	V	35 ft/sec	v	27.2 ft/sec
6. Max. safe deceleration	A	128.8 ft/sec ²	a	780 ft/sec ²
7. Deceleration safety factor		1.5		1.5
8. Ultimate deceleration	*A ₁	193.2 ft/sec ²	a ₁	1169 ft/sec ²
9. Oleo pogo stroke length (69% eff.)	H _O	6.87 ft.	h _O	8.25 in.
10. Collapsible pogo stroke length	H _C	4.75 ft.	h _C	5.7 in.
11. Impact velocity needed to achieve ultimate deceleration A ₁	V ₁	42.8 ft/sec	v ₁	33.4 ft/sec
12. Safe impact force	F	188,900 lb.	F	1889 lb.
13. Ultimate impact force	F ₁	279,280 lb.	f ₁	2792.8 lb.
14. Oleo spring rate F ₁ /H _O	K _O	40,652 lb/ft	k _O	339 lb/in
15. Collapsible spring rate F ₁ /H _C	K _C	58,750 lb/ft	k _C	490 lb/in
16. Free drop time for ultimate load	T ₁	8.05 sec.	t ₁	1.005 sec.
17. Free drop height for ultimate load	S ₁	172.5 ft	s ₁	17.25 ft
18. Kinetic energy at ultimate impact	ε ₁	1,294,000 ft. lb.	ε ₁	1294 ft.lb.

* Subscript '1' refers to ultimate load.

TABLE OF DIMENSIONLESS RATIOS

Length	$\frac{L}{l} = \frac{10}{1}$
Mass and weight	$\frac{M}{m} = \frac{W}{w} = \frac{605}{1}$
Gravity and accelerations	$\frac{A}{a} = \frac{G}{g} = \frac{.165}{1}$
Velocities	$\frac{V}{v} = \frac{1.282}{1}$
Forces	$\frac{F}{f} = \frac{100}{1}$
Time	$\frac{T}{t} = \frac{7.78}{1}$
Moduli (force/area)	$\frac{E}{e} = \frac{1}{1}$
Densities of materials	$\frac{D}{d} = \frac{.605}{1}$
Energies	$\frac{\mathcal{E}}{\epsilon} = \frac{1000}{1}$
Moments of inertia	$\frac{I}{j} = \frac{6.05(10)^4}{1}$
Angular velocity	$\frac{\omega}{\omega} = \frac{.1285}{1}$
Angular acceleration	$\frac{\alpha}{\alpha} = \frac{.165}{1}$
Momentum	$\frac{p}{p} = \frac{77.8}{1}$
Kinematic viscosity	$\frac{\lambda}{\lambda} = \frac{12.85}{1}$

4.1 TRI-COLLAPSIBLE OUTRIGGER

Figure 1 shows the finished concept with struts in collapsed position. Figure 2 shows a strut extension in exploded form.

The landing pads are saucer shaped in this photo (interchangeable as discussed in paragraph 4.5) to reduce bearing pressure on the surface at impact.

The principle of absorbing landing shock with frangible rings involves the absorption of impact energy as a non-repeatable operation by circularly rupturing a stack of rings of reliably predictable tension yield by forcing them over a cone. The rings would be forced over the taper by applying force to the top of the shorter cylinder (see static press in Figure 3.).

A theoretical formula was derived approximately equating impact force and ring dimensions for rectangular cross-section rings:

$$F \cong hnt s_t \left(\frac{\tan \alpha + \mu}{1 + \mu \tan \alpha} \right), \text{ where}$$

F = impact force
 t = ring wall thickness
 n = number of rings
 s_t = tensile yield of ring
 h = height of ring
 μ = coefficient of friction between ring and taper
 α = taper angle

The optimum taper angle was established as approximately 10° . For 6063 T-5 and 7073 T-6 soft aluminum over stainless steel, μ approximated .8 (dry coefficient of friction under extreme load); and $h = .1$ ".

The preliminary drop tests established an approximate correction factor of $1/3$ to the right side of the equation. Ring thickness for model drop heights of 2 to 4 feet varied from .010" to .022". Rings of aluminum were chosen because of lightness, convenient ring tensile yield, availability, and cost.

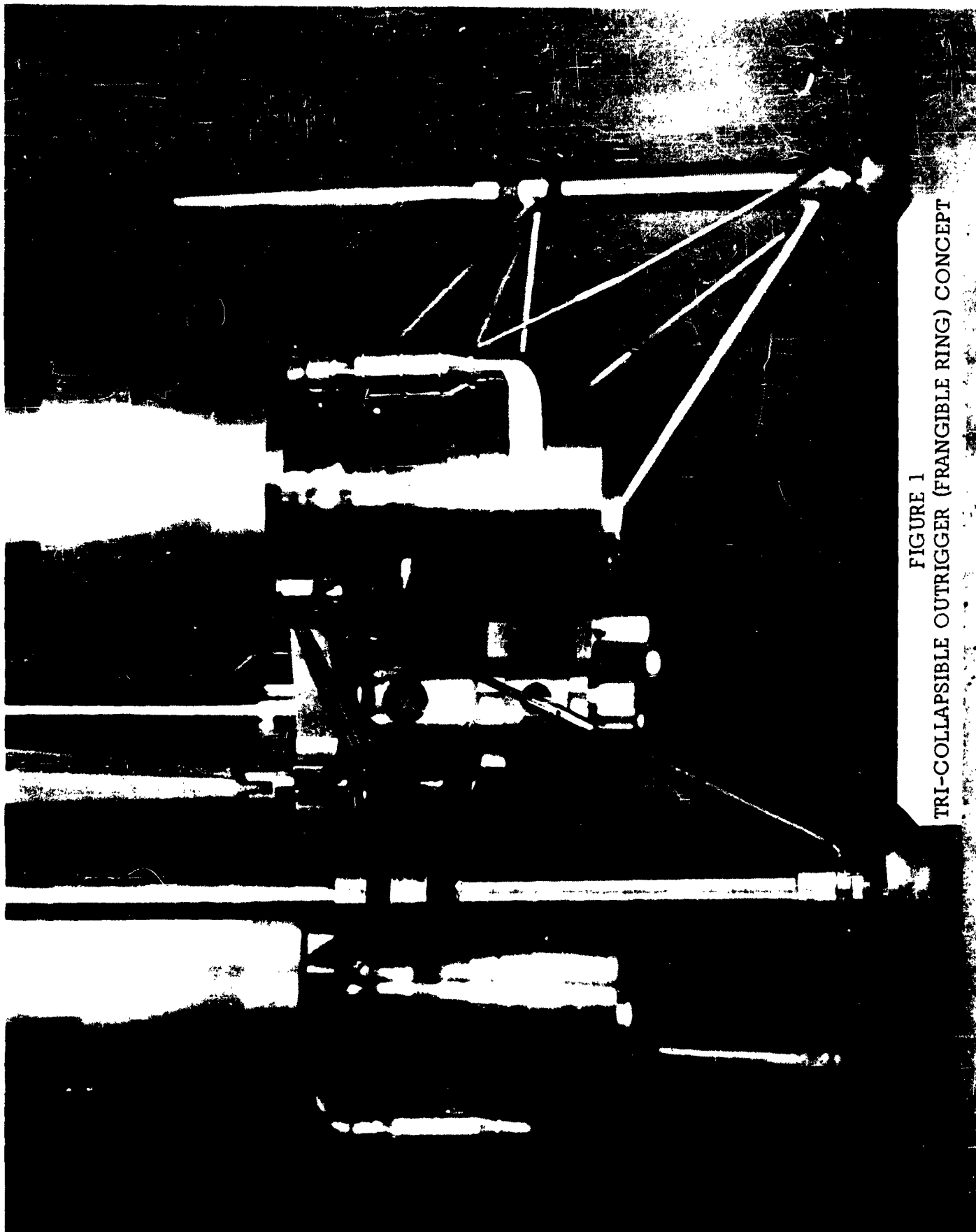


FIGURE 1
TRI-COLLAPSIBLE OUTRIGGER (FRANGIBLE RING) CONCEPT

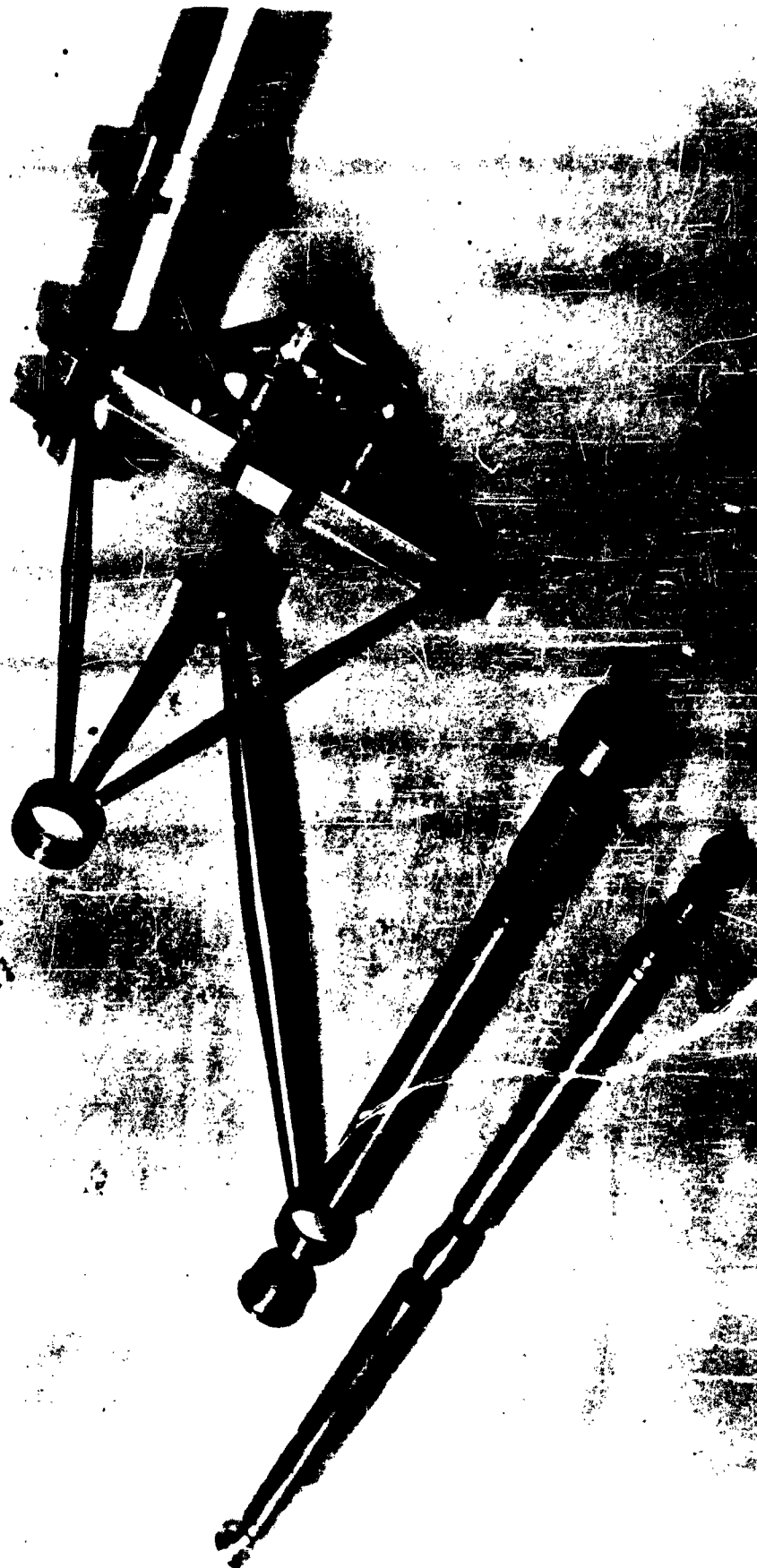
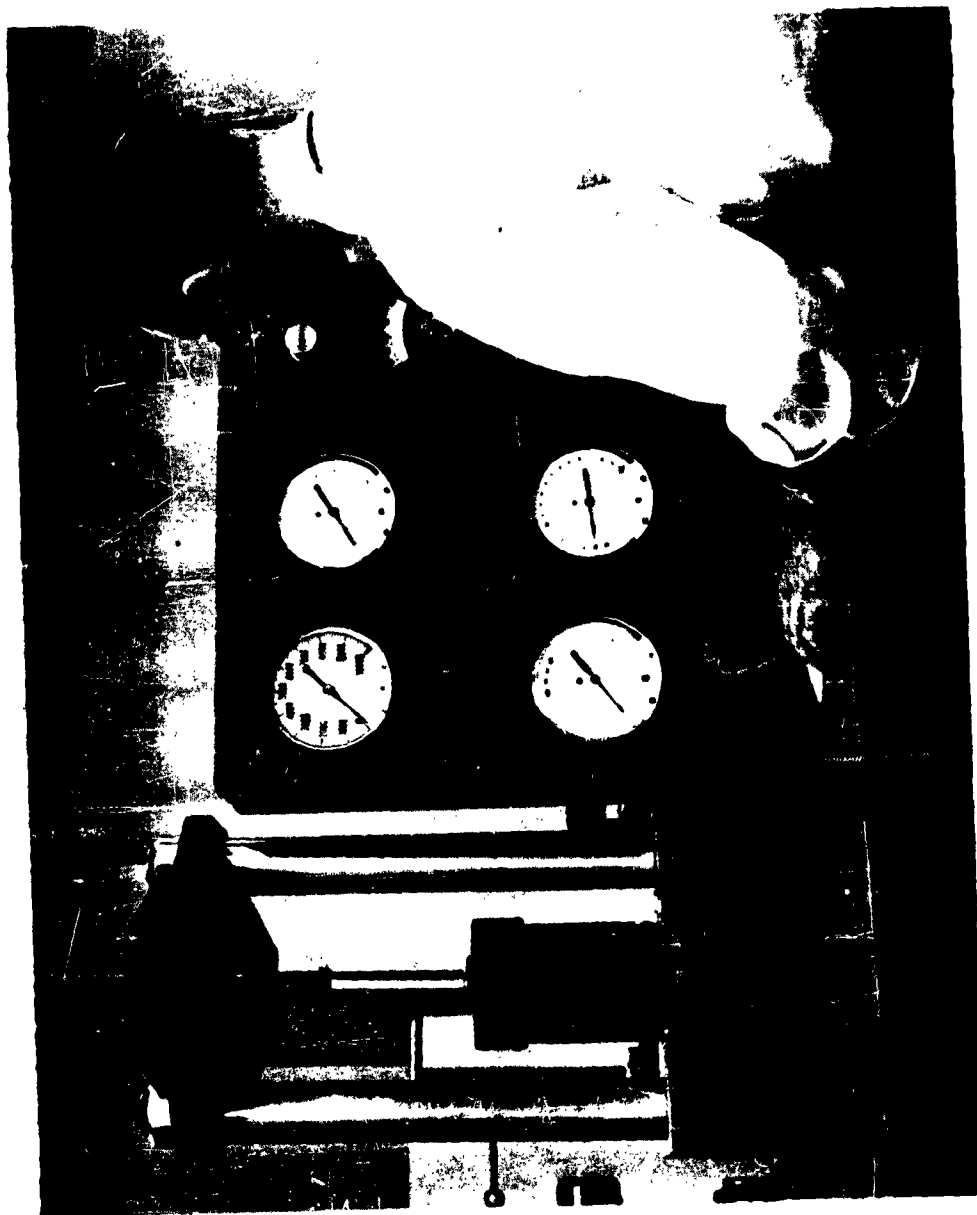
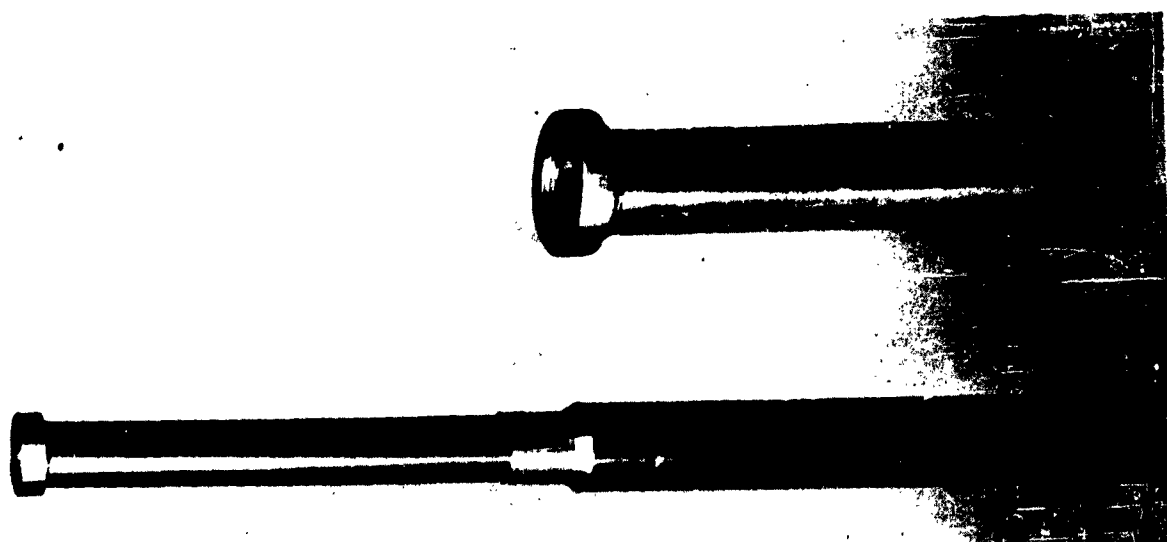


FIGURE 2
TRI-COLLAPSIBLE C-TRIGGER (EXPLODED VIEW)



STATIC-FORCE PRESS FOR EXPERIMENTAL FRANGIBLE RINGS

FIGURE 3
EXPERIMENTAL FRANGIBLE RINGS



Concerning problems encountered, it was found that radial clearances within the telescoping tubes were very important in controlling stack-up of fractured rings.

Testing the triple vertical configuration showed that a slight jamming of rings during fracturing caused the strut to impose instantaneously a greatly magnified impact force to the strut extension members. This phenomenon caused the extension structure to collapse due to the shortened effective stroke length. Although the extension members were stressed for a full 11.5 ft. drop, they failed when the much greater load was applied. It is suspected that shock wave phenomena also entered into this failure. Future testing then would require strengthened strut extensions and better fracture programming of rings.

This concept is considered worthy of further development. Its advantages include simplicity of operation, economy; a very low weight ratio, 100% efficiency of strut action, and self stabilization. It is relatively insensitive to temperature variations and other aspects of space environments.

As for all concepts modeled, the table in paragraph 4.6 shows relative mass ratios as developed for this concept.

4.1.1 Frangible Ring Pogo

This is a sub-concept of the one described above. Figure 4 illustrates it mounted in the test bed. Figure 5, lower, shows the frangible pogo in exploded form.

Its preliminary testing was very successful. Its mass ratio is lowest of all concepts (only .84% of total). However, it requires the use of an additional system for stabilization—being single-strut, hence with anchor stabilization it has a total mass ratio of approximately 2-1/3%.

The determination of optimum frangible ring dimensions for this sub-concept imposed the same problem as for the concept in paragraph 4.1. In testing, this sub-concept was the simplest of all to model. It had fewer parts and there were no test malfunctions.

NOTE: It should be noted that mass ratios shown herein represent model mass ratios. In developing completely satisfactory full-scale systems, the ratios may vary.

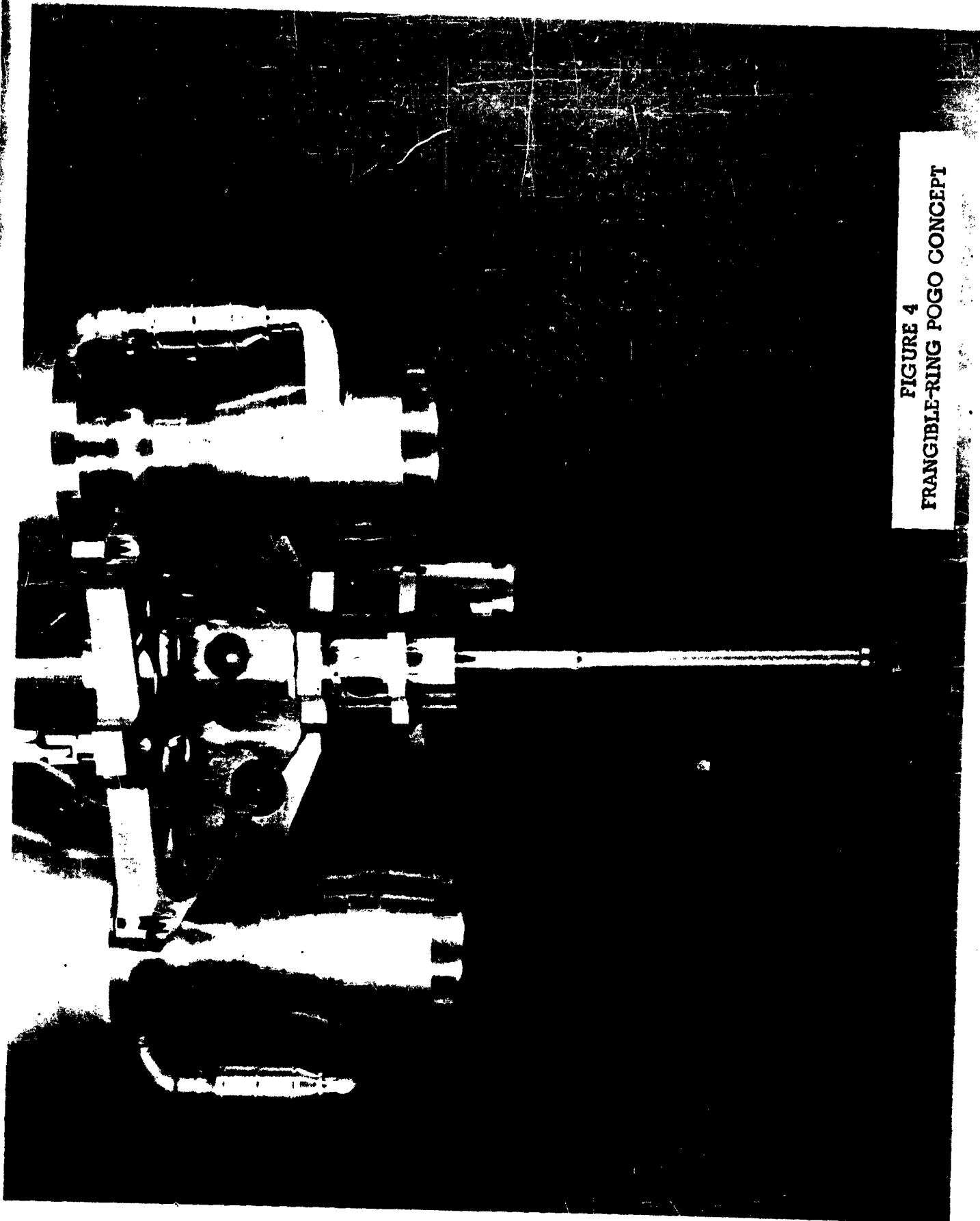


FIGURE 4
FRANGIBLE-RING POGO CONCEPT

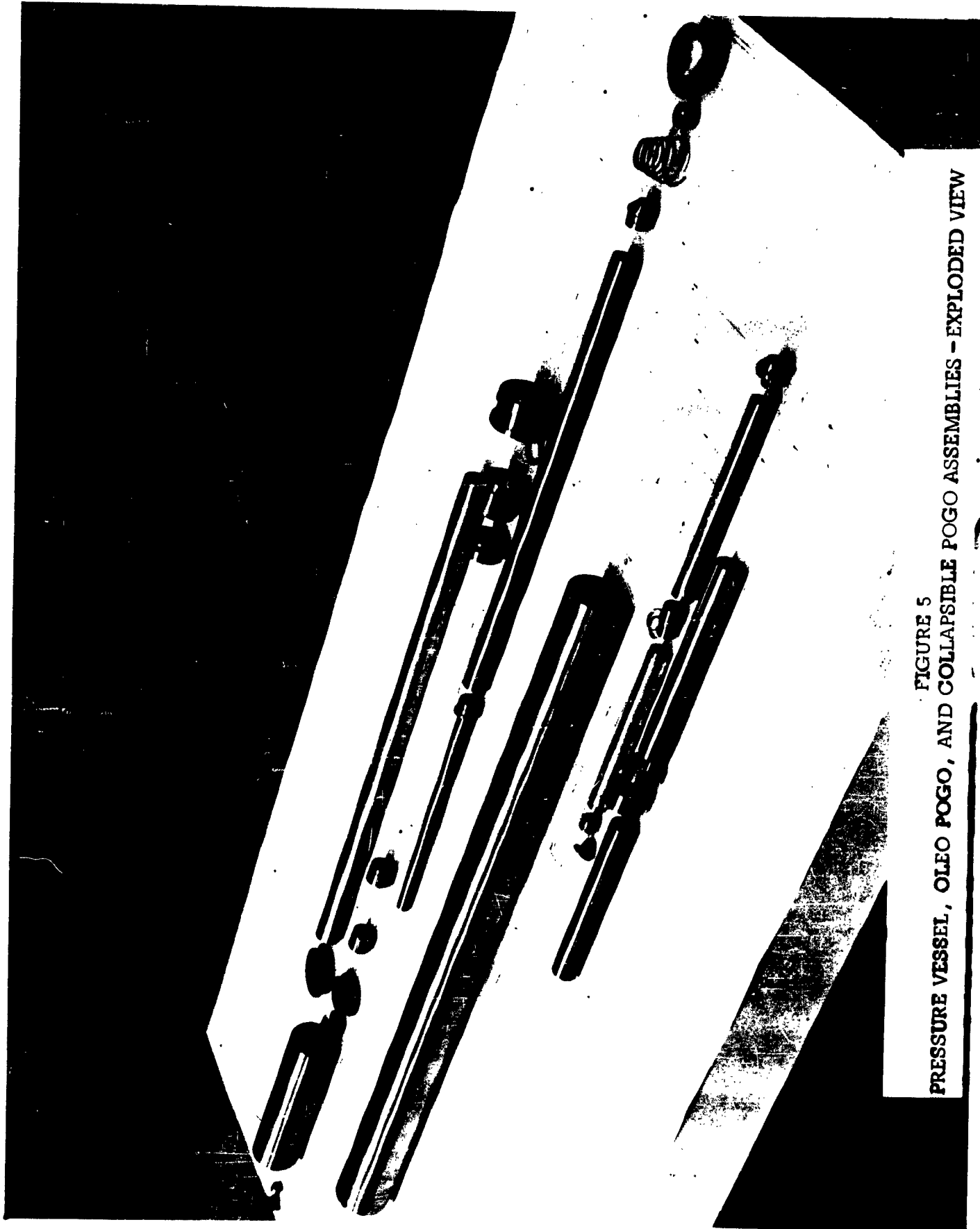


FIGURE 5
PRESSURE VESSEL, OLEO POGO, AND COLLAPSIBLE POGO ASSEMBLIES - EXPLODED VIEW

4.1.2 Departure Capability

With minor adaptations, a 12-1/2 cu. in. high-pressure vessel, Figure 5 upper left, was fitted to the upper end of the pogo cylinder to provide a departure capability.

Inside the bottle, a firing mechanism ignited a charge of black powder by resistive heating, by means of a capacitor discharge. The gas pressure produced drove the pogo piston downward (or the vehicle upward) with a calculated initial velocity.

The general formula describing the forces and motions of this system was derived as:

$$Mx \frac{d^3 x}{dt^3} + K \left(\frac{Md^2 x}{dt^2} + W \right) \frac{dx}{dt} = 0, \text{ where,}$$

M	=	mass of vehicle
t	=	time
K	=	adiabatic constant for pressurizing gas
W	=	vehicle weight
x	=	stroke length of piston
$\frac{dx}{dt}$	=	velocity of piston at any point
$\frac{d^2 x}{dt^2}$	=	acceleration of piston at any point
$\frac{d^3 x}{dt^3}$	=	rate of change of piston acceleration at any point

Theoretically, this system could impart an upward velocity to the model test bed to lift it to an ultimate height of approximately 50 feet (earth). More thorough testing is required to determine the overall capability of this system to assist lunar departure.

The following table gives approximate charges of the black powder required for preliminary departure testing for both the Frangible Ring Pogo and the Oleo Pogo (discussed in para. 4.3.1 below).

Vehicle Jump	OLEO POGO		FRANGIBLE RING POGO	
	Powder Charge	Est. Max. Pressure	Powder Charge	Est. Max. Pressure
h	w	psig	w	psig
1 ft.	8 grams	935	10 grams	1225
2	11	1385	12	1540
3	13	1695	15	2015
4	17	2365	19	2685

These charge figures were derived experimentally by preliminary departure testing. Powder charges required for each jump height proved greater than the values computed by formula. The difference is due, in large part, to sliding frictional forces between the moving parts.

The theoretical formula, neglecting frictional forces, for finding peak pressure is:

$$P_2 - 14.7 = P_1 (V_1/V_2)^k, \text{ or}$$

$$P_2 = (7.67 w^{1.21} - 14.7) \text{ psig, where:}$$

$$P_1 = \text{atmospheric pressure} = 14.7 \text{ psia}$$

$$P_2 = \text{max. peak pressure of reaction (psig).}$$

$$V_2 = \text{volume of pressure bottle, } 12.5 \text{ in.}^3$$

$$V_1 = 49.02(W) \text{ in.}^3 - \text{weight-volume coefficient of black powder times the weight of powder.}$$

$$K = 1.21, \text{ mean adiabatic constant for combustion products of powder.}$$

The differential equation above and the simple relation, $PA = ma + w$,* enabled the engineers to arrive at approximate powder charges needed for preliminary tests.

Comprehensive testing would provide an empirical correction factor for this gas formula.

* Where, P = max. peak pressure w = test bed weight
A = piston head area of Pogo a = test bed peak acceleration
m = test bed mass

4.2 IMBEDMENT ANCHOR

Figure 6 is a schematic of a unique imbedment anchor system from which the design of the scaled experimental equipment was developed. Three anchors, each 120° apart, were considered adequate for stabilizing a vehicle, providing they imbed at the same time and maintain proper tension on the lines. Figure 7 shows the system mounted in the capsule. Three (3) additional anchors were added for testing reliability.

The requirements of the system include that anchors fire simultaneously, then imbed in the surface. The lines were to be prevented from feeding out after anchor contact, then the lines had to be tensioned properly. Also, the system should be able to operate and hold on irregular surfaces of varying compressibilities.

Figure 8 is a photo of the system in exploded form -- upper left to lower right shows the reels for winding anchor lines, the lines, line brakes, and snubber (solenoid operated), firing springs, loading barrels (screw into capsule ring), and the anchors.

Each anchor line contains two (2) miniature insulated conducting wires leading to the solenoid. The power source is three (3) sets of three (3) 9-volt dry cells in series-parallel (27 volts to each solenoid). The batteries are located, three (3) each, in each of the three (3) fuel tanks to be part of the scaled liquid O_2 mass in order that C.G.'s and radius of gyration of tanks are maintained.

The anchors are spring released inertially on impact of the model. As the anchor strikes the surface, a 25-caliber primer and several grains of powder are ignited (see Figure 9 for anchor design). The ensuing reaction gases are contained in the anchor body and jetted rearward from the anchor tail.

Inside the anchor body, the high-pressure gas closes a pressure switch, completing the circuit to the line-brake and snubber as well as providing an extra impulse to the imbedding anchors. The entire sequence requires approximately 25 milliseconds (in model time).

It should be noted that the anchor system was scaled primarily for similitude of kinematics, forces, and restraints as these quantities, rather than anchor geometry, were important in concept testing.

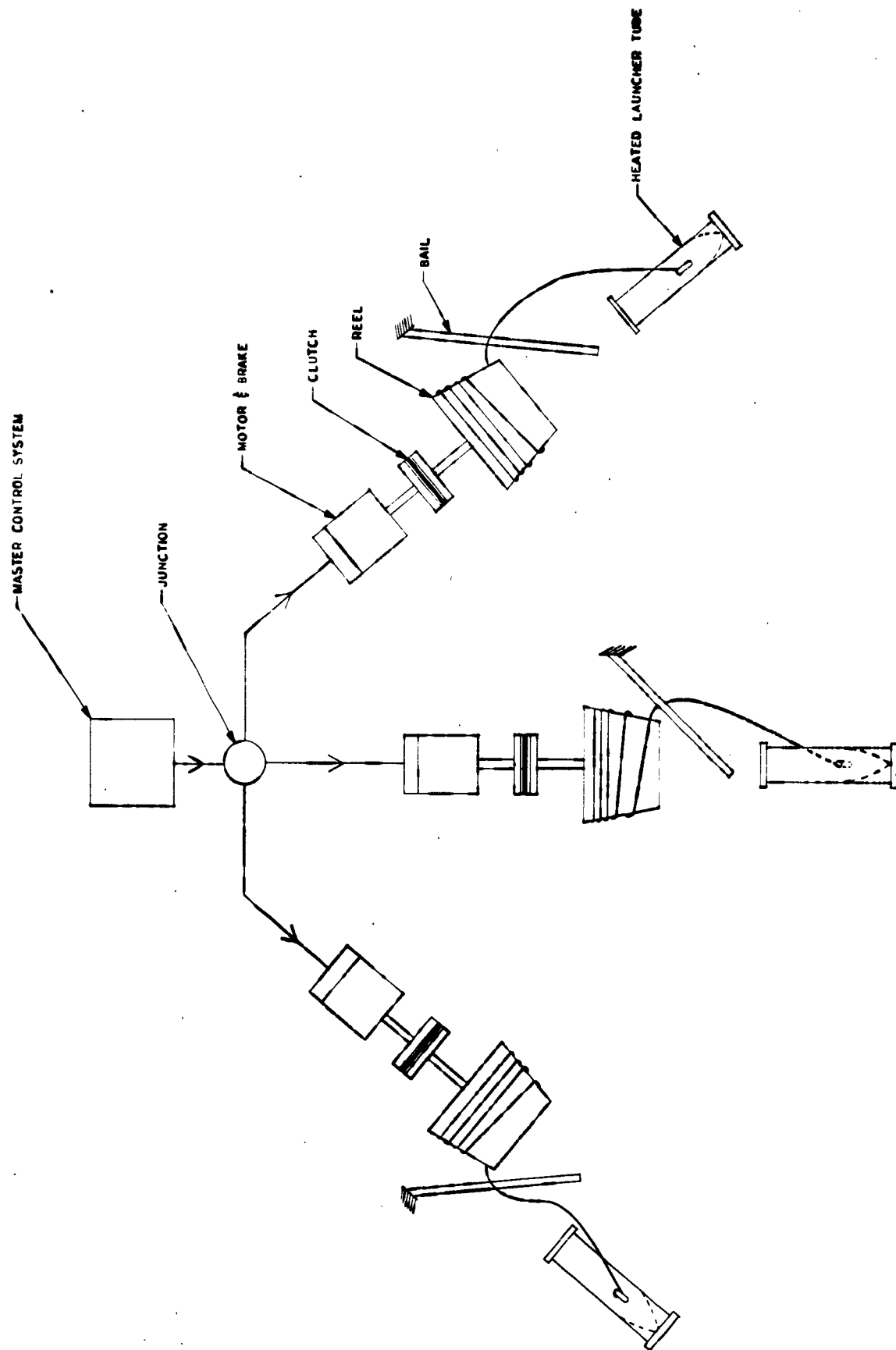
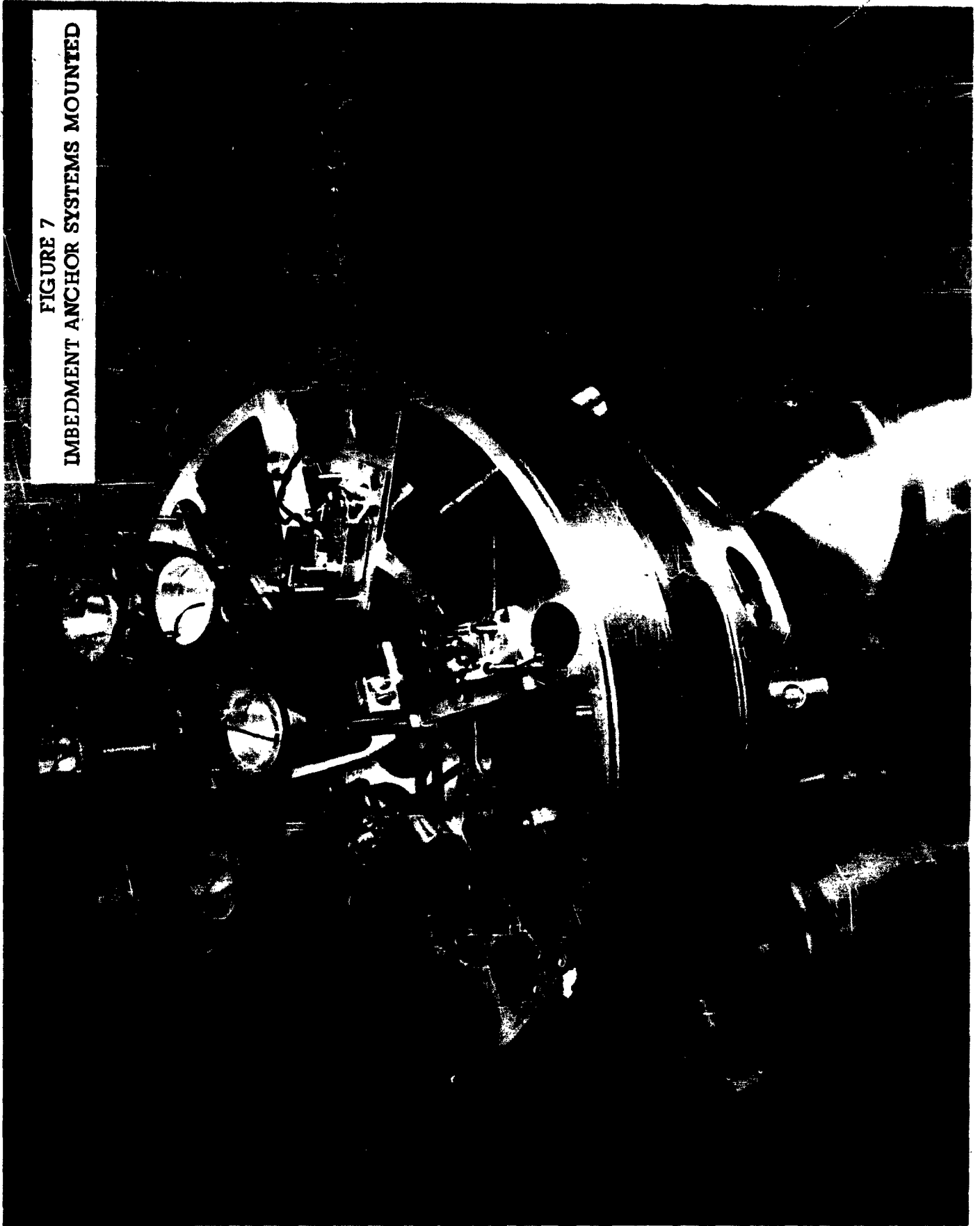


FIGURE 6
SCHEMATIC OF ANCHOR SYSTEM

FIGURE 7
IMBEDMENT ANCHOR SYSTEMS MOUNTED



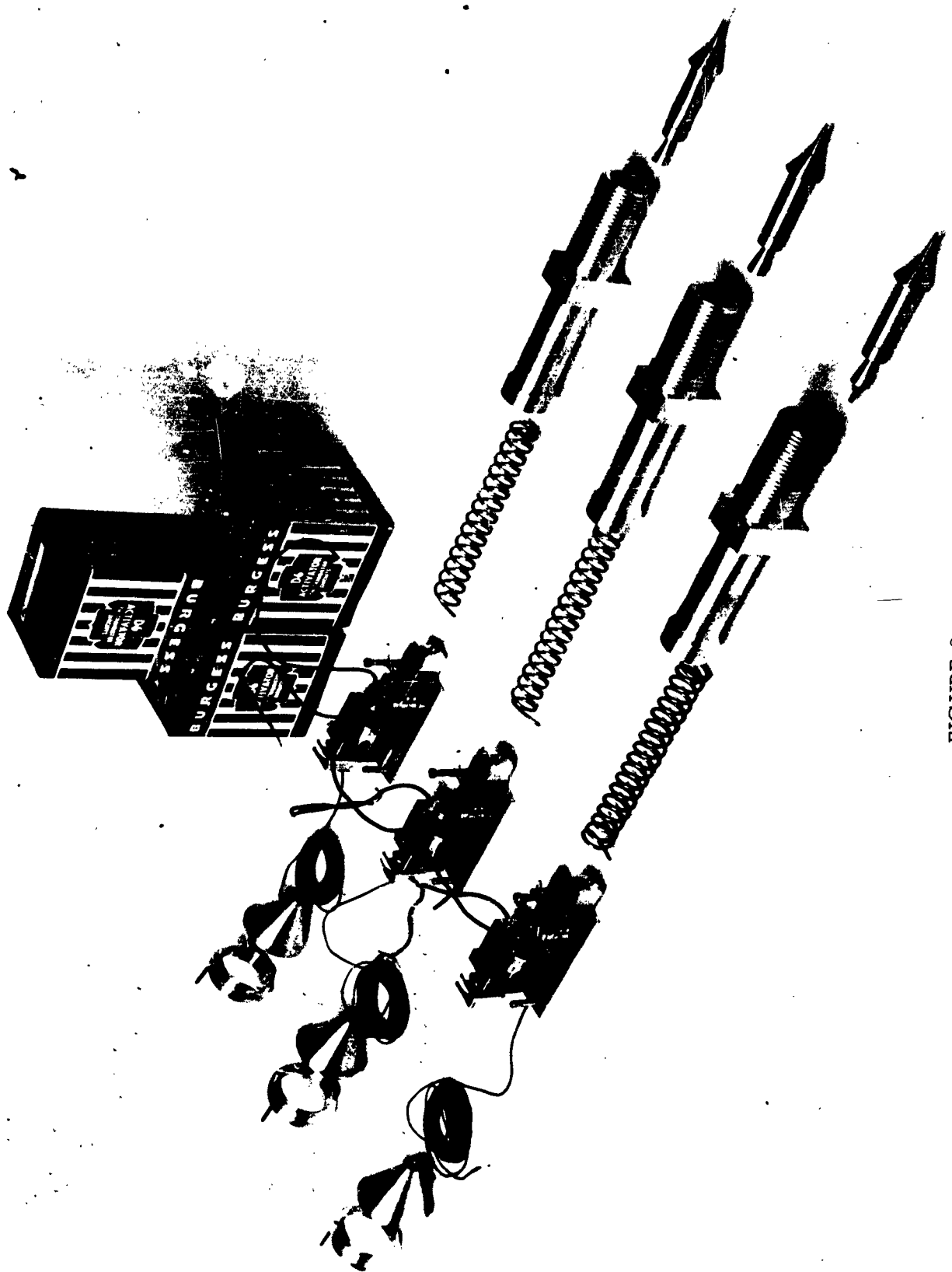


FIGURE 8
IMBEDMENT ANCHOR SYSTEM, EXPLODED VIEW

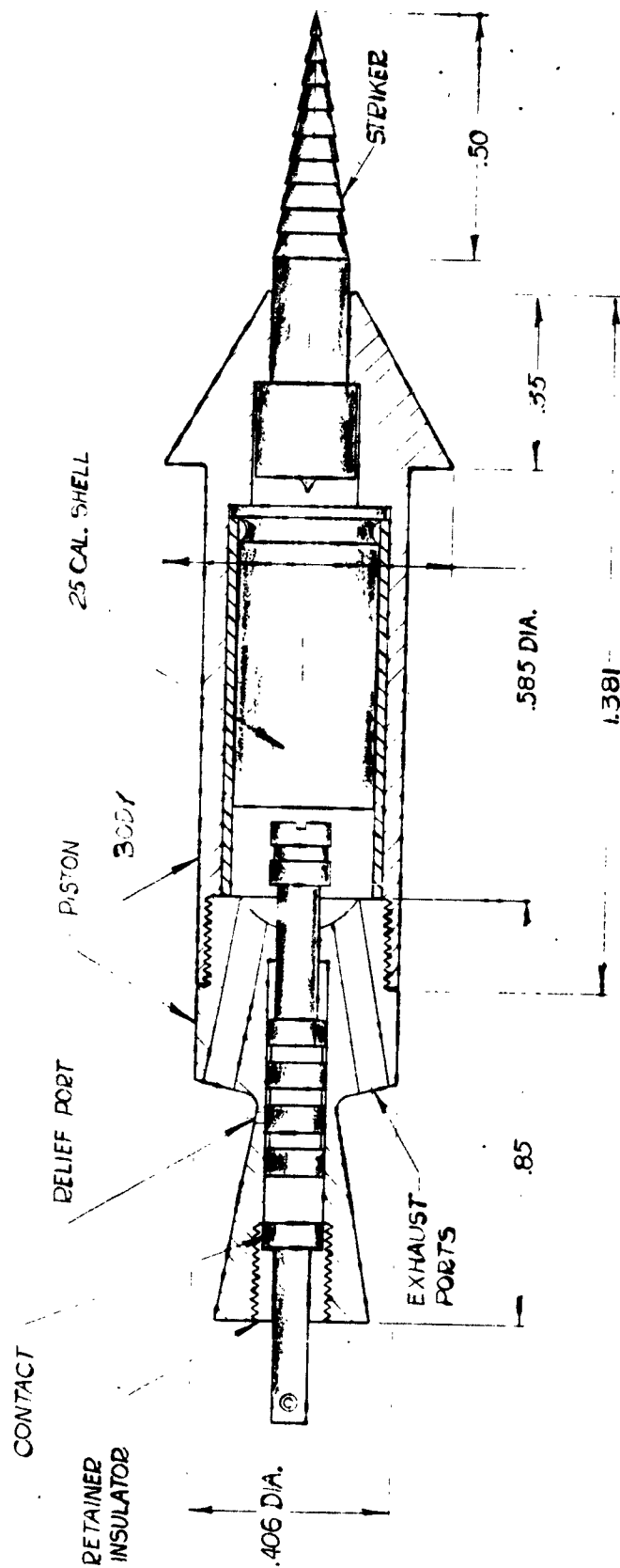


FIGURE 9
BASIC IMBEDMENT ANCHOR DESIGN

4.3 OLEO POGO

The experimental equipment in exploded form appears in Figure 5, upper portion. Figure 10 is a photo of the pogo mounted in the centerpost of the test bed.

Basically, this concept involves known landing gear principles, being an air-oil system in which hydraulic fluid is forced between an orifice and moving metering pin when impact force is applied to the pin-piston assembly.

Preliminary testing of this concept was very successful. While its weight is somewhat greater than the frangible-ring pogo, its load-absorbing ability is very predictable and it, of course, can be used repeatedly.

Comprehensive testing would indicate in what areas more weight can be removed from the parts to provide a significant weight reduction. Additionally, the problem of seals and fluids exposed to a space environment would require more detailed testing.

4.3.1 Departure Capability

Figure 5 is a photo of the pressure bottle and pogo parts in exploded form. This bottle is also adaptable to the frangible-ring concept discussed previously.

Theoretically, the pressure bottle adapted to the oleo pogo can fire the test bed to a height in excess of 40 earth feet. As this would represent in excess of 400 lunar feet, this concept merits considerable consideration as a method of achieving launch assist.

4.4 TRIPLE-OLEO OUTRIGGER

Figure 11 shows this concept attached to the test bed with the struts in the extended position.

Most of the impact force is absorbed by the upper piston (oleo). The lower strut is telescopic only -- it provides for the spreading tendency of the feet during alightment. In landings on a surface with a friction coefficient of approximately .3 or more, or where there are obstacles, the feet will retract and not spread.

This concept went through its preliminary tests very successfully. While the weight of this concept equipment is some

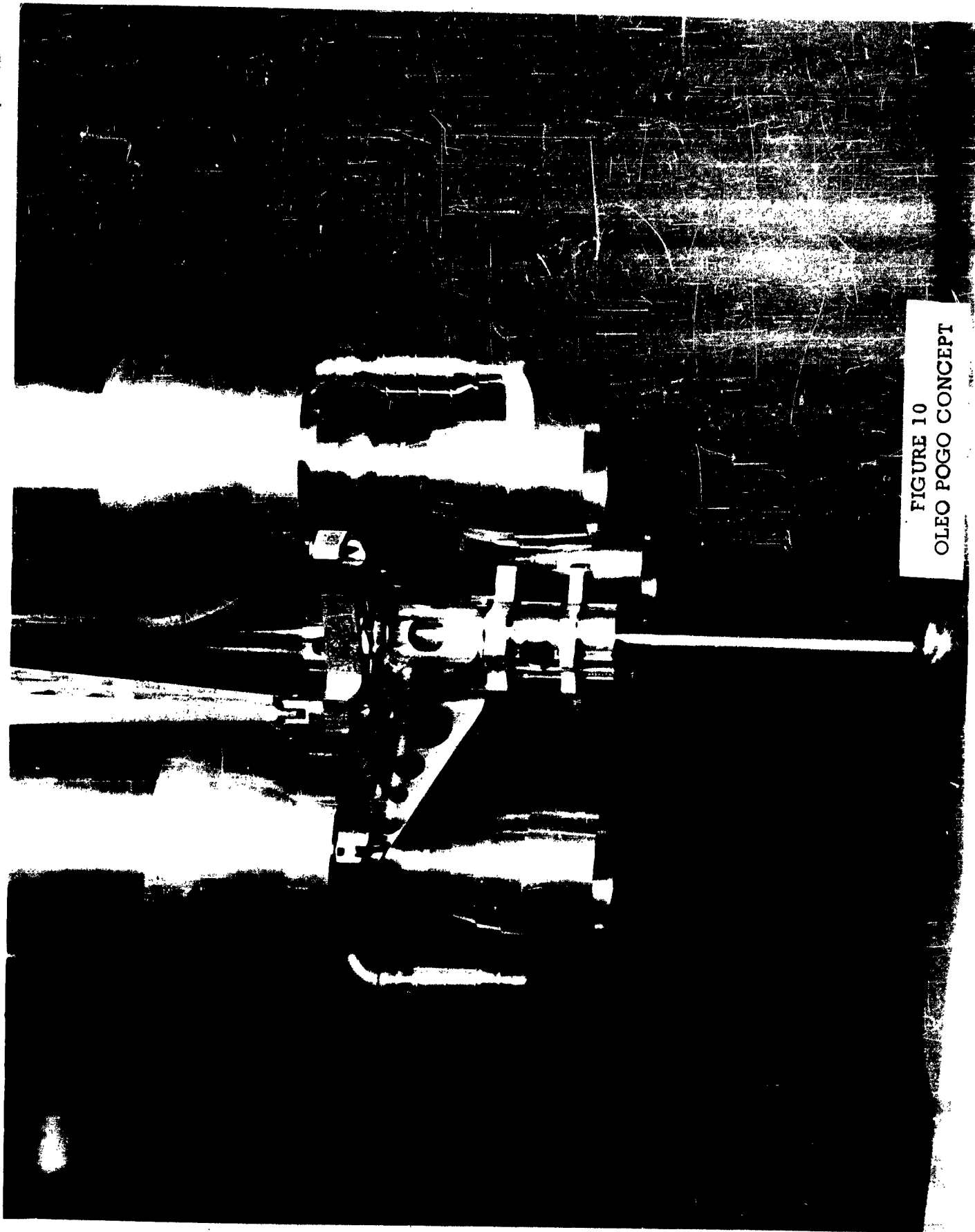


FIGURE 10
OLEO POGO CONCEPT

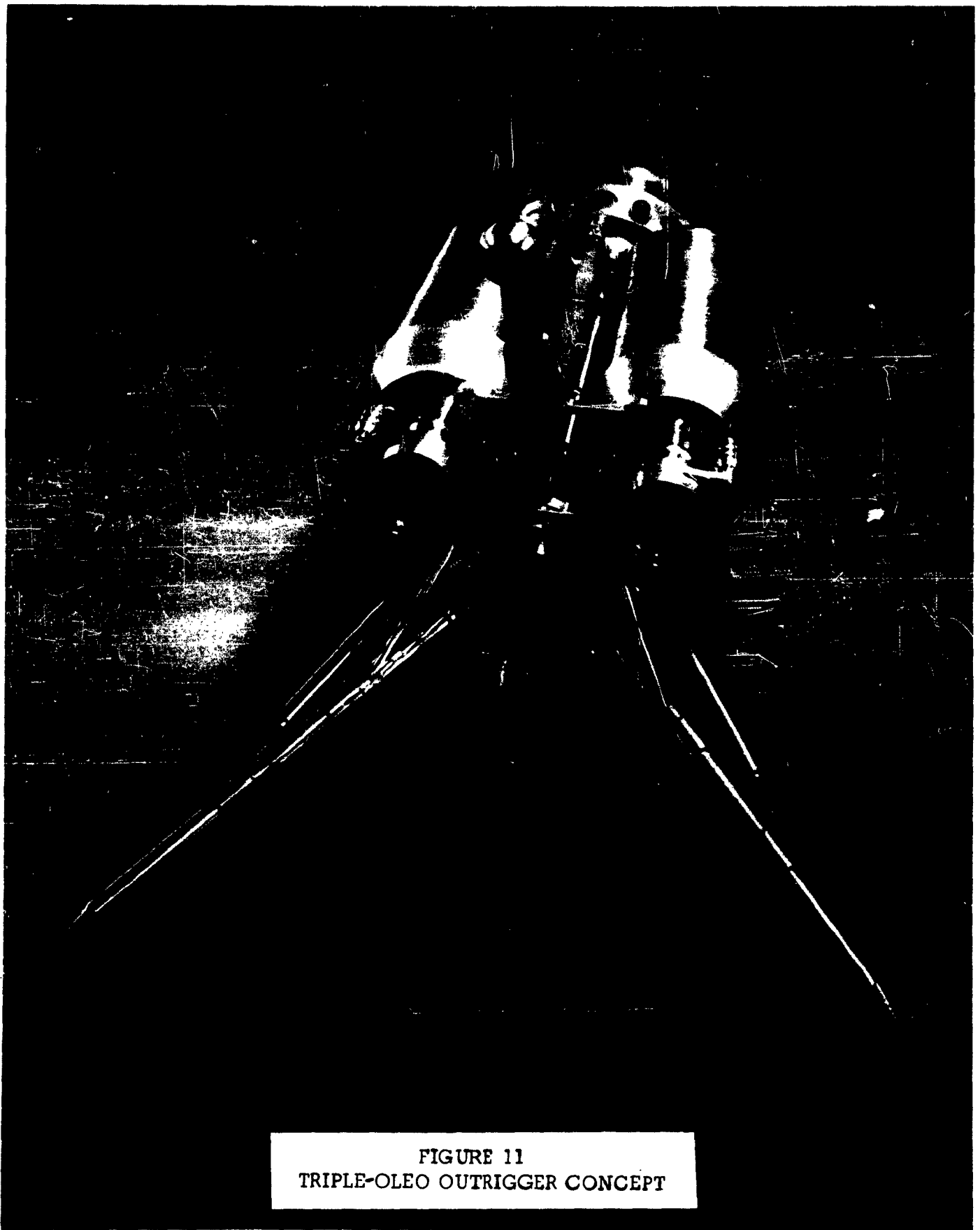


FIGURE 11
TRIPLE-OLEO OUTRIGGER CONCEPT

seven (7)pounds, the greatest of any concept, comprehensive testing should provide methods of reducing this weight to an acceptable percentage of total mass.

4.5 LANDING PADS

To accommodate various lunar surfaces, several alightment pad configurations were formulated. For soft surfaces, stainless steel hemispherical pads of scaled diameters 2", 4", and 6" were designed. For hard surfaces, a point contact was used. The figures provided herein illustrate the various pads.

The bearing pressure of full scale pads will vary from 25 psi minimum (soft dry sand) to several tons per square inch for the point contact (psi scale 1 to 1 for model to full scale).

Obviously, some data will be available on surface conditions long before manned extra-terrestrial alightments are made. Based on telemetered data, the optimum pads can be chosen. In the interim, the test apparatus provided as part of the contract will enable comprehensive drop tests to study surface reactions from the various alightment pads provided.

4.6 CONCEPT MASS RATIOS

The following table gives the mass ratios of concept to total vehicle mass of 75 lbs. Weights and percentages would appear to be reducible, in most cases, through further development.

	<u>Concept</u>	<u>Weight</u>	<u>% of Total</u>
1.	Tri-collapsible outrigger	3 lbs. 10-1/2 oz.	4.9 %
	(a) Collapsible pogo portion	10 oz.	.84%
	(b) Departure capability portion	1 lb. 4-1/2 oz.	1.7 %
2.	Imbedment anchor		
	3 anchors	1 lb. 14 oz.	2.5 %
	6 anchors	3 lb. 7 oz.	4.55%
3.	Oleo Pogo (alightment)	15 oz.	1.25%
	(a) Departure (less fluid)	10-1/2 oz.	.88%
4.	Triple Oleo Outrigger	7 lb. 8 oz.	10.00%

5. STRUCTURAL AND HUMAN FACTOR CONSIDERATIONS

A brief study was conducted during this project to obtain a useful comparison between the effects of shock loads on structures and living payloads in order to establish important parameters which must be considered in the future in designing structures and shock mitigation systems. The material presented in paragraphs 5.1 and 5.2 represents a compilation of contributions by CPI as well as the results of studies made of other organizations.

5.1 STRUCTURAL CONSIDERATIONS

Although the times and forces involved in deceleration during shock mitigation are easily arrived at by the formulas, $F = mV^2/2s$, $F = ma$, etc., the really critical quantities in complex systems are not so readily computed. Failure in a beam or structure sometimes occurs at load values much different from those arrived at by routine calculations.

For example, consider a uniform axial force, quickly applied to a beam of regular cross-section. Classical mechanics tell us that, in the loaded beam the maximum intensity of stress, s , in a fiber y distant from the axis equals $F/A \pm My/J$ psi, where F = end load, A = cross-sectional area of beam, M = max. moment due to bending, and J = moment of inertia of beam.

However, in many structural designs with suddenly applied loads, the problem of interacting shock waves also arises. The basic equation describing particle motion of the beam, as a stress wave, is $v = s/dC$, where

v	=	particle velocity in stress wave
s	=	stress in the fiber
d	=	mass density of material
C	=	velocity of sound in material

This formula describes a compression wave which, on reaching the other end of the beam, reflects back as a tension wave. The total stress at any point in the beam is generally the algebraic sum of the initial compressive stress and the reflected tensile stress. It is interesting to note that the full value of load stress, s , is experienced in tension when the load duration is less

than L/C , where L = beam length. The load-time durations involved with high strength steels such as used in aircraft landing gear, for example, are of the order of .005 sec.

Further, the expression, $v = s/dC$, can be reduced to $v = C\epsilon$, where ϵ = strain produced in the beam material. For high strength steels, $C = 17,000$ ft/sec. and a tolerable $\epsilon = .005$ (tensile strain to yield point neglecting strain-rate effects), $v = 17,000 (.005) = 85$ ft/sec. (particle velocity in stress wave). Experimental values of critical impact velocities, resulting in tensile fracture rather than bending and/or compression, are in the range of 100 to 200 ft/sec.

It is interesting to speculate how a typical shock mitigation system would behave when the deceleration time, t , $< L/C$, or $Ct/L < 1$. (As an orbiting free body, it would move in a discontinuous, or vibrating fashion). In any event, for this reason, the system would be very difficult to analyze mathematically.

The study of a transition of stress-wave motion in a beam or shock mitigation members to a relatively uniform vibration response in its natural modes is most complex. One outstanding simplification, however, can be stated; that is, vibratory response of a structure, mass-spring or distributed-mass, is dependent only on the velocity change of the loading pulse if the duration of loading is less than about $1/4$ the fundamental natural period of the structure. Additionally, the relationship between velocity change (Δv), and relatively slowly applied deceleration, a , sufficient to induce equivalent structural response or stress, is approximately: $a = \omega \Delta v$, where ω is the natural circular frequency of the structure.

For the steel beam, this expression can be reduced to $\Delta v = 2C\epsilon/\pi$ ft/sec.* Estimates of failures caused by instabilities in columns or cylindrical shells, as used in typical aircraft or space vehicle configurations, are close to this value.

When the more severe condition of lateral loading occurs on the beam, experimental results show that $\Delta v = .3C\epsilon$. When loading duration is longer than approximately .8 of the fundamental natural period of the beam, the effects in terms of stress and strain are comparable to those for steady state loading.

* Substituting: $\omega = \frac{\pi C}{2L}$, $a = \frac{\epsilon C^2}{L}$

When one wishes to reproduce shock wave patterns in test models, the ratios (prototype to model) of moduli and densities, as closely as possible, should equal unity; and geometric scaling should be maintained. By so doing *, the same materials can be used in the model and a scaled time history of motions and shock waves can be preserved.

When properly applied, model testing is a valuable tool in deriving optimum configurations of load members having low safety-factors where interaction of stress waves become very complex.

The foregoing data and formulae apply very well to the shock mitigation problems entertained in some of the orbital rendezvous concepts presented by CPI. The shock mitigation problems actually are very similar to those imposed by impulsive accelerations as experienced in orbital maneuvers; however, they occur in the opposite direction.

5.2 HUMAN FACTOR CONSIDERATIONS

While forces and reactions of structural members themselves are relatively difficult to analyze, living payloads pose an equally complex problem. Experiments ** in forces and reactions, made with mice and men and corresponding to those made on structural beams, showed that critical changes in velocity (ΔV) were as follows:

Critical ΔV for man = 80 ft/sec. approx. (causes mild shock)

and

Critical ΔV for mouse = 40 ft/sec. approx. (produces
50% mortality)

The max. deceleration levels corresponding to these critical velocity changes were:

$a = 24$ g's for man, and

$a = 1500$ g's for mouse

* In the lunar model system, made by CPI, the ratios $E/e = 1$ (moduli), and $D/d = .605$ (densities).

1

** Made by Mr. M. Kornhauser of the General Electric Company.

Figures 12, 13, and 14 show velocity change, ΔV , plotted against average acceleration, minimum time, and distance (in each case) for the structural beam, the man, and the mouse. The plots cover the spectrum from the impulsive zone, statically applied loading zone, and intermediate zone (.25 to .8 of the fundamental natural period of the beam). Figure 12 shows a curve for the axially-loaded beam as well as the transversely-loaded beam. Generally, damage occurred when a velocity change and average acceleration combination fell above and to the right of a sensitivity curve (Figure 12). When points fall above each of these curves, damage will occur.

It can be seen that the mouse generally outlasted the man and beam although, in some instances, the man is the strongest. The reason for the living payload's unexpectedly good performance is probably due to the resilience of their bodies, or the relative absence of shock waves caused by impulsive loading. With proper "anti-g" protection (such as liquid-supported devices), man's tolerance can be increased.

An impact of lunar alightment would be hundredths of a second duration. Orbital rendezvous, on the other hand, could impose severe velocity changes and for longer durations during thrust maneuvering and grappling. Maneuvering could impose forces on crew or structure which are within the danger zones as shown in Figures 12 - 13.

Prolonged velocity changes must be avoided, especially in the danger areas. For humans at maximum accelerations, this duration appears to be about 1/10 second, and for transverse structures, about 1/100 second.

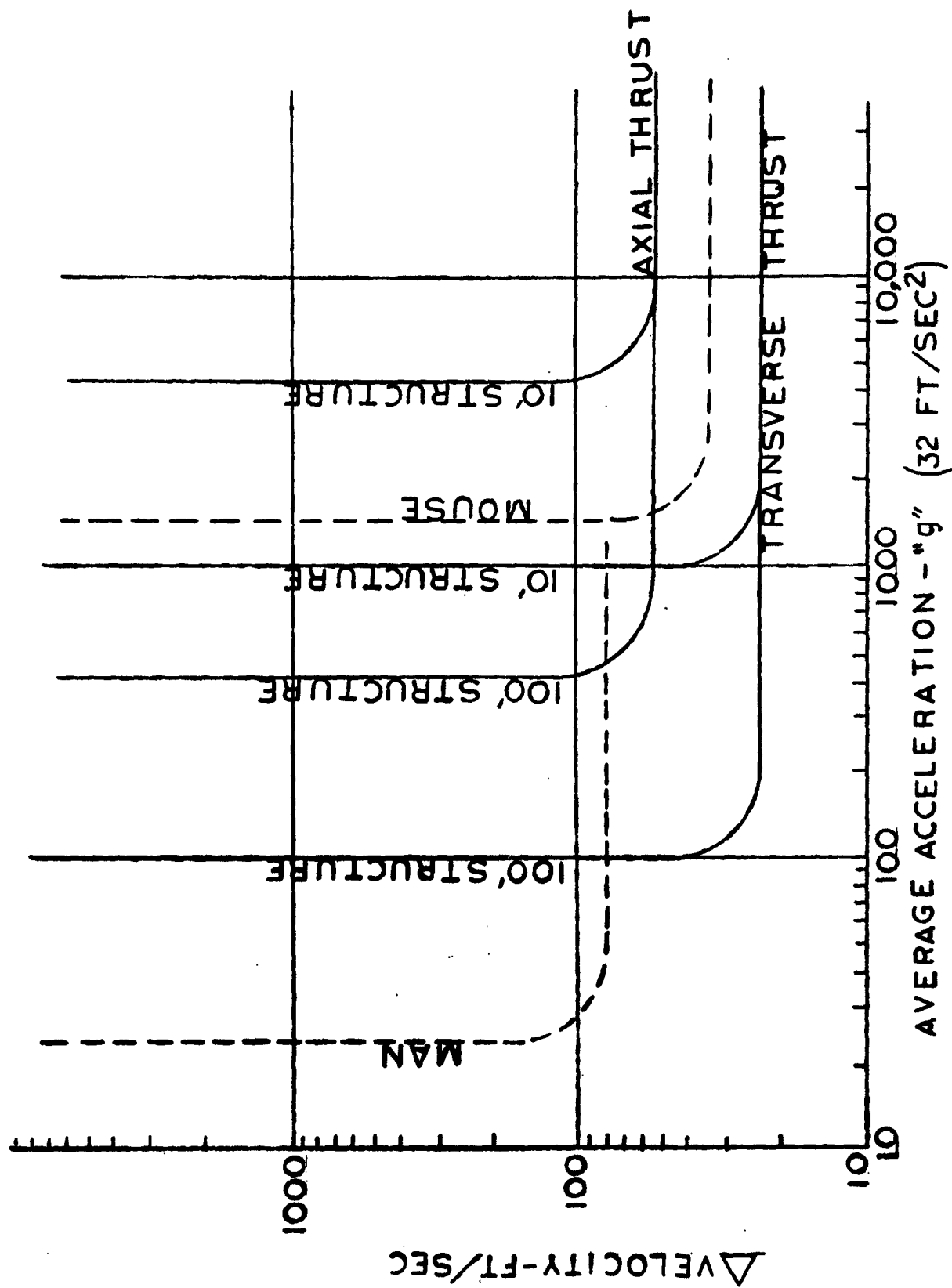


FIGURE 12
IMPACT SENSITIVITIES FOR MICE, MEN, AND STRUCTURES

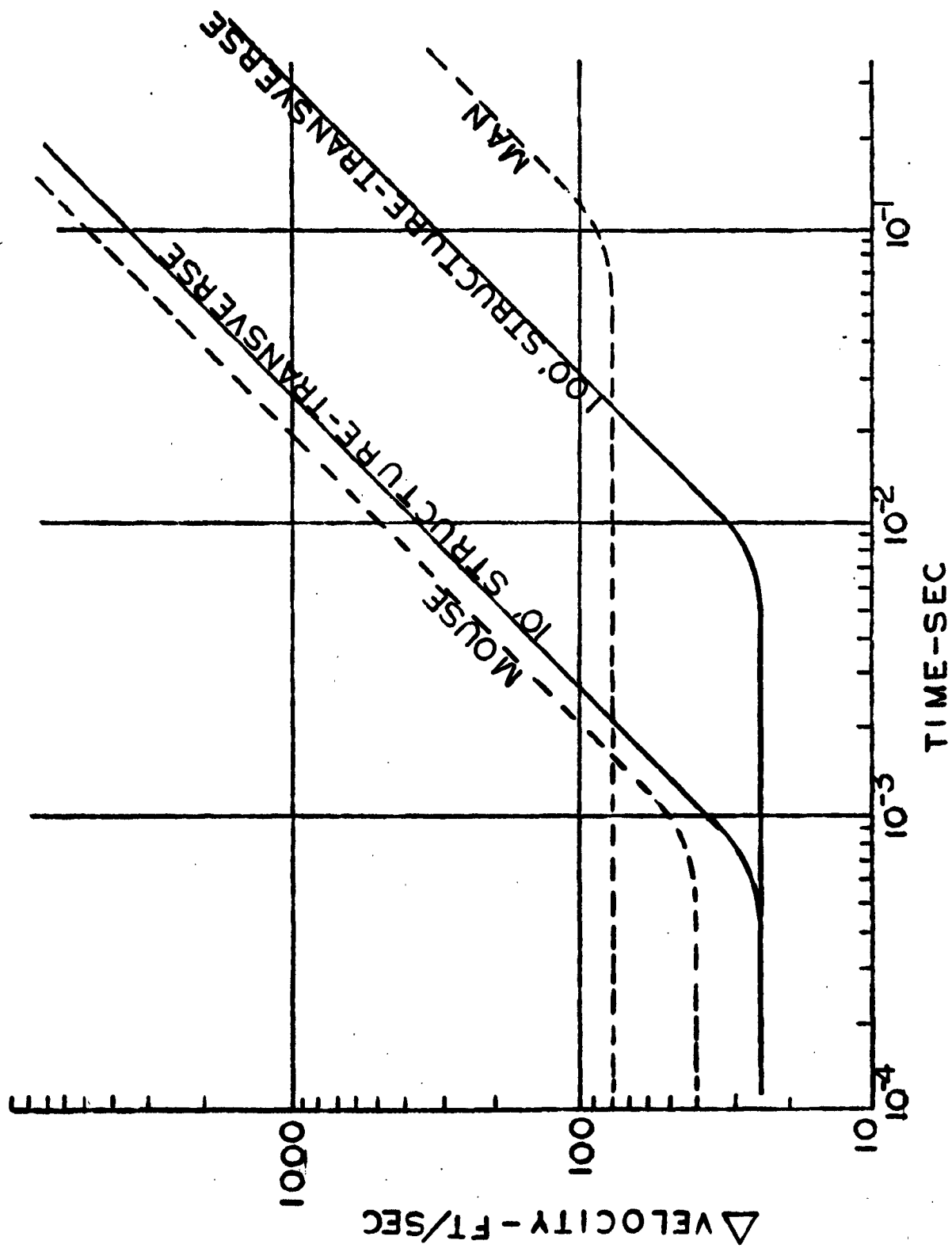


FIGURE 13
MINIMUM TIME vs. VELOCITY CHANGE

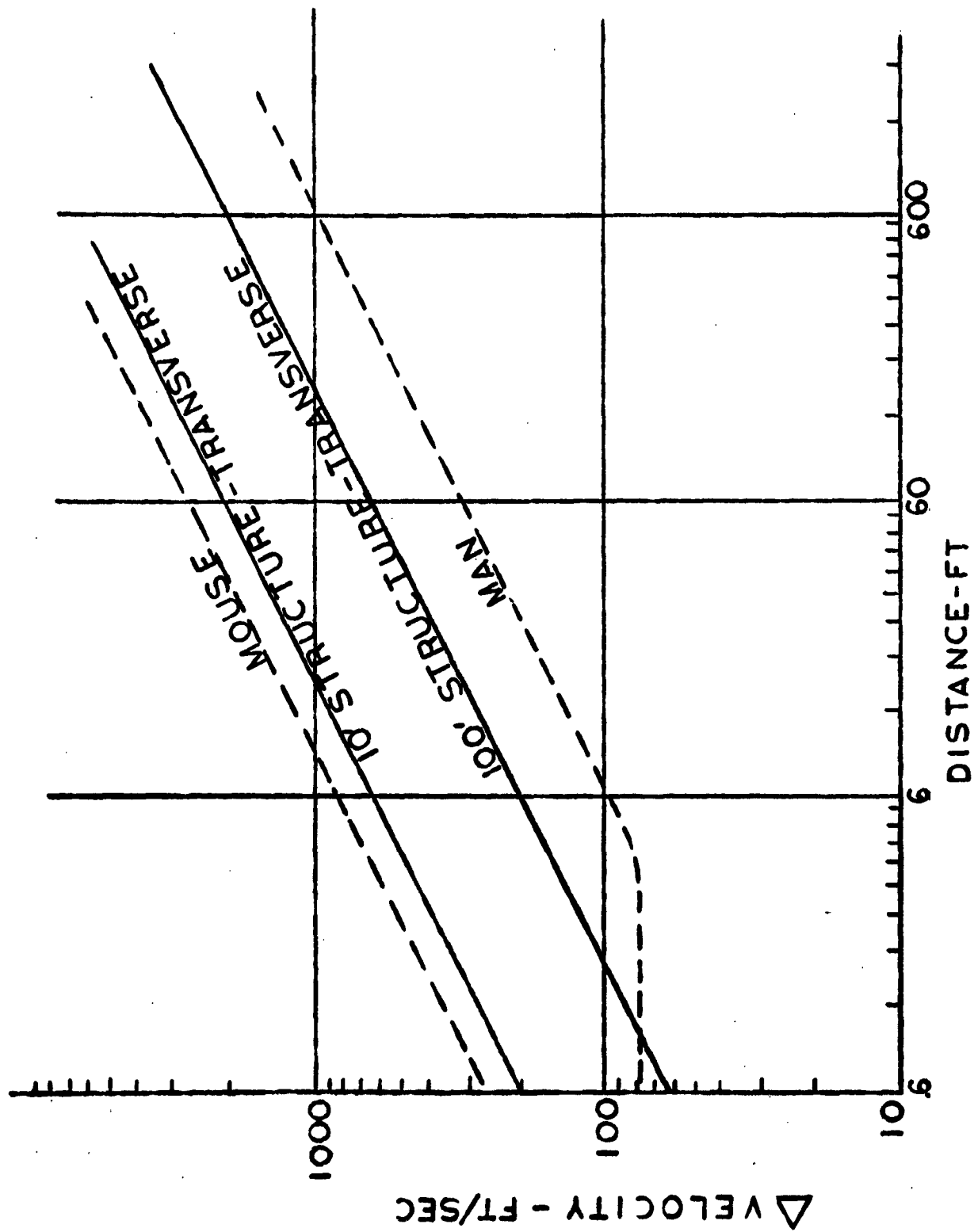


FIGURE 14
MINIMUM DISTANCE vs. VELOCITY CHANGE

6. SPACE ENVIRONMENT EFFECTS ON MATERIALS

As use of any or all the concepts presented depends greatly on available materials, preliminary surveys were made of developments in high-strength materials, effects of thermal shock on high-strength materials, high-energy irradiation of structural materials, thermal and high-energy irradiation of lubricants and fluids, the possibilities for providing thermal protection by metal coatings, and certain vacuum effects.

6.1 HIGH-STRENGTH MATERIALS

Of all structural materials, steels show greater promise of becoming even stronger in the future (by increasing crystal purity and bonds).

High-alloy steels in the 500 ksi tensile range are under development by a number of industrial laboratories. By an elevated temperature-forming process, the Ford Motor Company has produced a material similar to AISI 4340 with tensile and yield strengths in excess of 400 ksi and with elongations of 6%.

Ryan Aeronautical has produced strengths up to 340 kpsi in AM 355 stainless steels by foil rolling to very high reductions. Resulting material, however, had low ductility. Nevertheless, on the basis of accomplishments to date, it is conservative to predict that steels with tensile strengths approaching 500 ksi will be available in five to ten years. They will probably have the following characteristics:

- a. High F_t y/f_t ratio, approaching unity.
- b. Low ductility, less than 5% elongation.
- c. Limited to forms of rolled sheets, as hot or cold working to high reduction is necessary to achieve high strengths.
- d. Elevated temperature strength limited to 700° - 800°F.

Above about 800°F, all known steels rapidly lose their tensile and yield strengths. The only material that can be relied upon for reasonable strength at these levels and higher are refractories; but they, unfortunately, to date, have embrittlement problems when shock loaded.

6.2 THERMAL SHOCK

For shock mitigation structures destined for service in exo-atmospheric operations, thermal-shock problems should not be significantly different from those already being encountered by satellites. High ductility in a material seems to be the most effective characteristic for countering thermal shock short of controlling the thermal shock itself -- by shielding, thermal re-radiation, heat sinks, thermal cycling, etc.

The minimum temperatures to be encountered may prove even more serious than the maximum temperatures. All steels and most non-ferrous metals experience marked embrittlement at the low temperatures (-150° to -300°F). Mechanical shock resistance at these low extremes decreases by several orders of magnitude in high-strength steels and certain brass alloys. The solution to the thermal shock problem may be more readily achieved by controlling the temperature spread rather than mitigating the effects of temperature extremes.

6.3 RADIATION EFFECTS

Few definite conclusions have been reached regarding specific radiation effects on structural materials. The subject is extremely complex, as radiation effects are dependent upon many variables, among which are:

- a. Chemical content of the material.
- b. Crystal structure, degree of cold work, internal stresses, and prior thermal and mechanical history of the material.
- c. Temperature at which radiation occurs.
- d. Precise intensity, wave frequency, and duration of the radiation.

Some generalizations can be made, however:

- a. Metals and alloys are generally more resistant to radiation damage than other materials.
- b. Iron, Carbon Steels, Molybdenum, and

Tungsten (body-centered cubic structure) have shown tendency to embrittlement and low impact strength after neutron irradiation.

- c. **Face-centered cubic structures suffer ductility losses, but do not become excessively brittle.**
- d. **Density may decrease.**
- e. **Dimensional changes can occur in metals with preferred grain orientation or lattice anisotropy.**
- f. **Generally, mechanical strength can be expected to increase while ductility decreases. These effects decrease with the amount of prior cold work or residual stress.**

6.4 LUBRICANTS

As yet, no fluid lubricants or greases are known to be usable in vacuums at -50° to 200°F with temperature extremes of -200°F to 500°F . A material having fluid characteristics at -50°F will probably exert a high vapor pressure at 500°F and consequently evaporate quite rapidly. However, fluids and greases are available which can meet these thermal conditions if they are adequately sealed to prevent vapor loss. One example of this type is: General Electric Silicone Oil SF-1000.

Another solution to this problem may be use of dry or solid film lubricants. An advantage of solid film lubricants is their independence of effects of temperature up to the decomposition point. No replacement of the lubricant would be required during operational life of the bearing surface.

Under nuclear radiation, the binder and base material of dry lubricants often show higher resistance to radiation dosage than do organic fluids or greases.

One of the best dry-types of lubricants found to date is that under development by the Naval Air Material Center. It provides a film composed of molybdenum disulfide and graphite with a sodium silicate binder. It is reported that same is stable from -300°F to 750°F to 240 hours running time. This film has demonstrated, in

thermal stability tests, that it outlasts the best military grease developed for high temperature use. Additionally, after exposure to gamma radiation of 5×10^7 roentgens, it still had satisfactory bearing characteristics.

6.5 FLUIDS

Virtually all mineral-based and synthetic oils are reasonably stable up to approximately 10^7 roentgens of high energy and corpuscular radiation. Exposure to 10^8 roentgens produces appreciable lubricant degradation by an:

- a. increase of viscosity, acidity, vapor pressure, foaming, metal corrosivity, and coking.
- b. decrease of flash point, auto-ignition temperature and lubricity.

Trends in radiation-resistant lubricant development indicate that a compromise in physical properties of lubricants may be necessary. Therefore, in advanced mechanical design for systems facing adverse environments, lubricants of any kind should be used only where absolutely necessary.

6.6 METAL COATINGS

Up through the infra-red spectrum, sprayed gold metal coatings on base materials can offer significant thermal protection to structures. The following table shows the reflectance (R) and transmittance (T) values for gold coatings.

Wave Length	Ultra Violet	Visible Spectrum						Near Infra-Red	Infra-Red
		Violet	Blue	Green	Yellow	Orange	Red		
Milli-microns		400-450	450-490	490-575	575-590	590-650	650-750	750-1000	1000-4600
% T	0.9-0.5	0.3	0.4	0.4	0.3	0.2	0.2	0.0-0.2	0.0-2.0
% R		39-42	42-46	46-61	61-63	63-70	70-80	80-95	90-103

The above values given for transmittance are relative to air. The reflectance values in the visible and near infra-red regions are relative to magnesium carbonate. In the infra-red wave lengths, reflectance values are relative to aluminum metal. The emissivity of the gold coating remains at 0.08 or lower, even when the base metal is as high as 1500°F. Emissivity values are obtained by using a black body of standard emissivity 1.0.

Gold coatings unfortunately possess poor abrasion and erosion resistance. Normal coatings of thicknesses of 0.000,005 in., therefore, prove unsatisfactory for thermal protection from hot exhaust gas impingement. However, vacuum deposited coats of silicon monoxide over the gold coating do provide needed protection from erosion while not affecting the reflectance of the gold under-coating.

For structures located near rocket engines, gold and silicon monoxide coatings appear very attractive for protection against the intense thermal radiation and hot exhaust gas impingement.

6.7 VACUUM EFFECTS

The lighter metals -- mag-lithium and magnesium, and even aluminum -- have a tendency to sublime in a vacuum. For extended exposure, this phenomenon could become serious for structures having thin walls. The heavier metals and certain plastics, however, have shown no tendency toward vacuum sublimation. If this does, in fact, become a problem with lighter metals, then coating them with heavier materials would be a solution to the sublimation problem.

Another, and possibly more serious, vacuum effect involves that of welding. When two like metals or similar type metals are in intimate contact in a vacuum, there is a tendency for them to weld together at any temperature due to the absence of air or foreign matter between them. This phenomenon can even occur on earth; however, it is rare because of the pervading atmosphere, lubrication present, and constant contamination. Dry-film type lubricants may be necessary between all contacting metallic surfaces when used in vacuums.

7. ADDITIONAL PROJECT PHASES

7.1 TEST APPARATUS

As a requirement of this project, CPI was to furnish adequate apparatus to test the basic design integrity of the concepts modeled. As the project developed, this equipment was defined as a drop platform with drop capability from heights up to 17 feet, and tether equipment to permit snatching the test bed model for departure maneuvers.

The basic apparatus constructed includes a platform 8 ft. square with the surface variable within 15° and providing varying consistency of surface for impact testing, a tethering cable and clamps, and a cable brake. These items are illustrated in Figures 15 and 16.

7.2 STAFF FILM

Lunar-time-scaled motion picture film was taken which depicts motions as they would actually be seen on the lunar surface. All maneuvers within the modeled concept's capabilities were recorded on film and have been arranged in logical sequence.

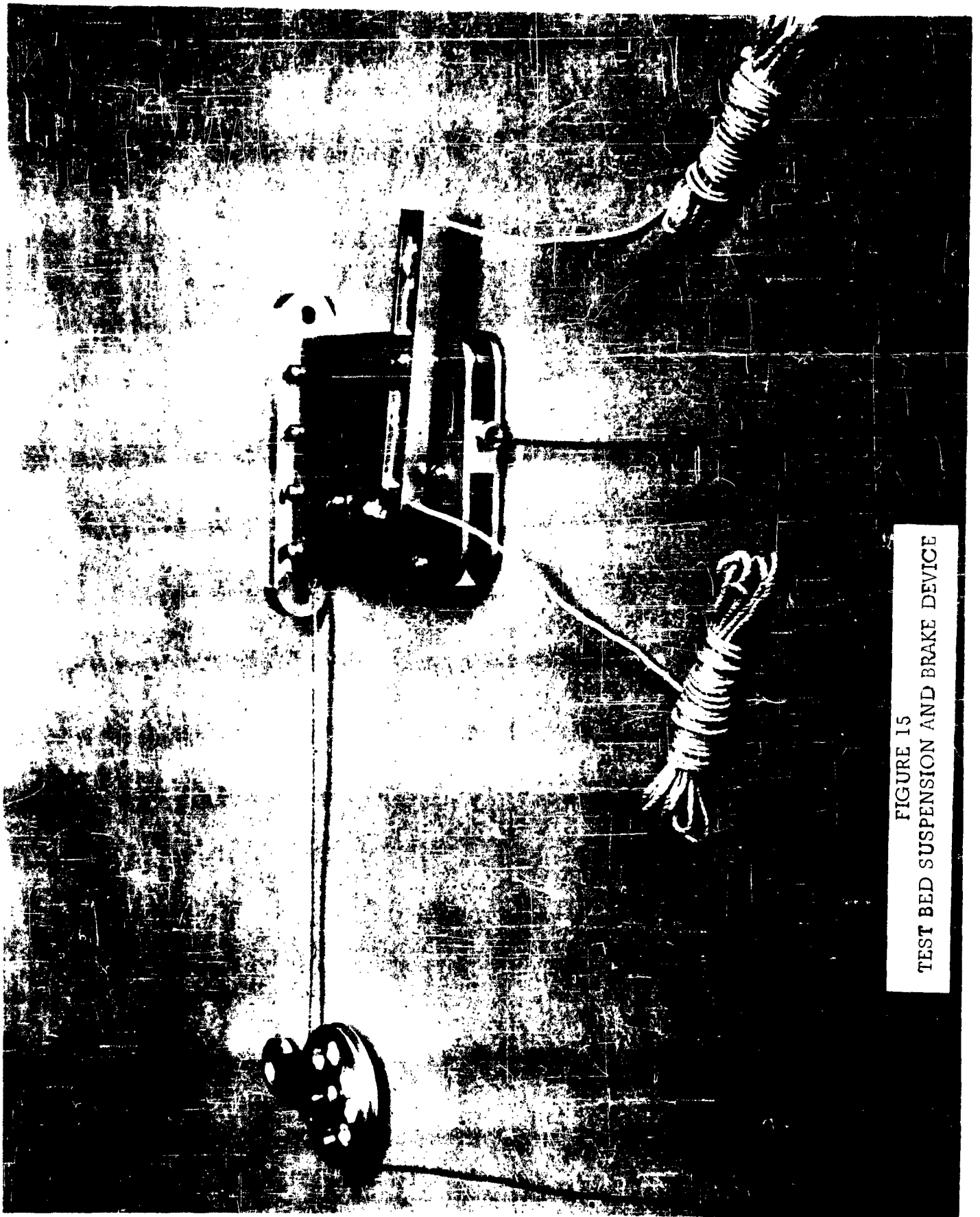


FIGURE 15
TEST BED SUSPENSION AND BRAKE DEVICE

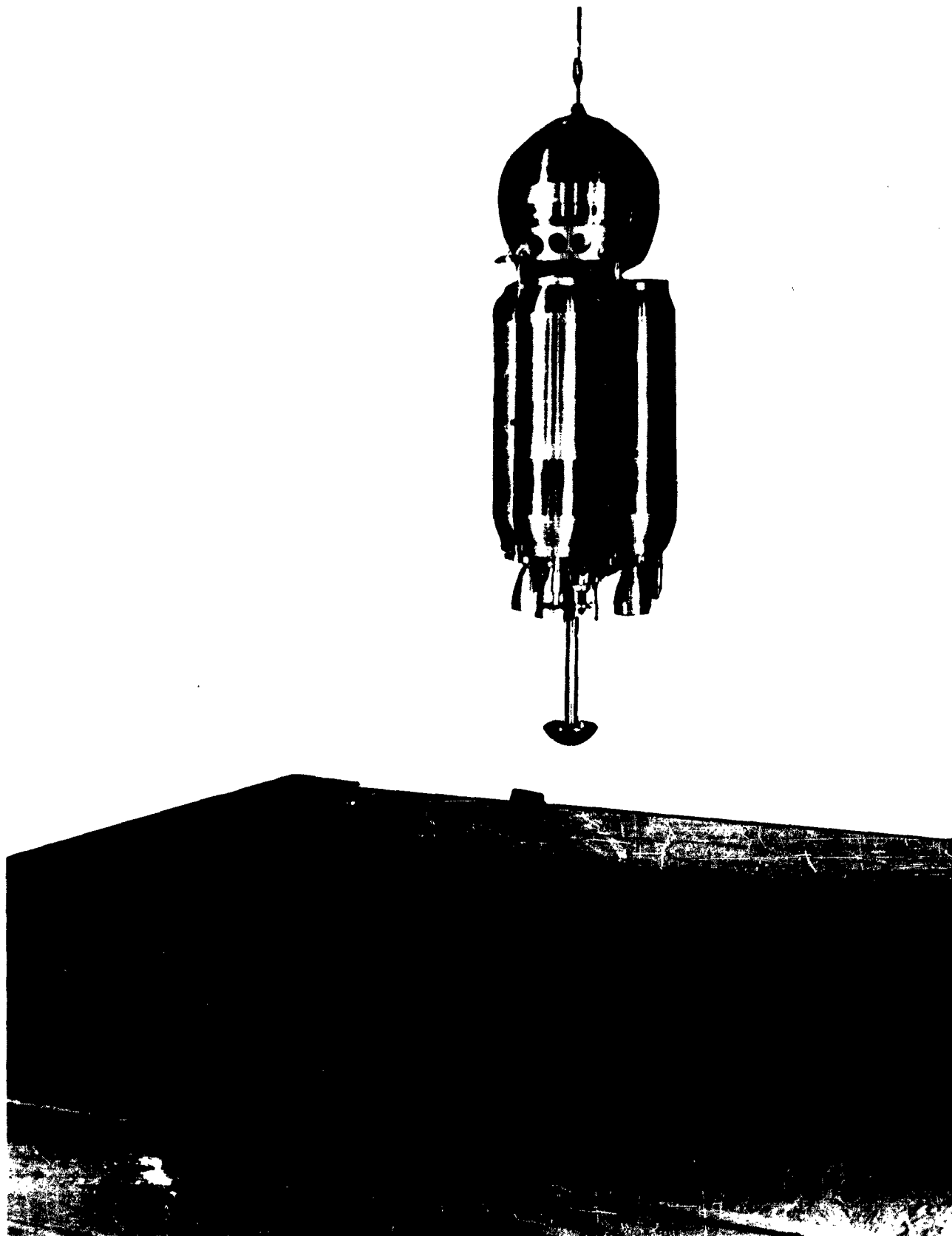


FIGURE 16
ADJUSTABLE DROP PLATFORM WITH TEST BED SUSPENDED ABOVE

8. CONCLUSIONS AND RECOMMENDATIONS

During the conduct of this project, it was concluded to be essential that appropriate attention be devoted to the development of shock mitigation equipment in order that it parallel work of all other aspects of advanced flight vehicles. This is essential in order to most efficiently derive the total vehicle system.

The type of shock mitigation equipment must receive early consideration in the design of the total vehicle, as for each type of vehicle and mission there appears to be an optimum shock mitigating system.

The program recently concluded establishes that the optimum shock mitigation system depends upon a variety of factors:

- a. Basic vehicle configuration, including center of gravity.
- b. Mass distribution of the vehicle.
- c. Allowable mass to be devoted to shock mitigation and requirements for repeatability.
- d. Landing dynamics and the surface characteristics to be encountered for the landing.

The concluded study has also demonstrated that mass ratios for shock mitigation equipment versus the overall mass of the vehicle can be derived based on analytical studies and testing with dynamic models.

8.1 ADDITIONAL STUDY INDICATED

As a result of this program, various new or extrapolated shock mitigation and stabilization concepts presented therein appear to offer promise and merit detailed examination for possible use in advanced flight-vehicle application. Specific concepts would include:

- a. The single strut pogo-type systems for use on irregular surfaces.
- b. The imbedment anchor stabilization concept for use with single strut systems on unprepared, irregular, and uncertain surfaces.

- c. The frangible ring method of one-time energy absorption.
- d. The gas-squib departure assist technique.
- e. Modified versions of conventional air-oil struts for exo-atmospheric use.

In addition, further study and research by cognizant agencies are essential with regard to the solid materials and fluids to be utilized in advanced vehicles and the effects thereon as imposed by the environment of extremely high altitude flight and operations on or near extra-terrestrial bodies.

8.2 TESTING MEDIA

As a further recommendation resulting from this study, CPI submits that evaluation models, dynamically-scaled in those areas requiring study, should be utilized wherever possible in addition to conventional analytical techniques, particularly with regard to flight problems associated with reduced gravitational fields. The results of utilization of such techniques will provide the basis for a framework from which the optimum of shock mitigation equipment can be selected for any type of vehicle based on the vehicle's required performance and mission criteria.

APPENDIX

This Appendix contains, in pictorial form, the concepts as they were initially submitted during the course of the project. They are divided into classes I, II, and III respectively, as pertaining to maneuvers performed at earth, in earth orbits, and on the lunar surface, and are numbered E-1, E-2; O-1, O-2; L-1, L-2, etc. The illustrations are intended to convey overall concepts and do not necessarily adhere to strict proportion or optimum design. Those concepts whose features were selected for further model study are indicated by "+". Although major refinements were made with many of the other concepts, they do not appear except in original form in order to avoid an excessively long report.

Class I	Earth Concepts (14 figures - 9 concepts)
Class II	Orbital Concepts (19 figures - 16 concepts)
Class III	Lunar Concepts (30 figures - 23 concepts)

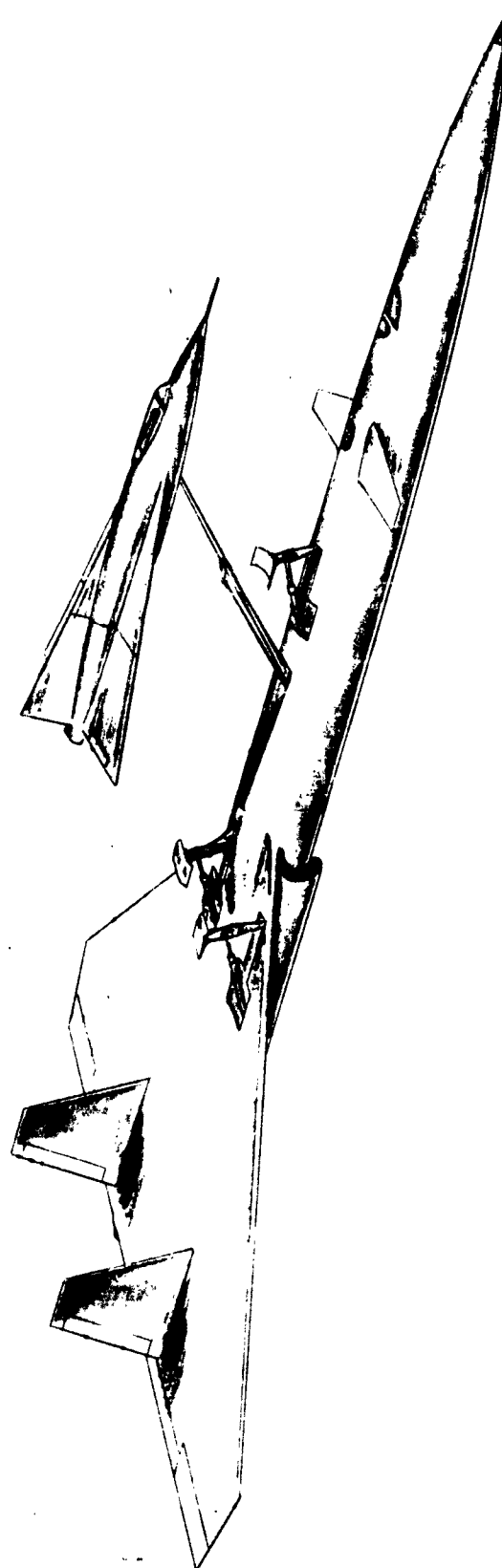


FIGURE 17
CONCEPT E-1 (DEPARTURE)
CONCEPT E-2 (RENDEZVOUS)
ORBITAL GLIDE VEHICLE AND SUPERSONIC CARRIER

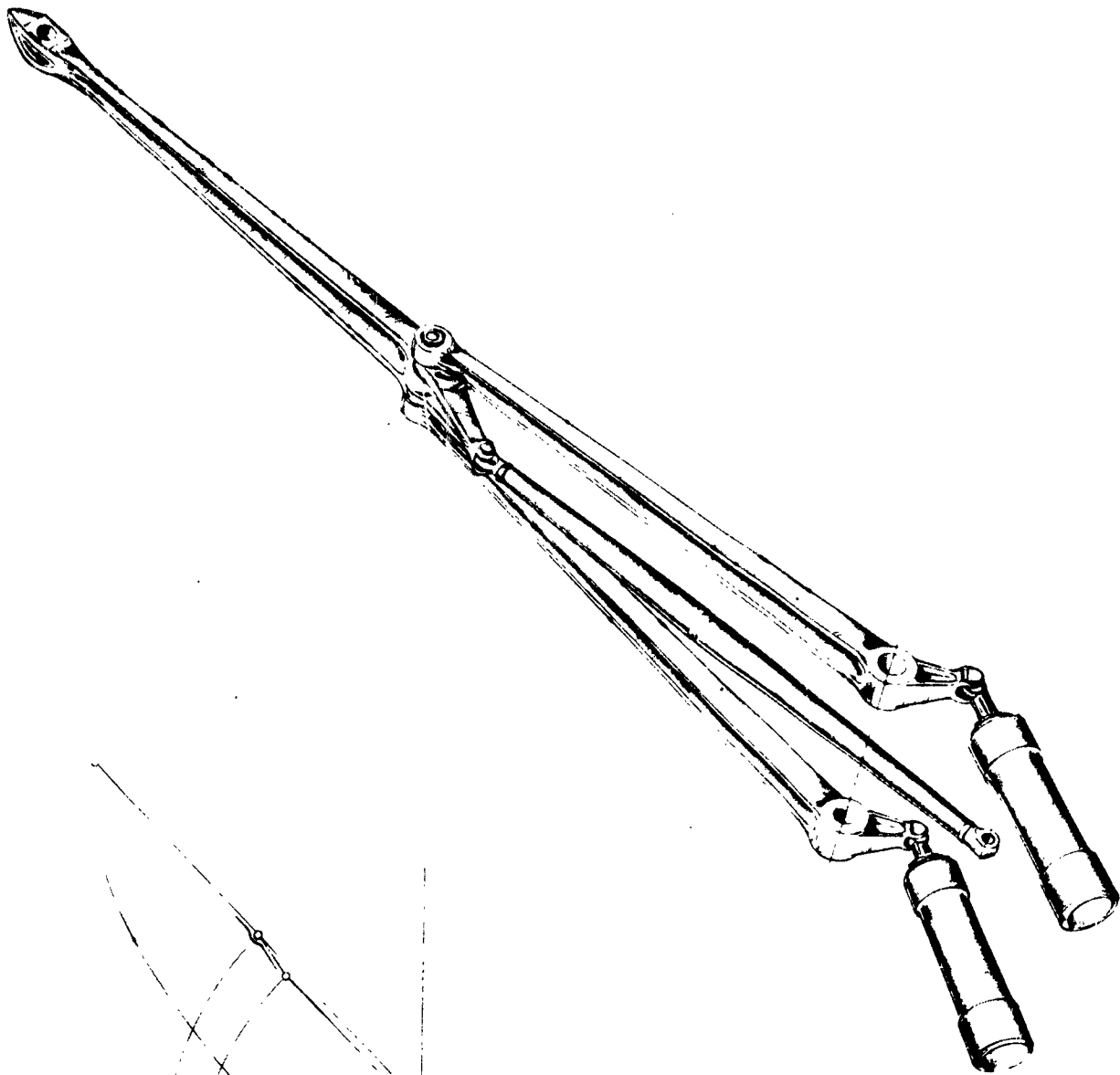


FIGURE 18
ATTACHING BOOM FOR TACTICAL VEHICLE FOR CONCEPT E-1 AND E-2

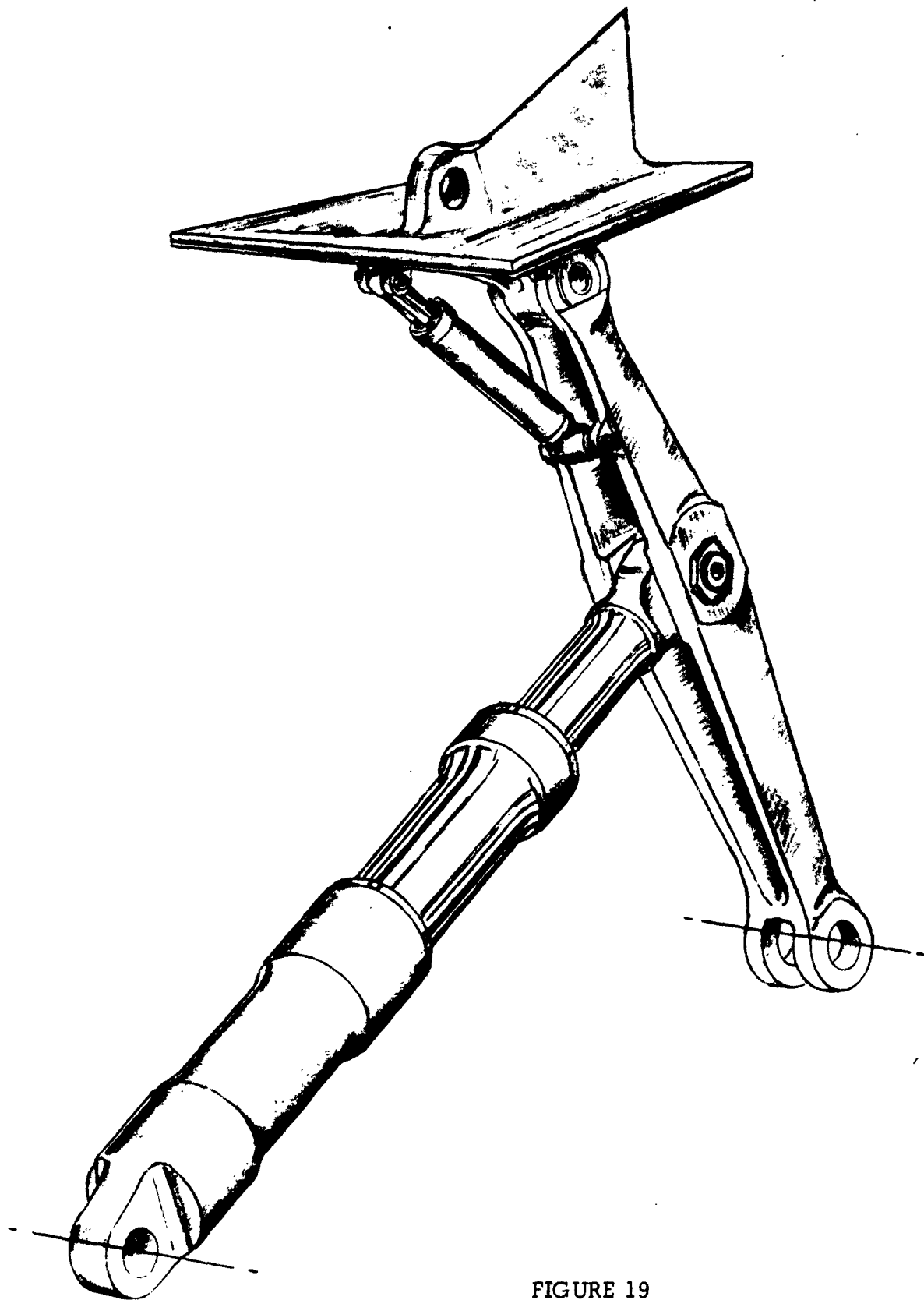
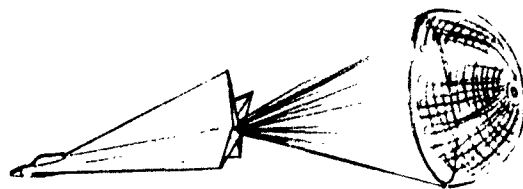
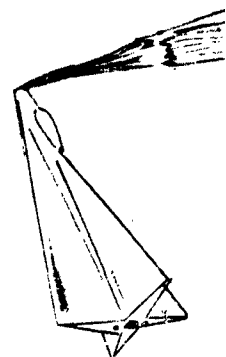


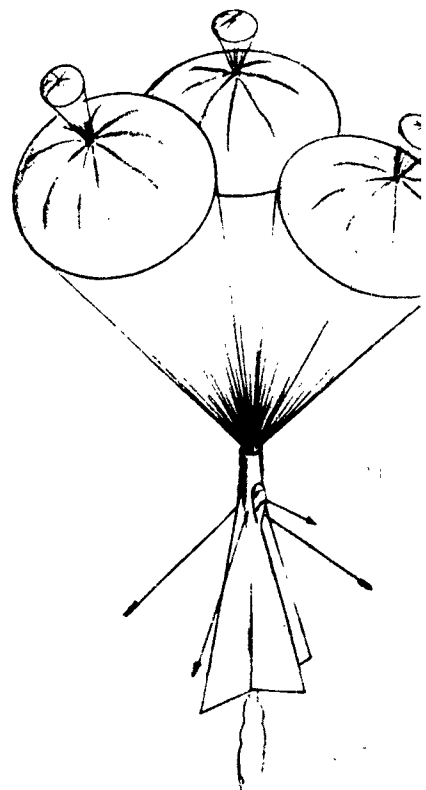
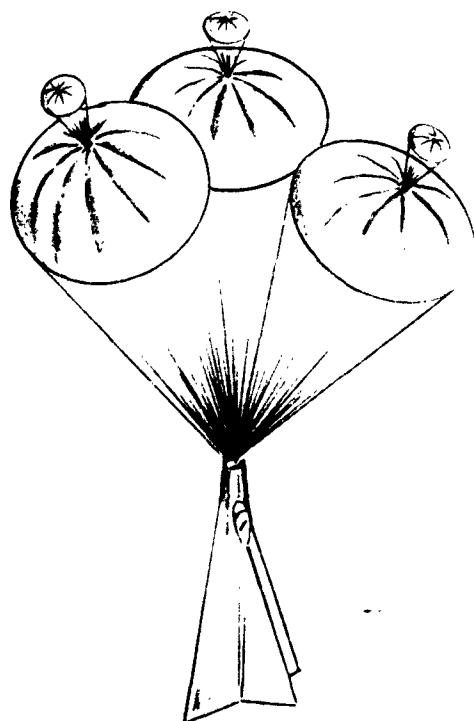
FIGURE 19
PYLON POD FOR TACTICAL VEHICLE FOR CONCEPTS E-1 AND E-2



VEHICLE DESCENDS TO LOW ALTITUDE AND DECELERATES
TO LOW SUBSONIC SPEED BY STEEL RIBBON CHUTE

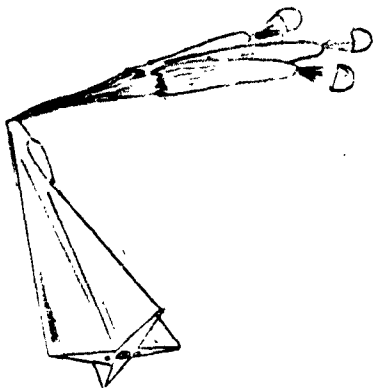


CONVENTIONAL PARACHUTE
POPPED AT 5,000 TO 10,000 FEET

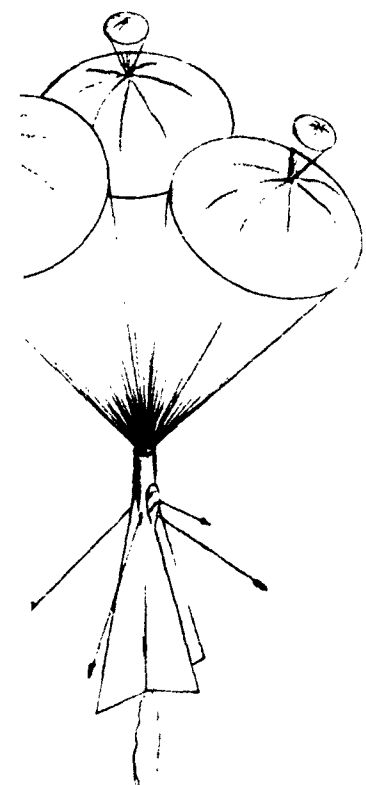
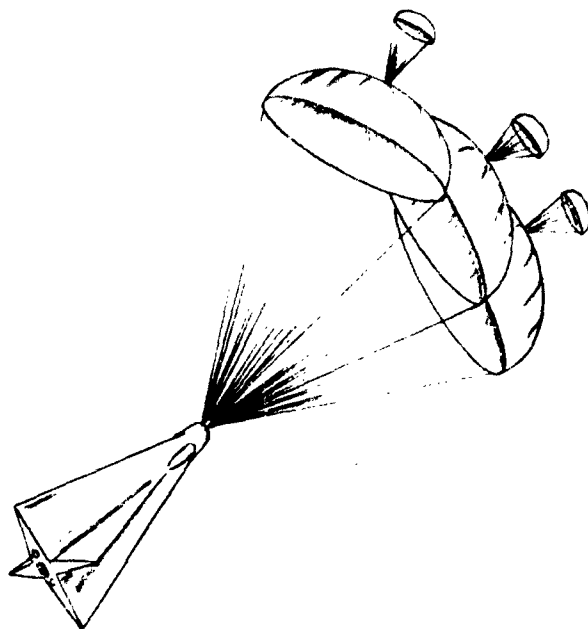


1

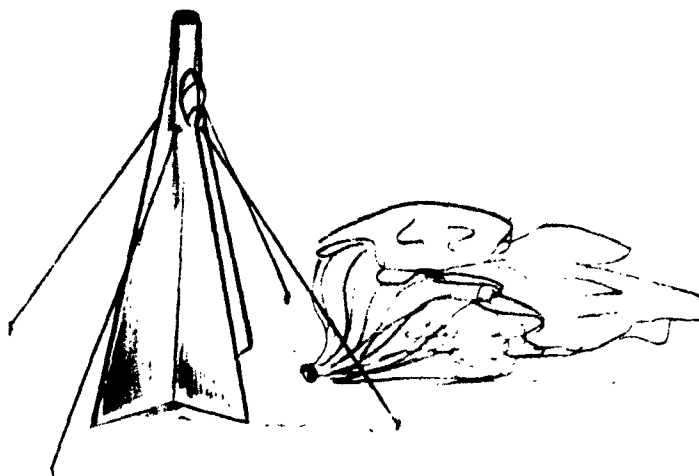
STABILIZING ANCHORS FIRED AT THE TIME OF DEPLOYMENT



CONVENTIONAL PARACHUTE CLUSTER
 OPENED AT 5,000 TO 10,000 FEET



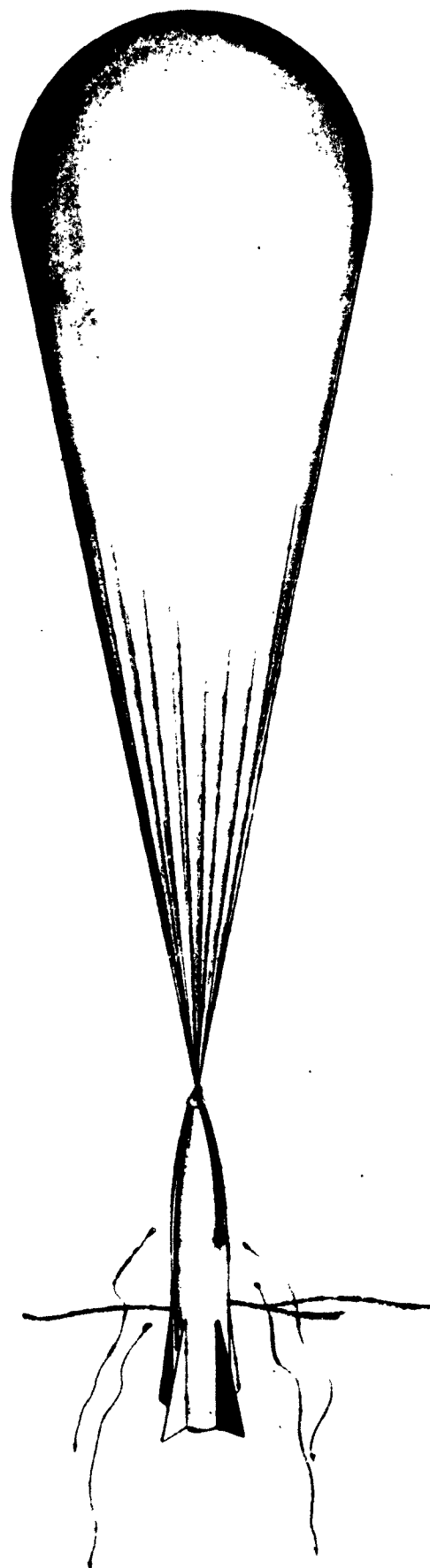
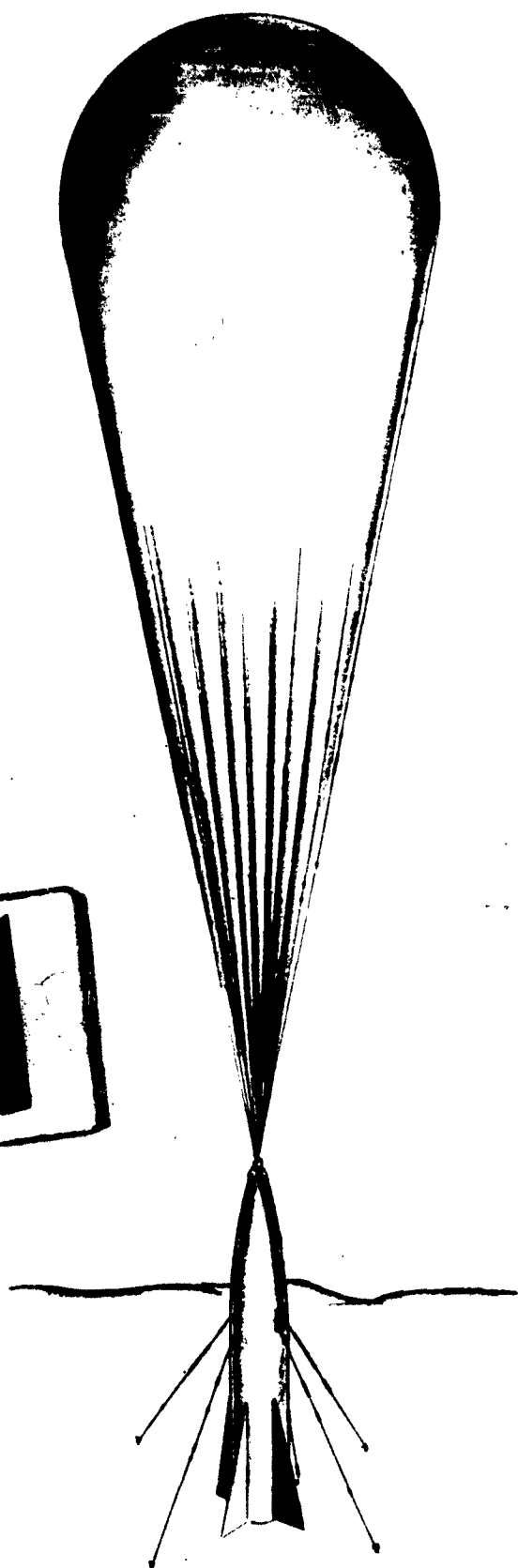
CHORS FIRED AT TOUCHDOWN

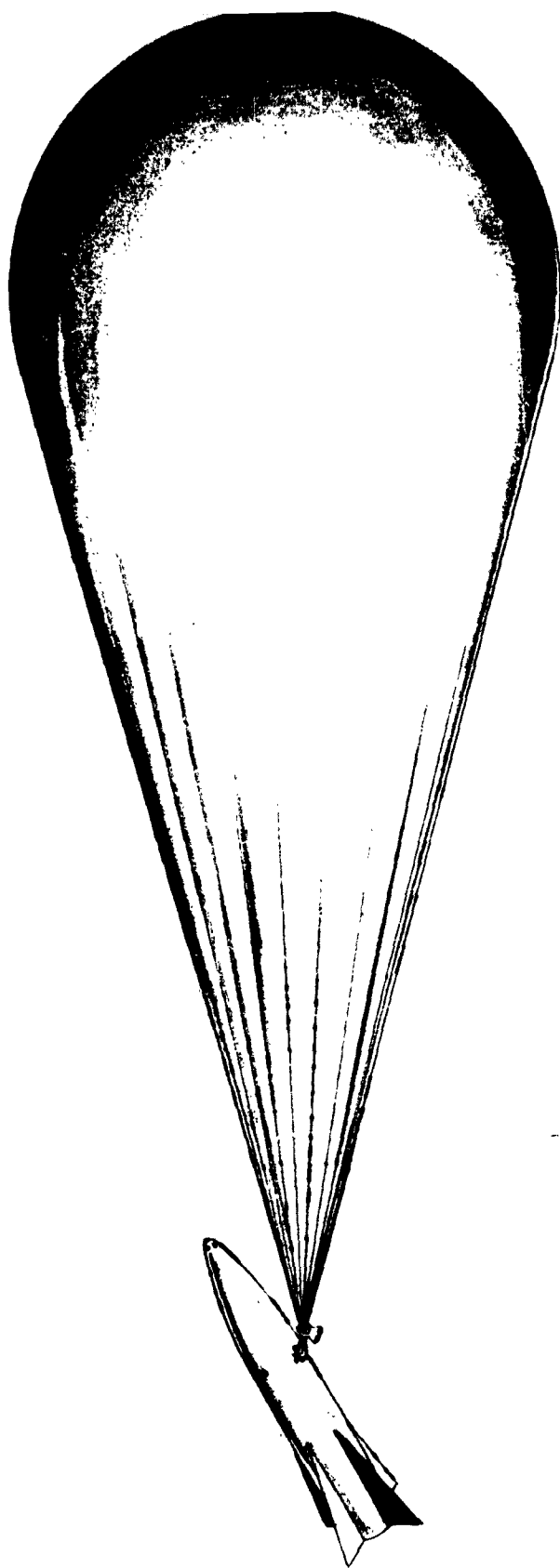


2

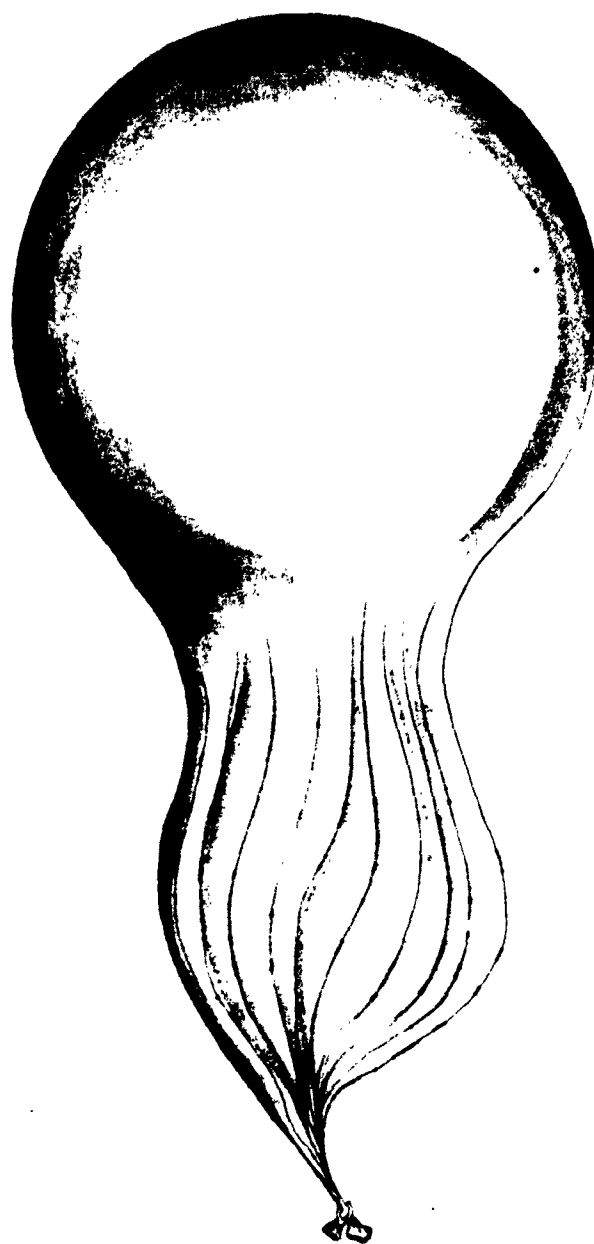
FIGURE 20
 CONCEPT E-3
 PARACHUTE ALIGHTMENT

1





SLOW VERTICAL ASCENT



ROCKET MOTORS FIRED AT 70,000
TO 100,000 - ABOVE MOST OF
ATMOSPHERE

2

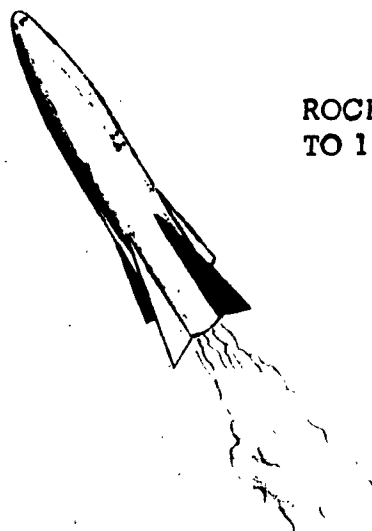
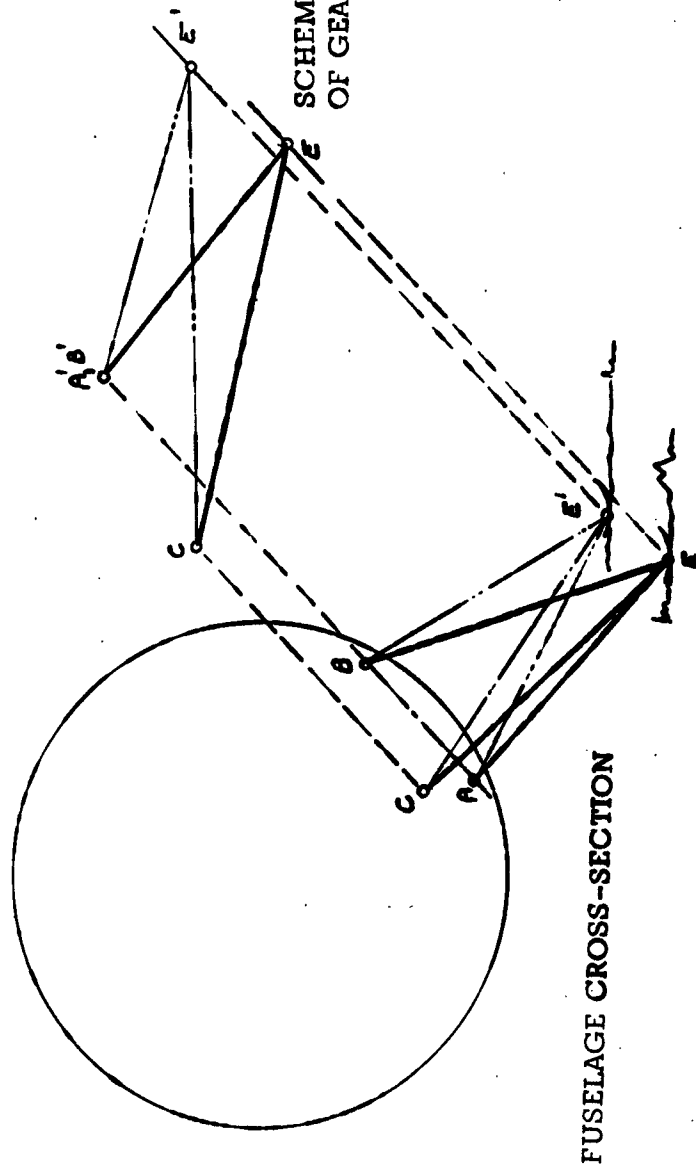
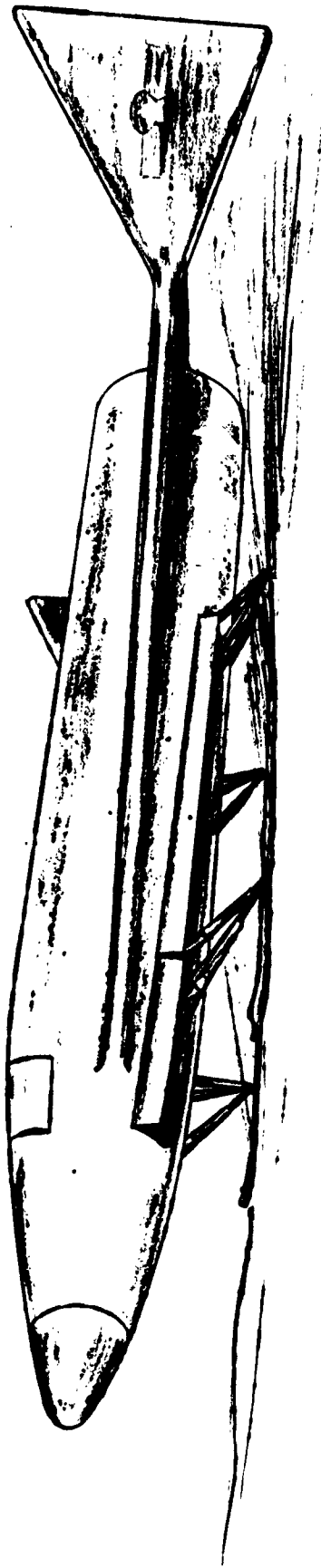


FIGURE 21
CONCEPT E-4
BALLOON DEPARTURE



FIGURE 22
CONCEPT E-5
SINGLE SKI ALIGNMENT ON PREPARED SITE



SCHEMATIC OF SIDE PROJECTION
OF GEAR SHOWING DEFLECTION

FUSELAGE CROSS-SECTION

FIGURE 23
CONCEPT E-6
CONVENTIONAL SKI ALIGNMENT ON PREPARED SITE

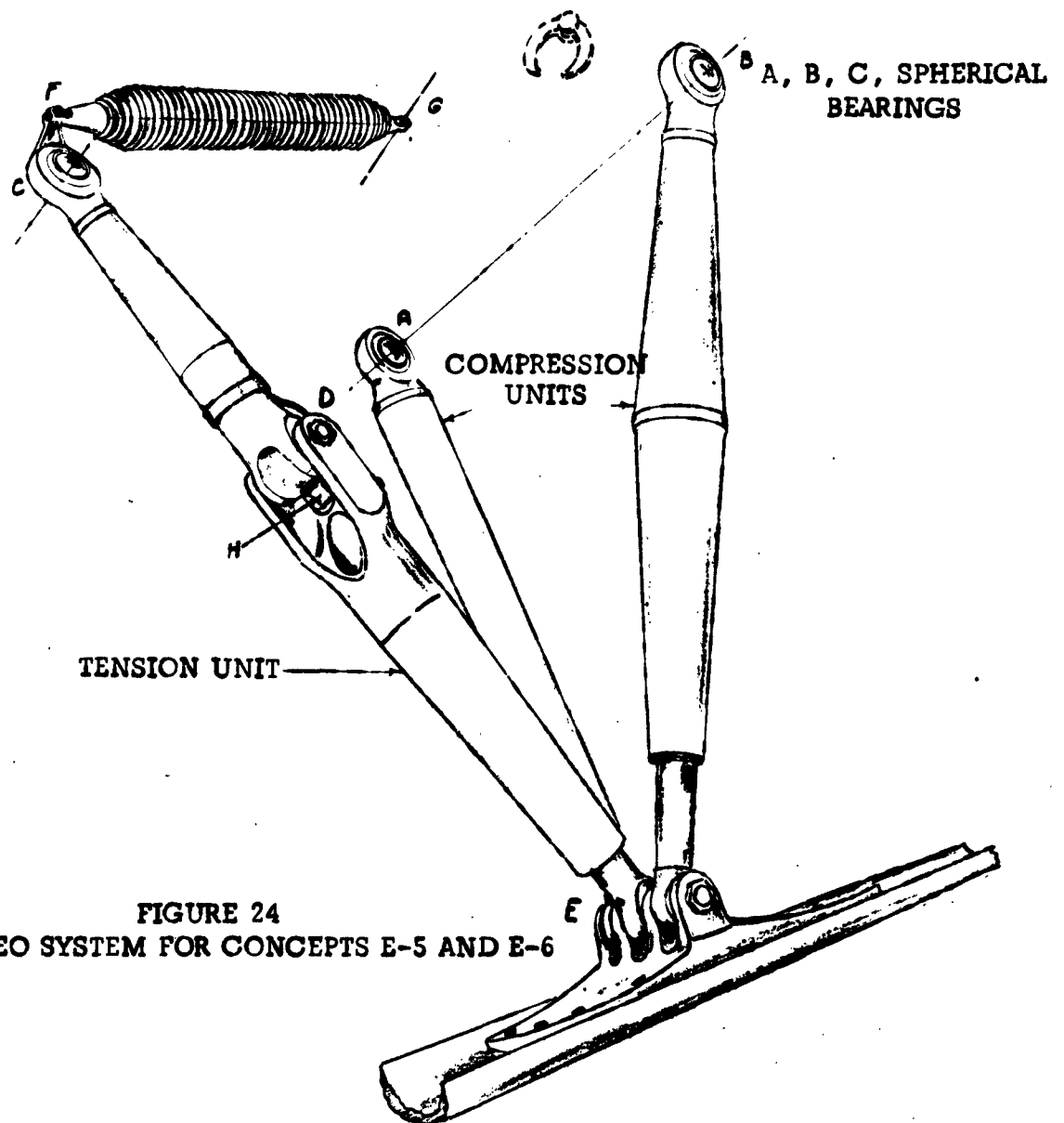
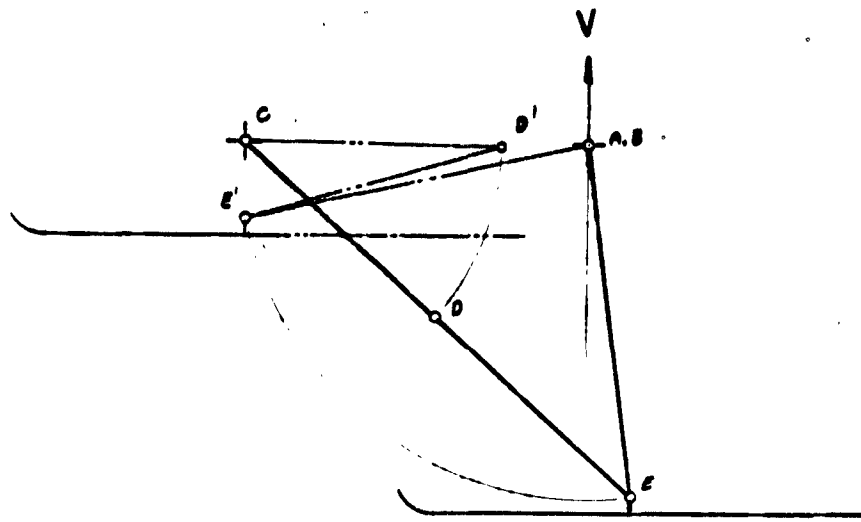
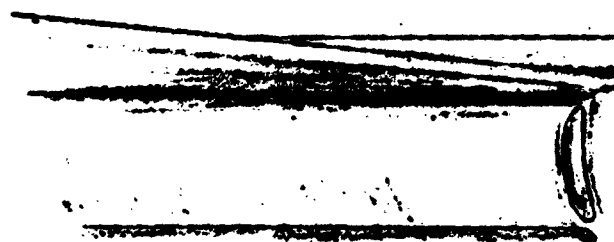
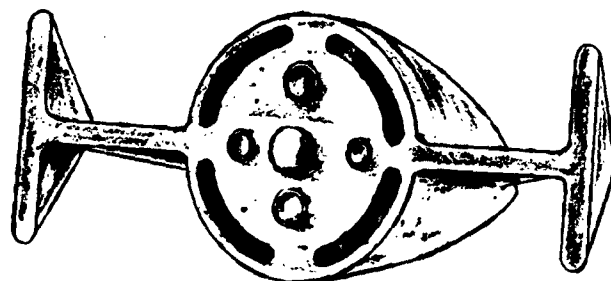
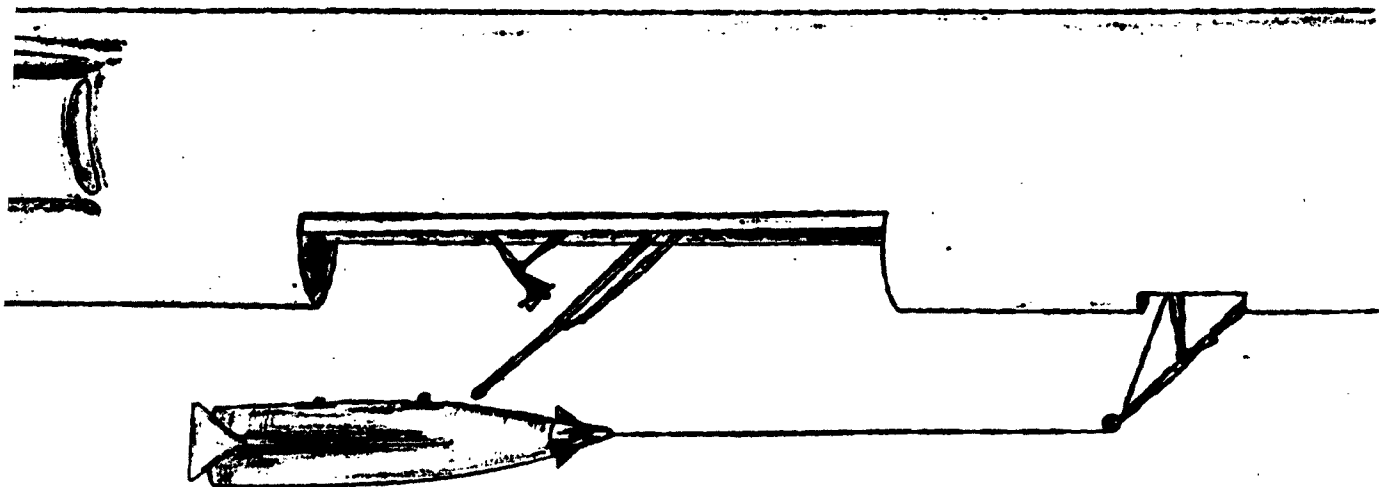


FIGURE 24
SKI OLEO SYSTEM FOR CONCEPTS E-5 AND E-6





2

FIGURE 25
CONCEPT E-7
RENDEZVOUS BY DROGUE CAPTURE - LOW ALTITUDE AND LOW SUBSONIC SPEED

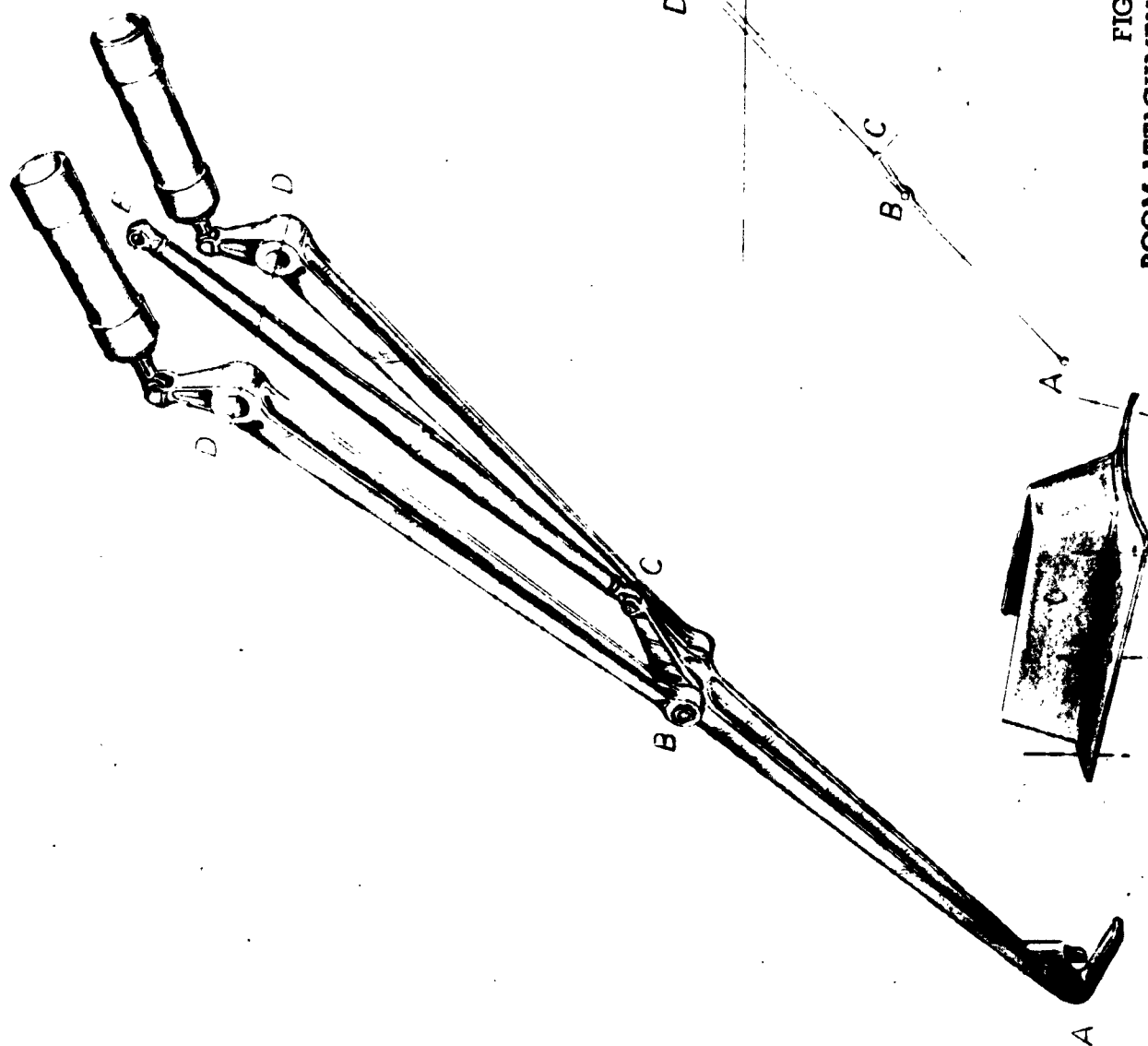


FIGURE 26
BOOM ATTACHMENT USED FOR CONCEPT E-7

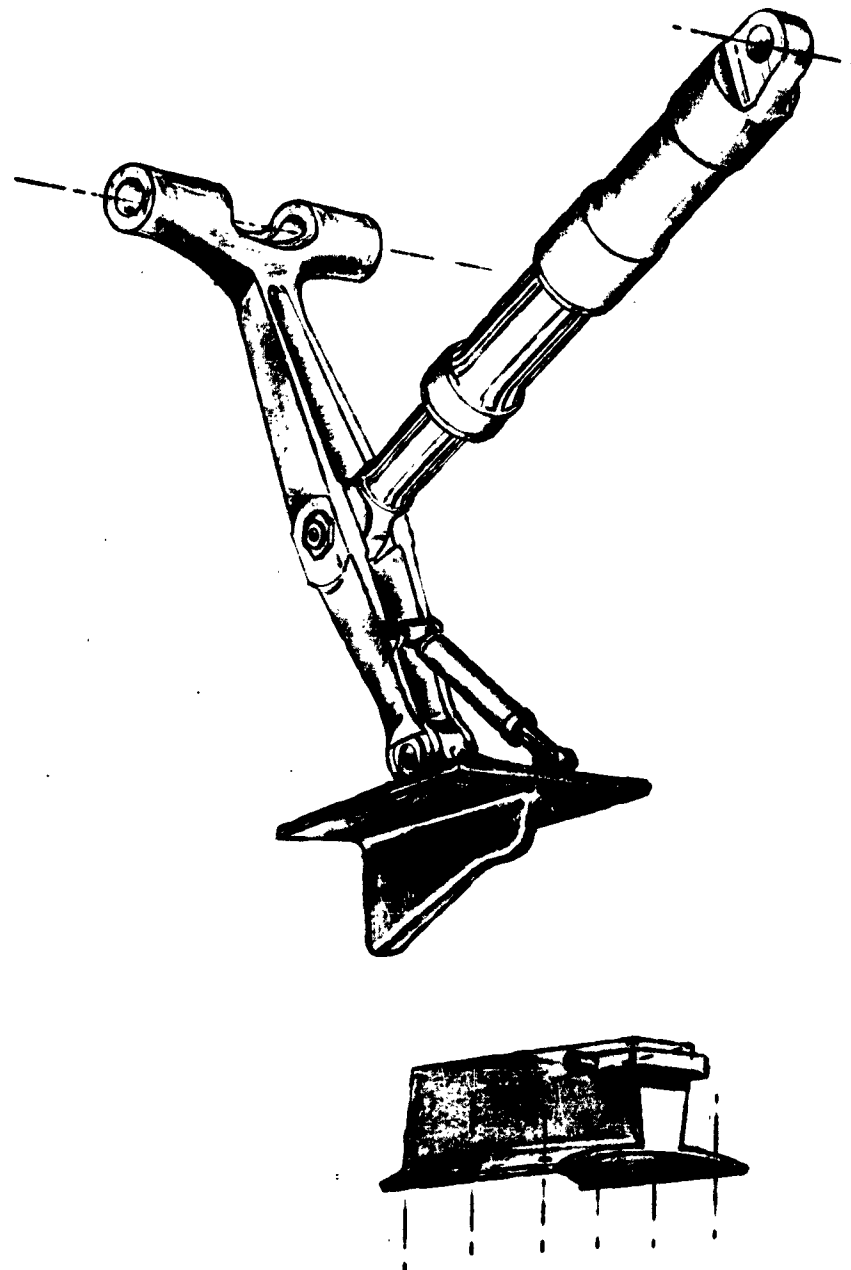


FIGURE 27
PYLON PAD USED FOR CONCEPT E-7

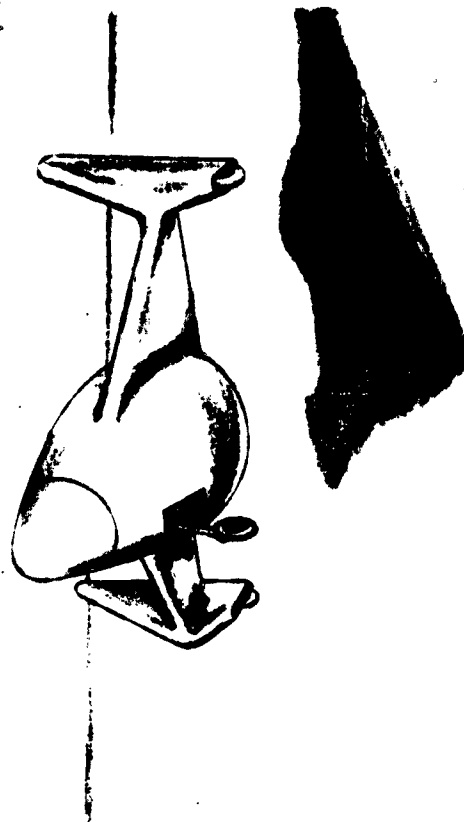
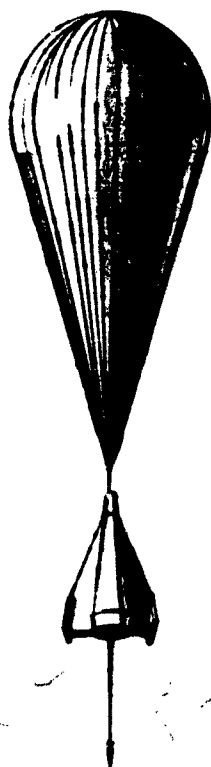
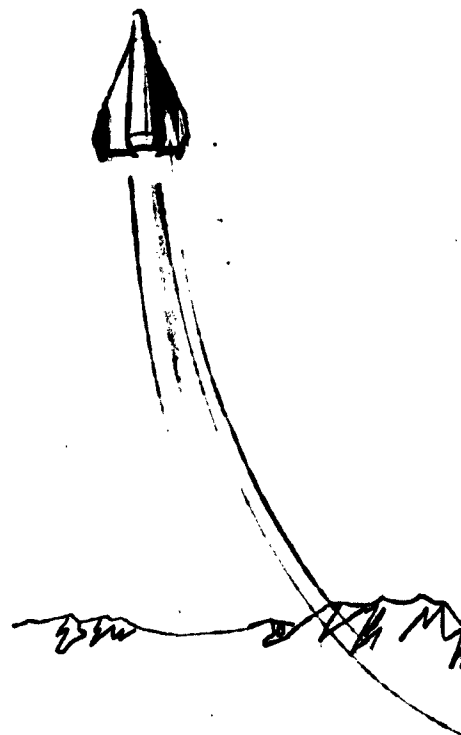
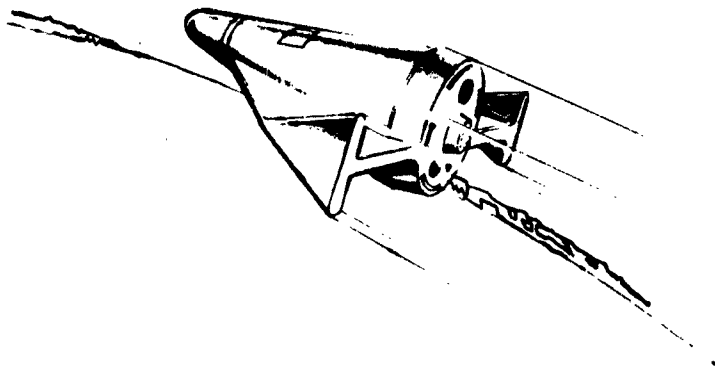
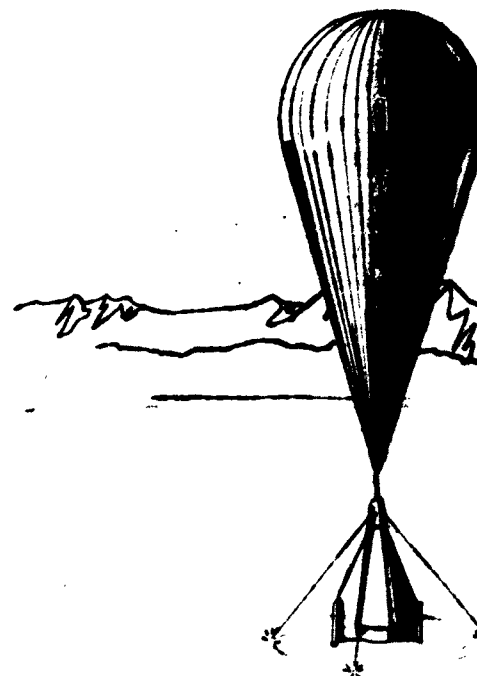


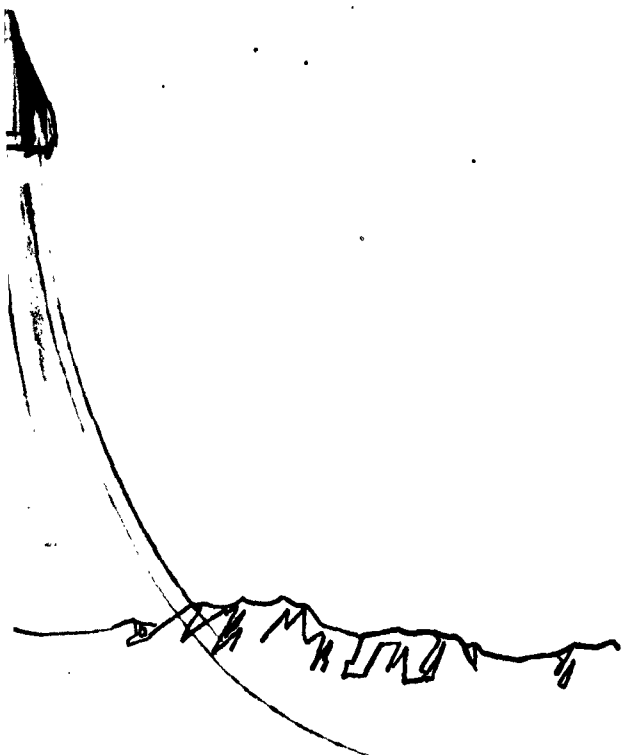
FIGURE 28
CONCEPT E-8
ALIGNMENT ON PREPARED SITE WITH TRICYCLE GEAR



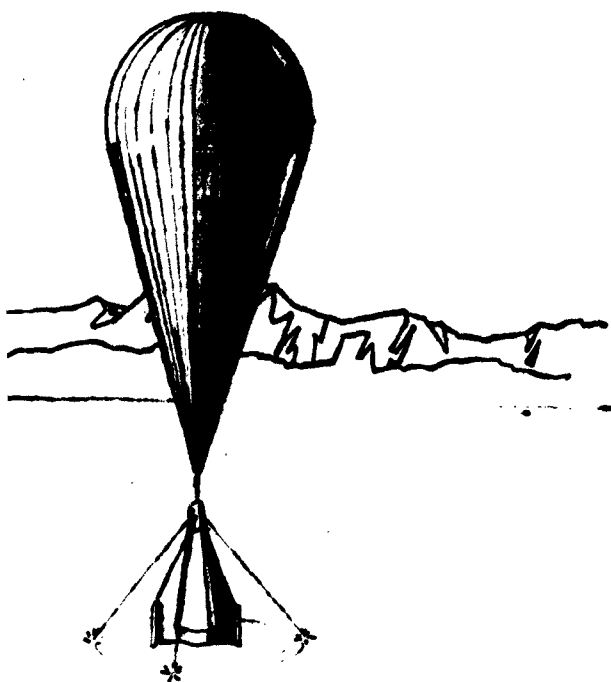
ANCHOR FIRED TO DAMPEN
OSCILLATION



ADDITIONAL ANCHORS
FOR STABILIZATION AT



BALLOON EJECTED WHILE VEHICLE
APPROACHES VERTICAL STALL,
ASSISTED BY RETRO THRUST



ADDITIONAL ANCHORS FIRED
STABILIZATION AT TOUCHDOWN

2

FIGURE 29
CONCEPT E-9
ALIGNMENT BY BALLOON DESCENT

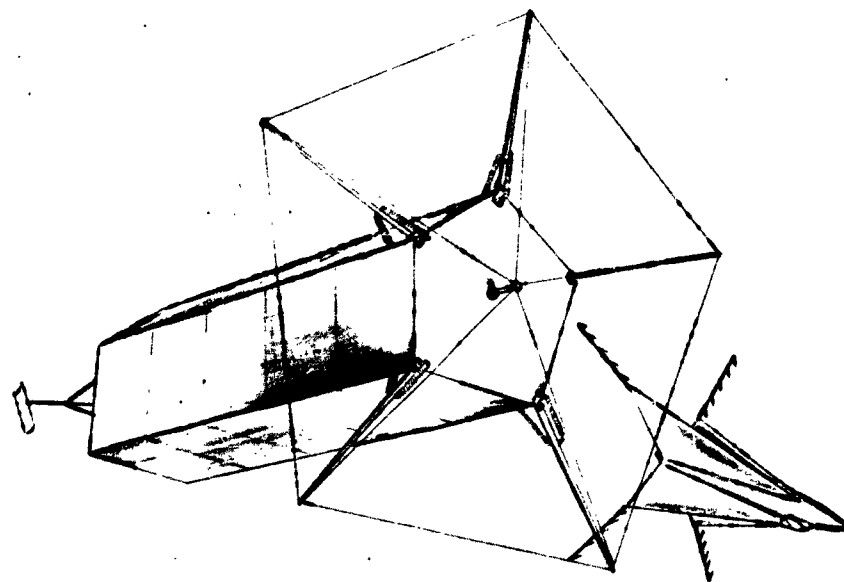
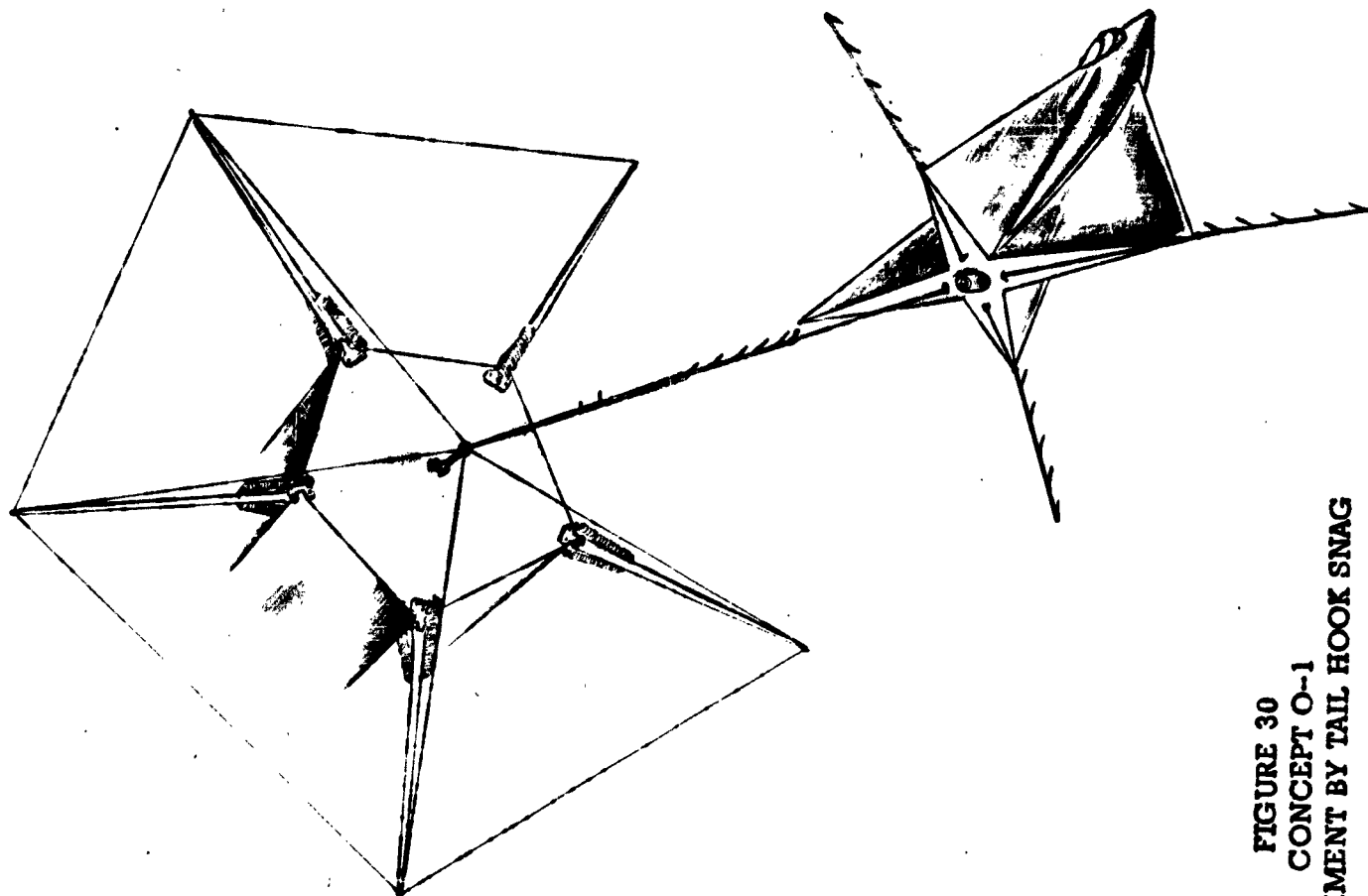


FIGURE 30
CONCEPT O-1
ATTACHMENT BY TAIL HOOK SNAG

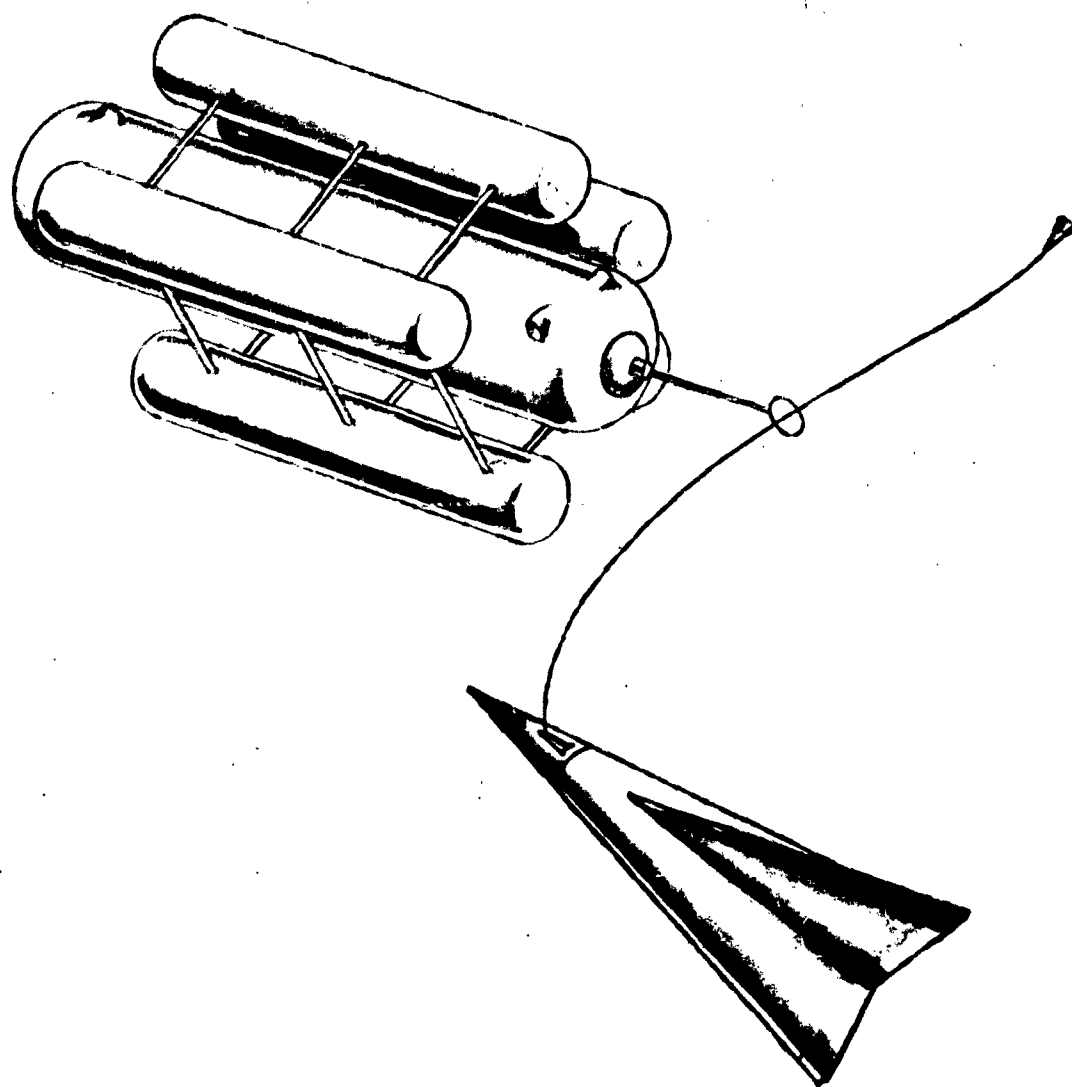


FIGURE 31
CONCEPT O-2
ATTACHMENT BY SELF-GUIDING PROBE THROUGH HOOP

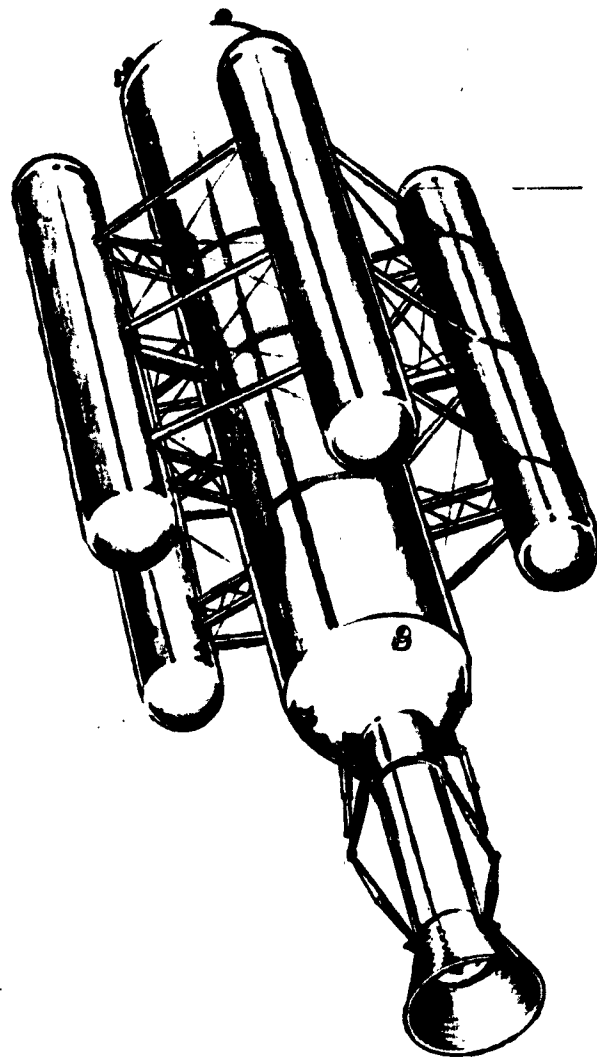


FIGURE 32
 CONCEPT O-3 (ATTACHMENT)
 CONCEPT O-4 (DEPARTURE)
 SHOCK MITIGATION BETWEEN TWO AXIALLY ALIGNED VEHICLES

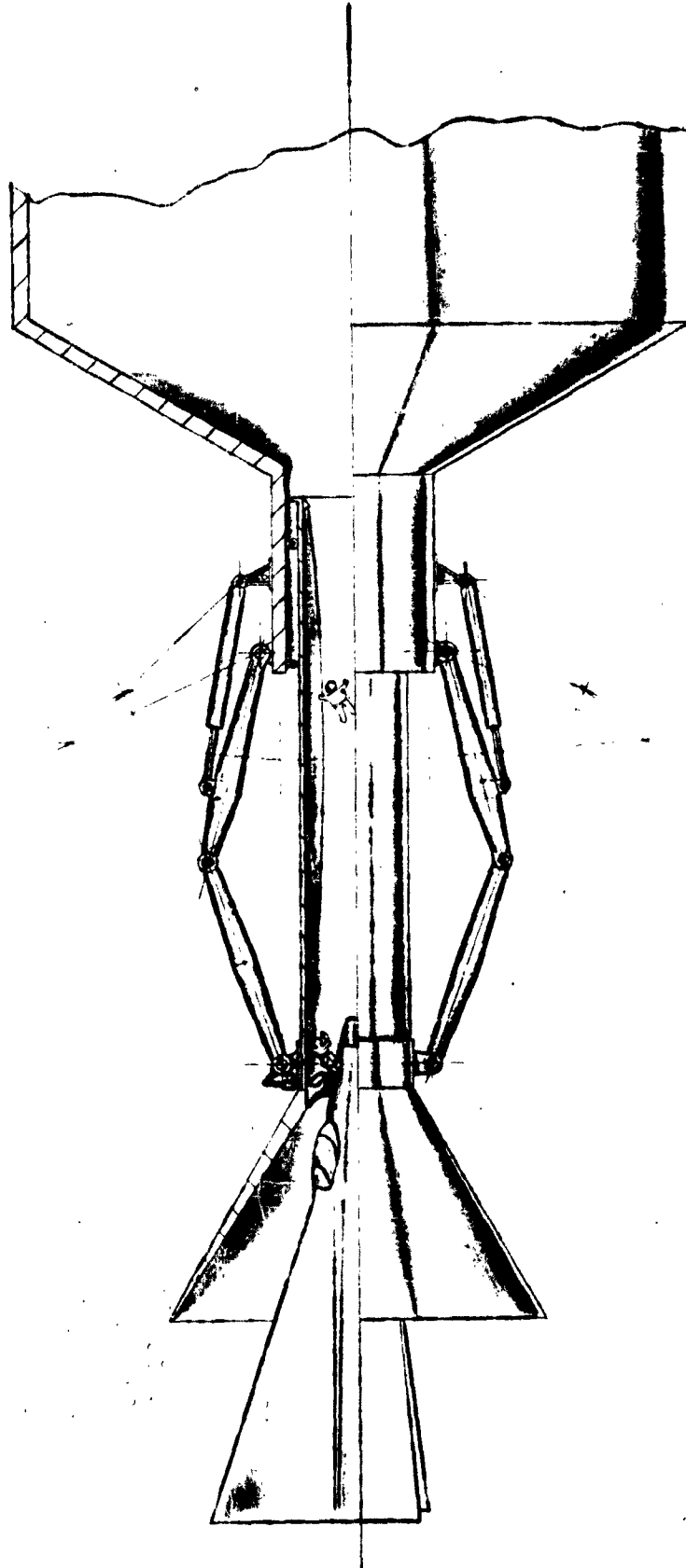


FIGURE 33
ARRESTING GEAR FOR STORING IMPACT ENERGY FOR
SUBSEQUENT EJECTION DEPARTURE - CONCEPT O-3
AND O-4

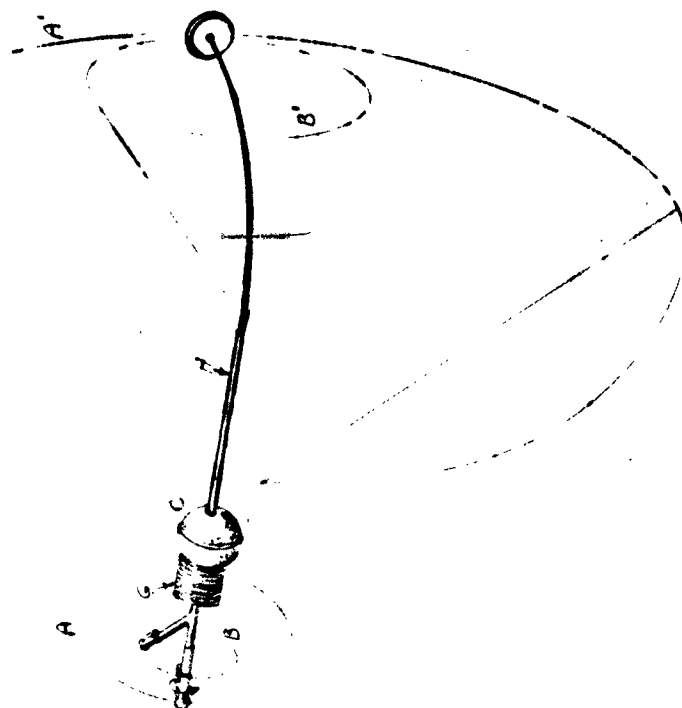
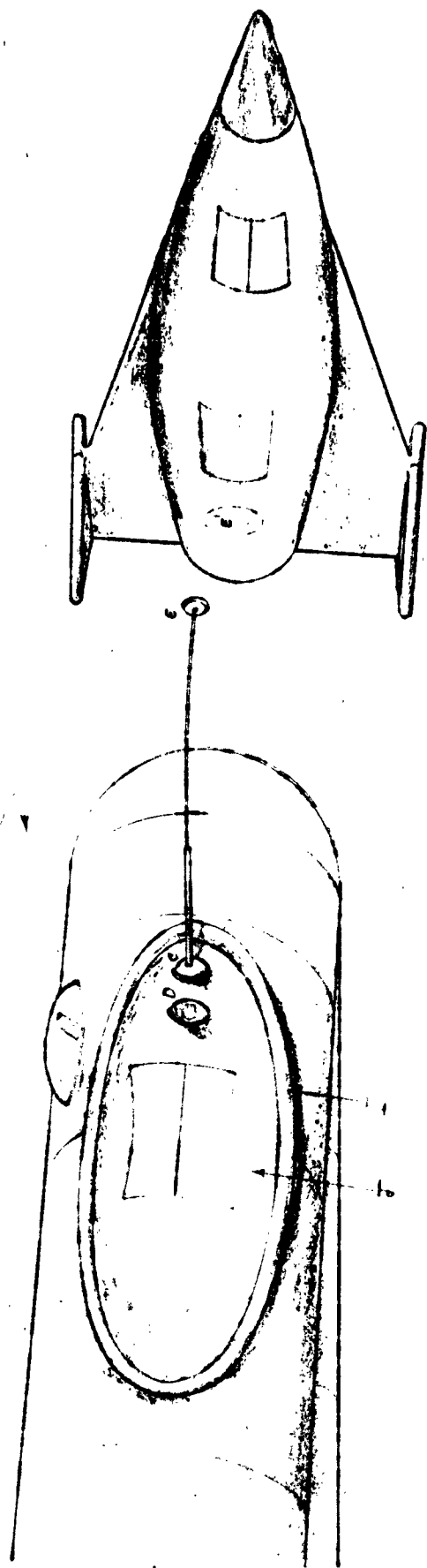
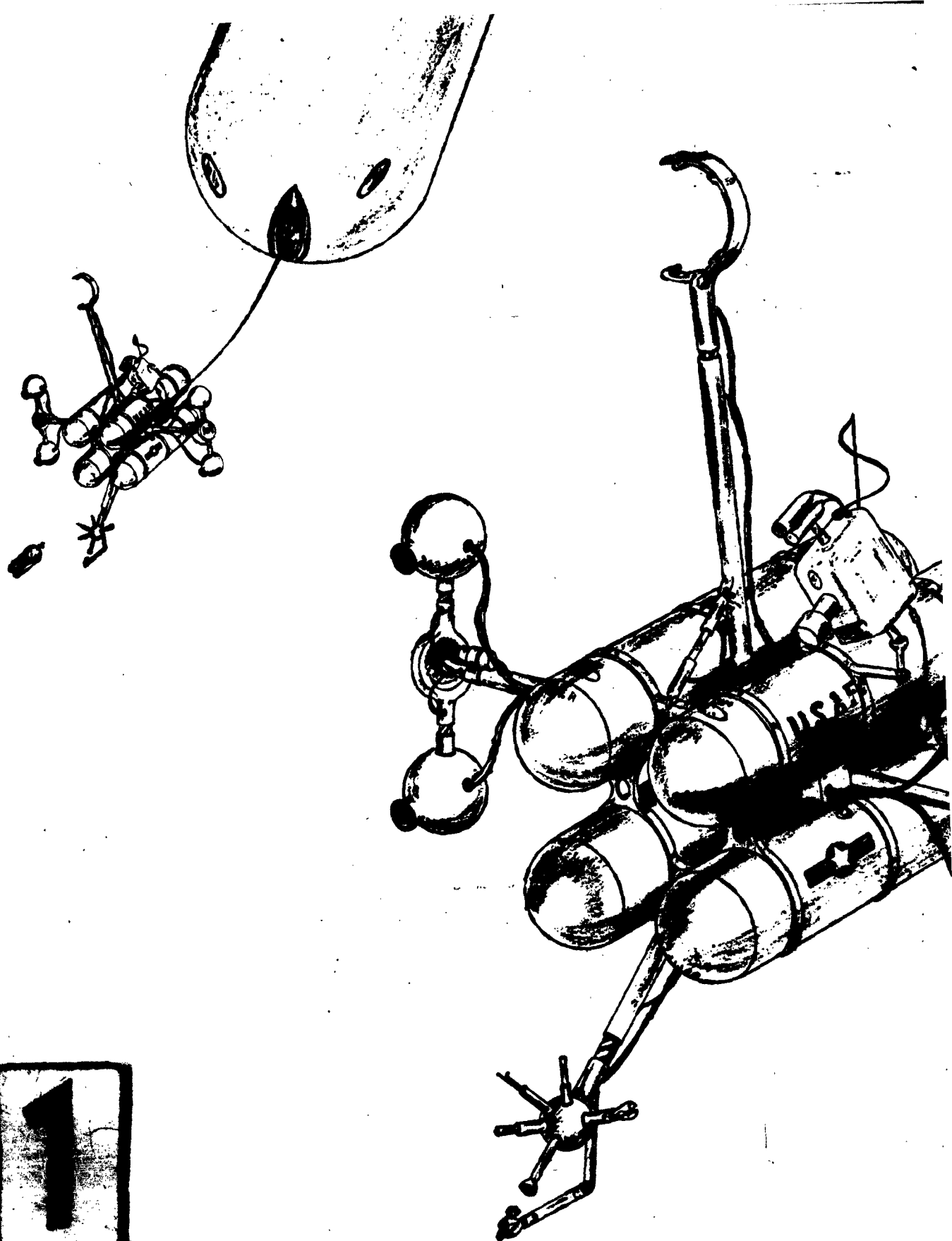
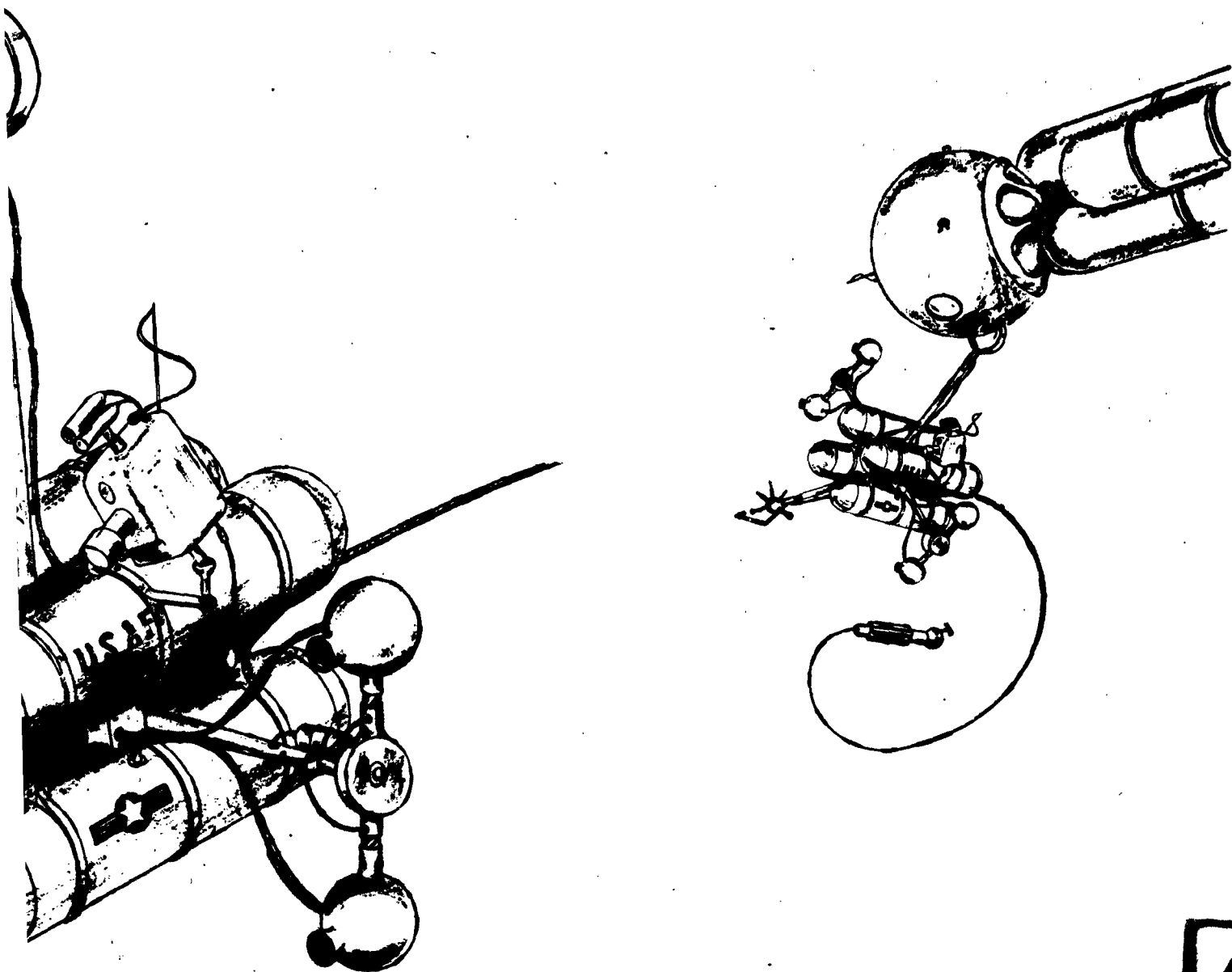


FIGURE 34
CONCEPT O-5
REMOTELY CONTROLLED MAGNETIC CONTACTOR ON FREELY SWINGING CABLE





2

FIGURE 35
CONCEPT O-6
RENDEZVOUS BY UTILITY TUG - REMOTELY CONTROLLED

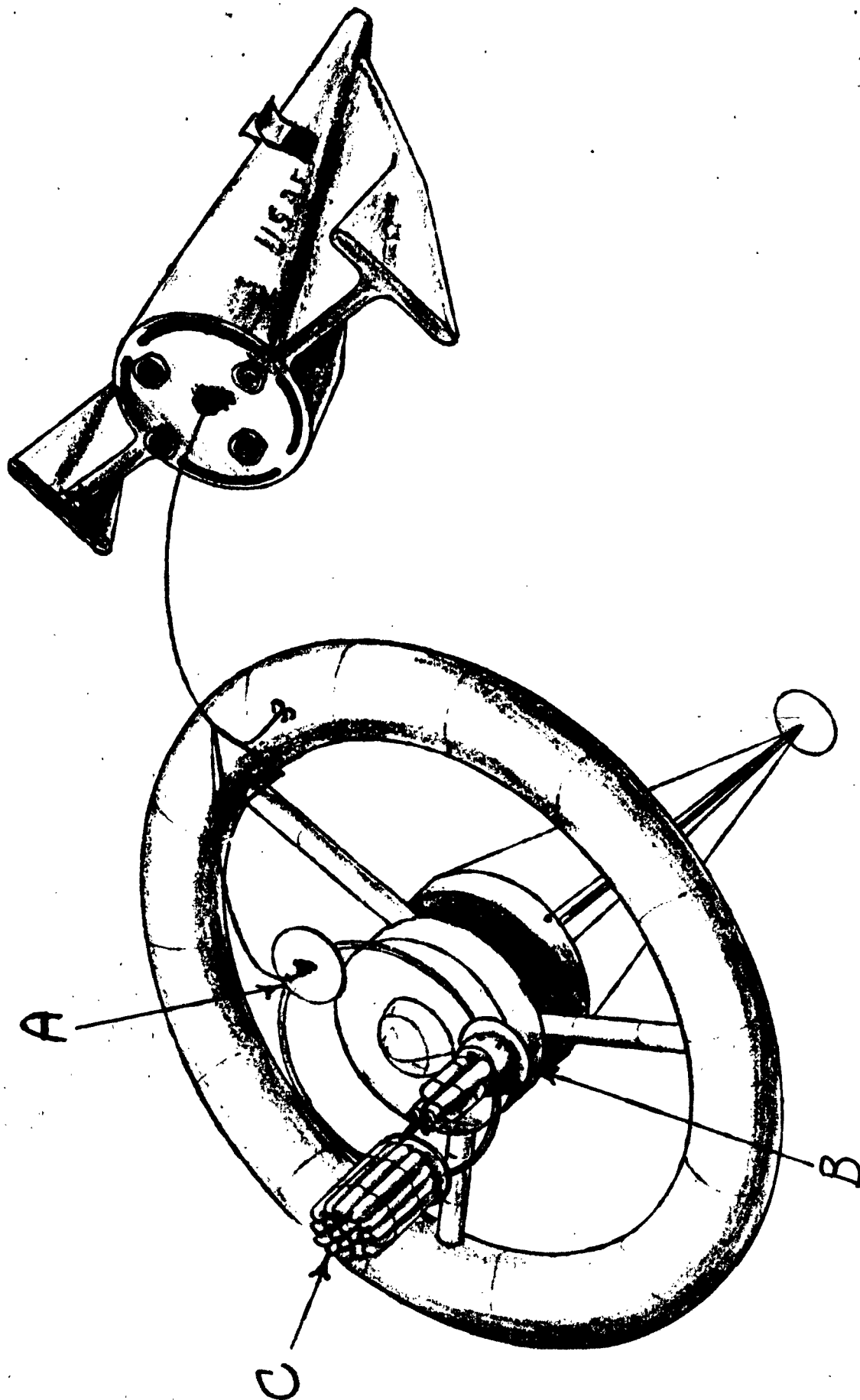


FIGURE 36
CONCEPT O-7
ATTACHMENT BY MECHANICAL GRAPPLING HOOK - CLOSE RANGE

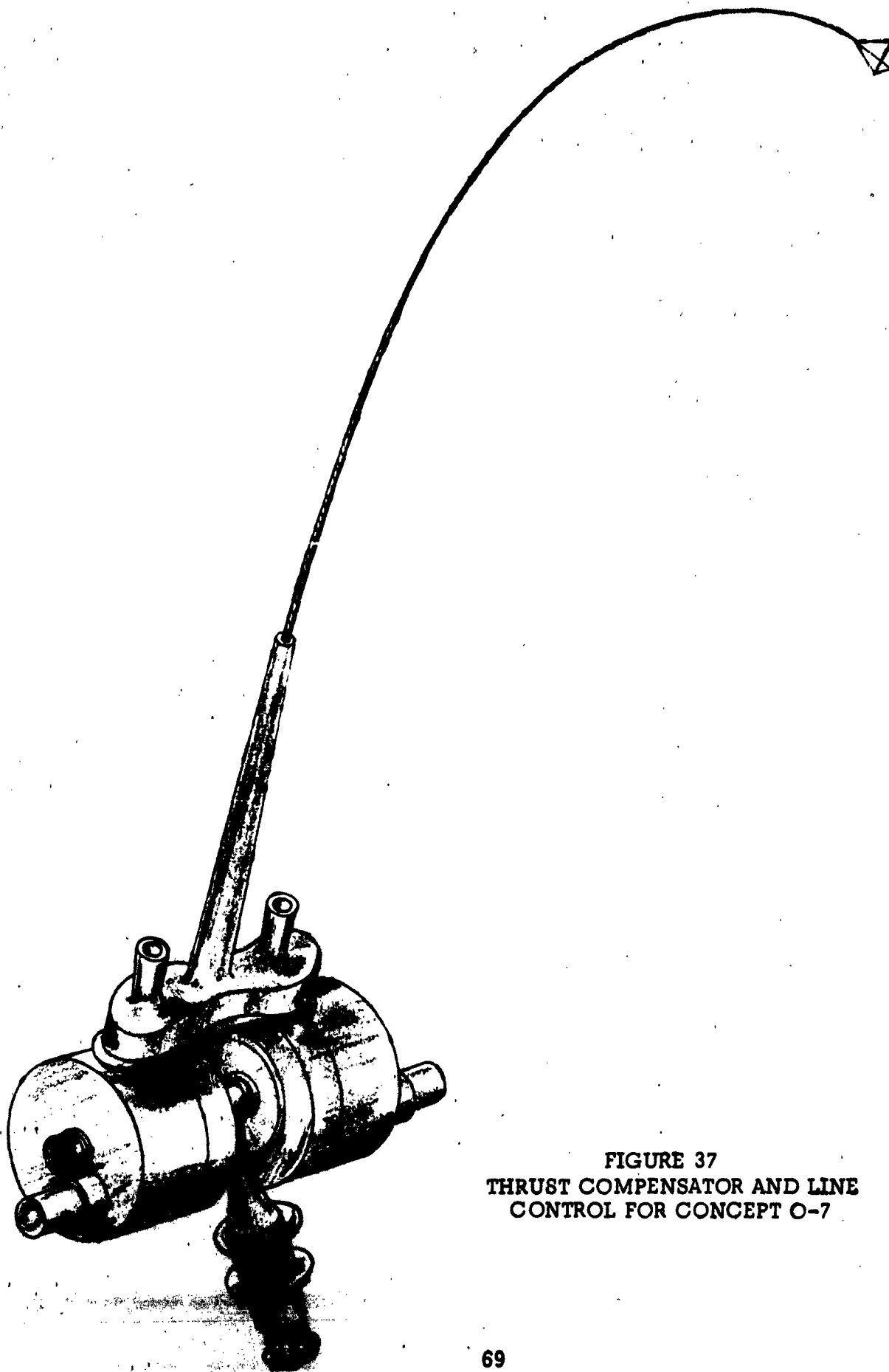


FIGURE 37
THRUST COMPENSATOR AND LINE
CONTROL FOR CONCEPT O-7

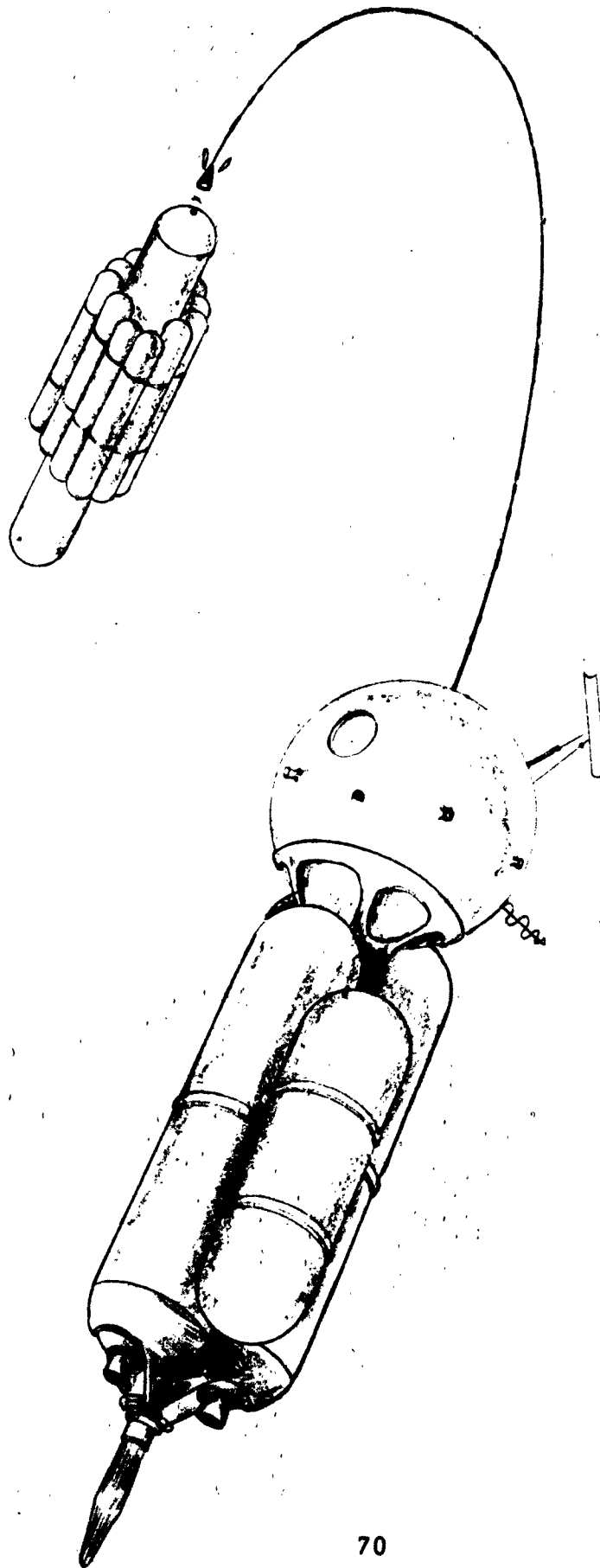


FIGURE 38
CONCEPT O-8
ORBITAL ATTACHMENT BY SELF-GUIDING PROBE

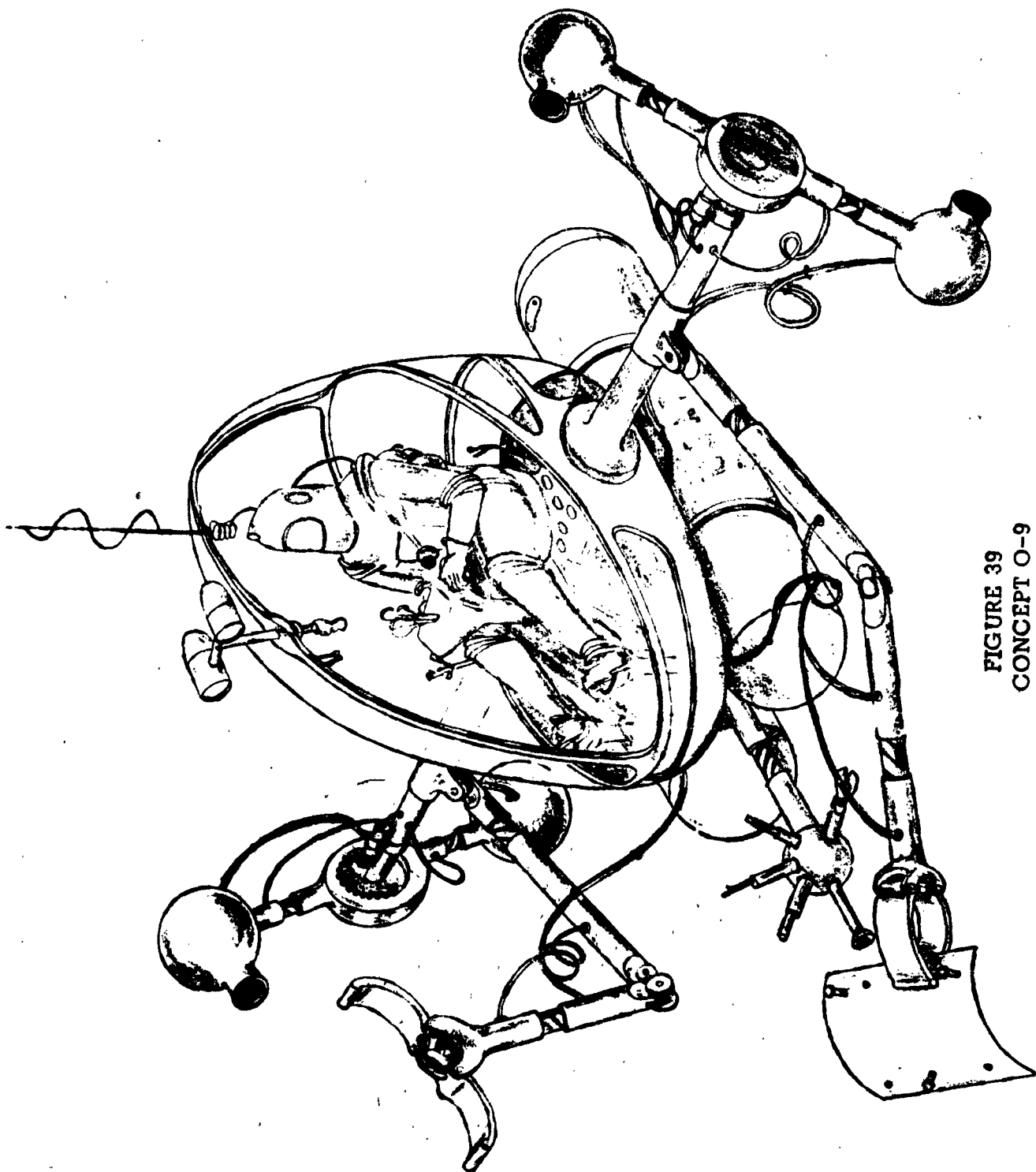


FIGURE 39
CONCEPT O-9
RENDEZVOUS BY MANNED UTILITY TUG

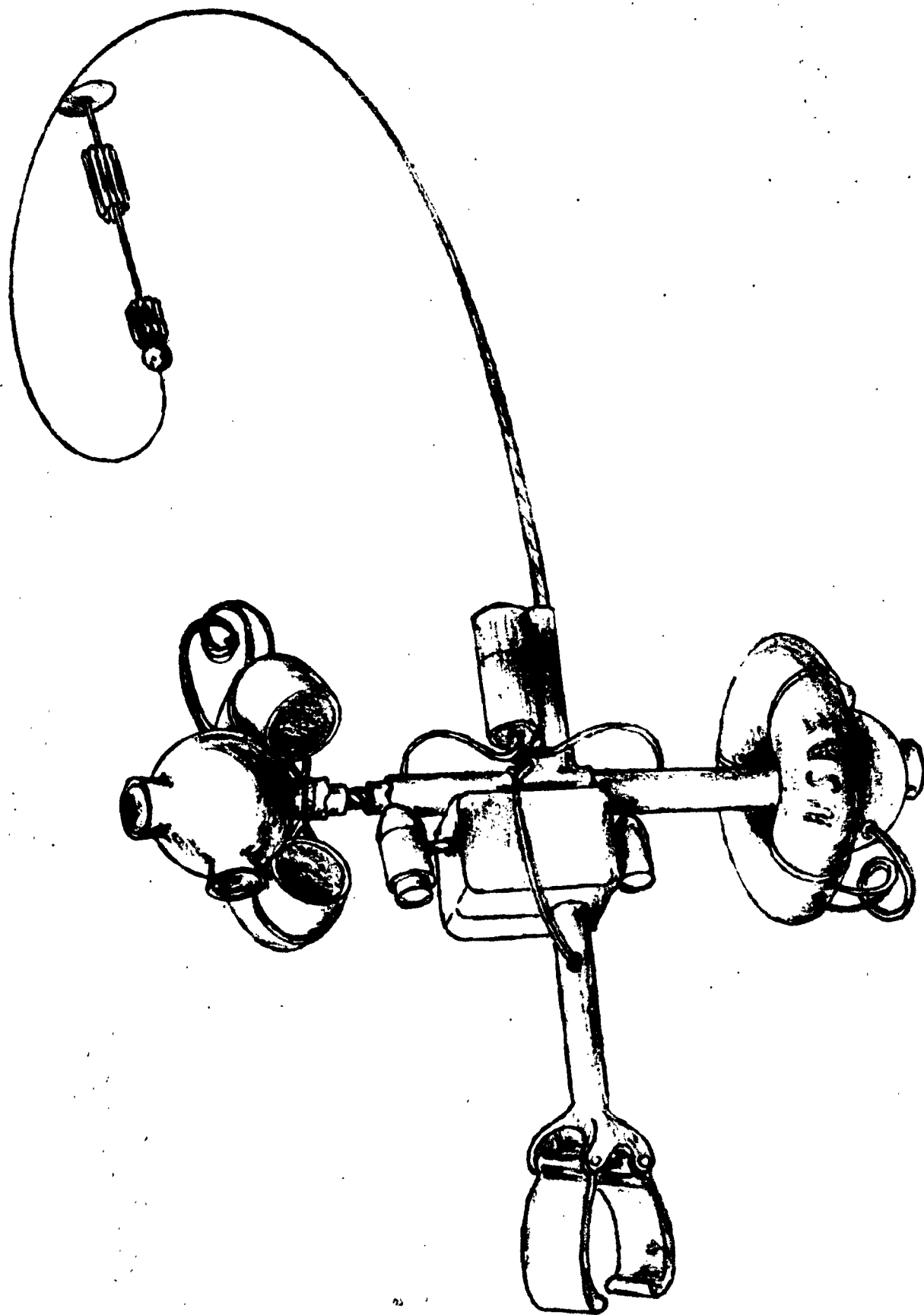


FIGURE 40
CONCEPT O-10
RENDEZVOUS BY SIMPLE, REMOTELY CONTROLLED TUG

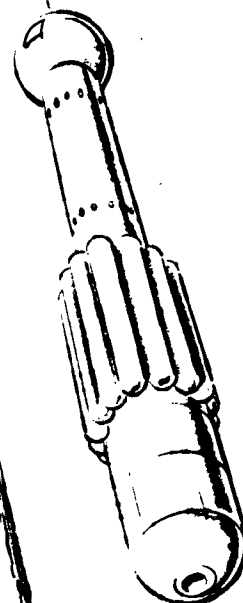
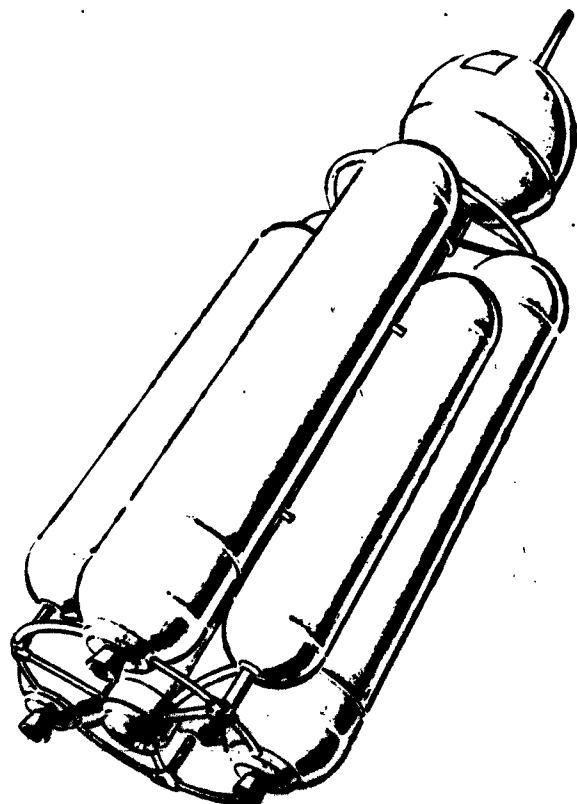


FIGURE 41
CONCEPT O-11
LONG RANGE ATTACHMENT BY PROBE AND DROGUE - HEAT OR LIGHT SENSITIVE

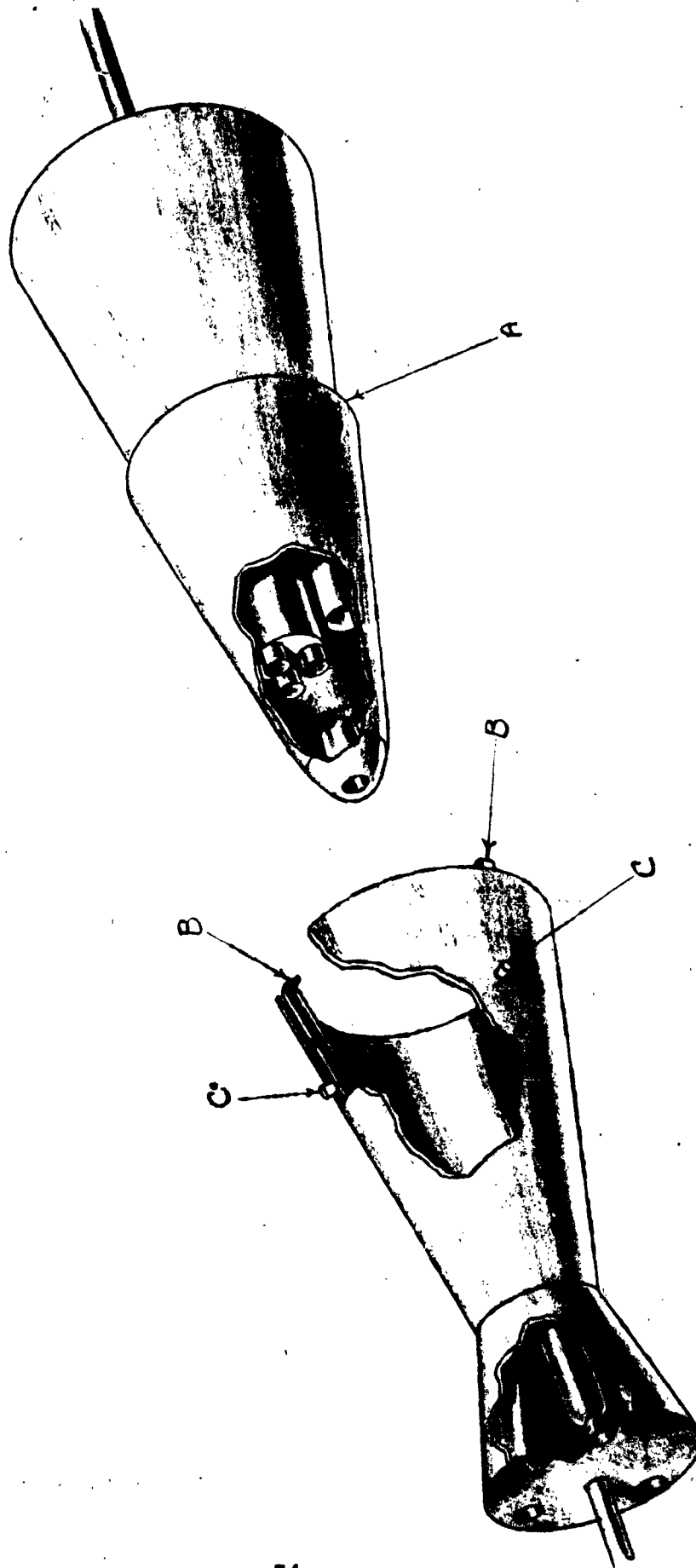


FIGURE 42
LATCH COUPLING FOR CONCEPT O-11

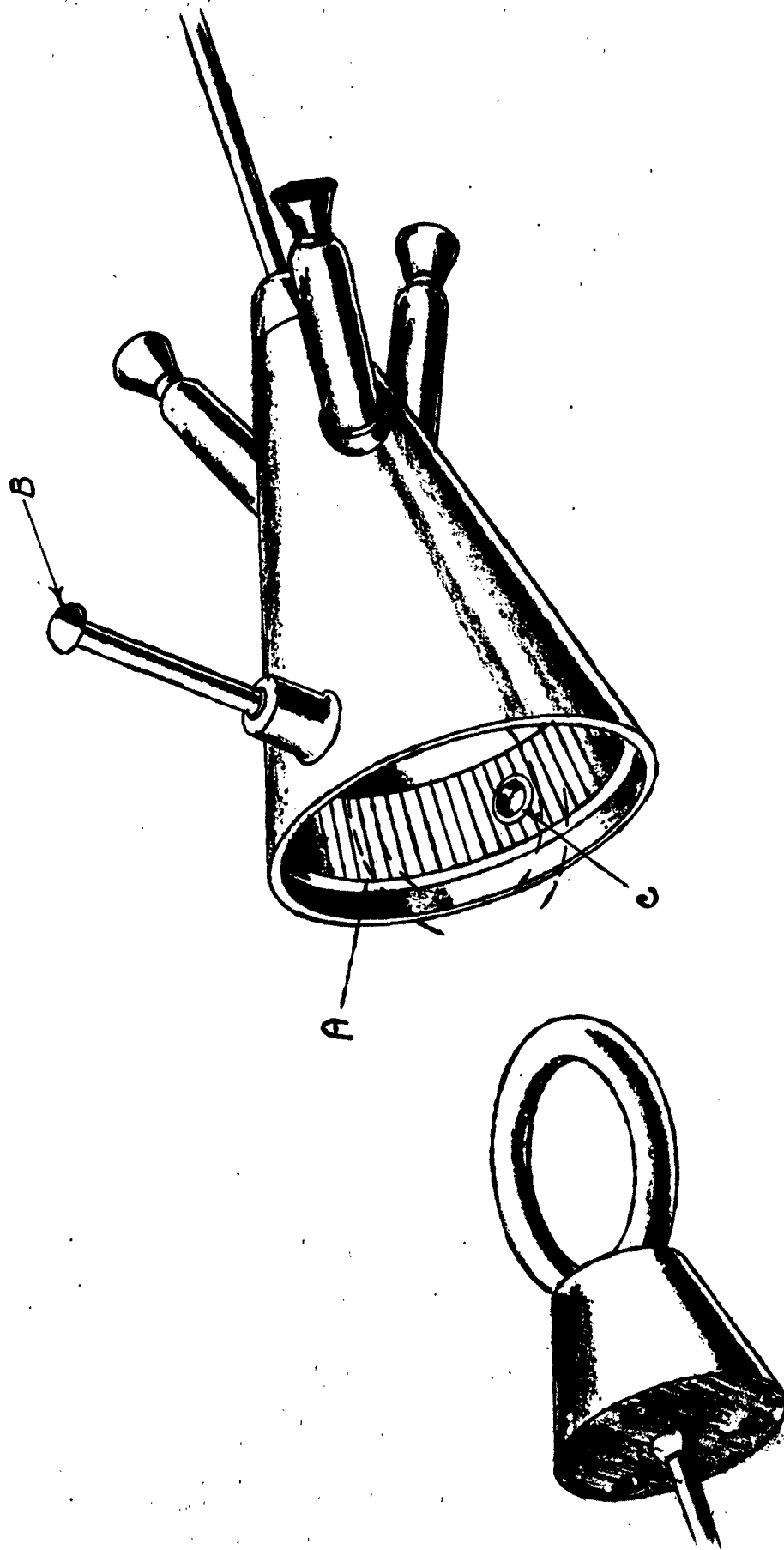


FIGURE 43
MECHANICAL MAGNETIC RING COUPLING FOR CONCEPT O-11

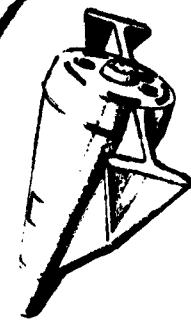
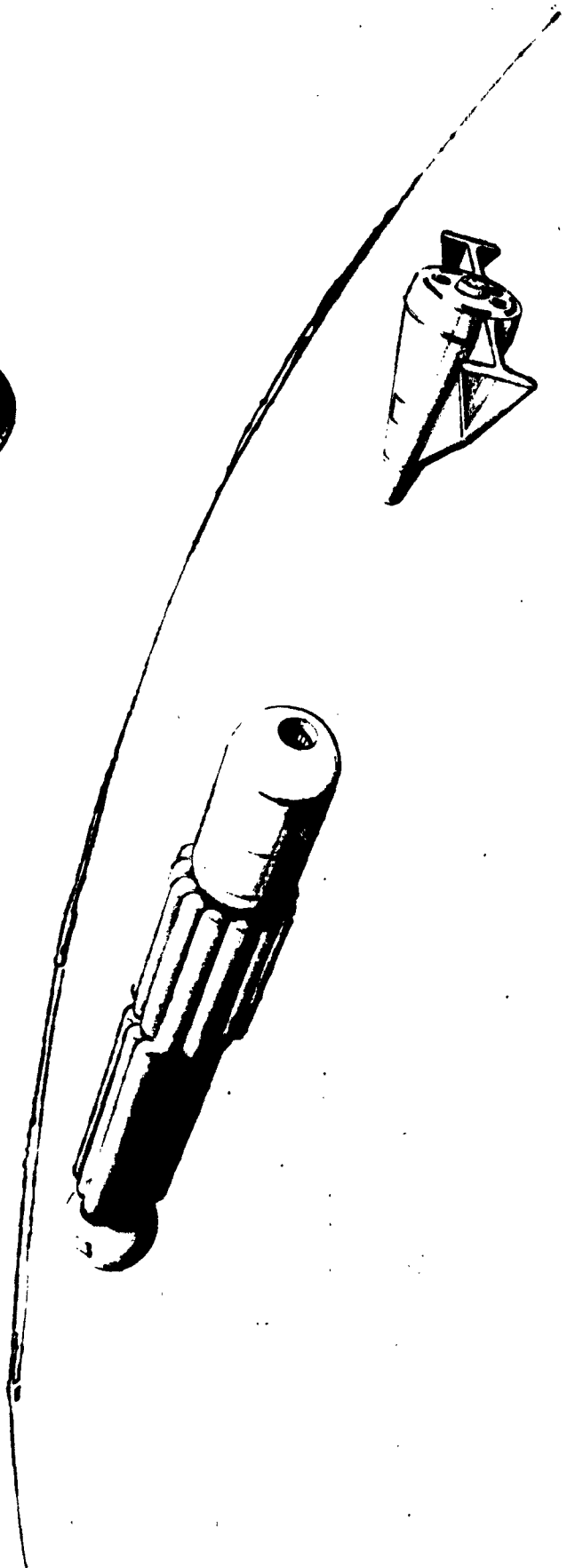


FIGURE 44
CONCEPT O-12
RENDEZVOUS OF AXIALLY ALIGNED VEHICLES BY PENETRATION

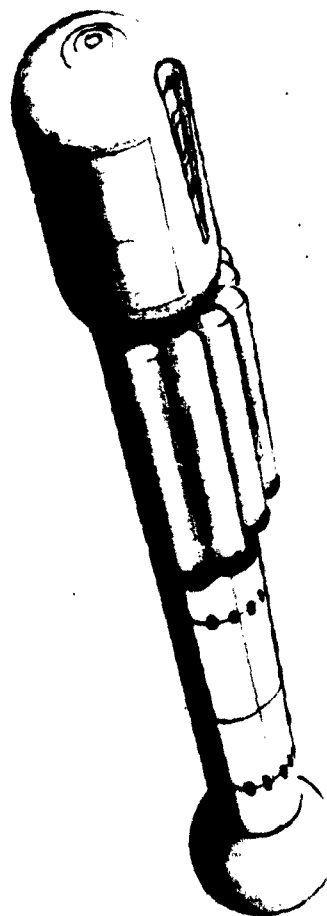
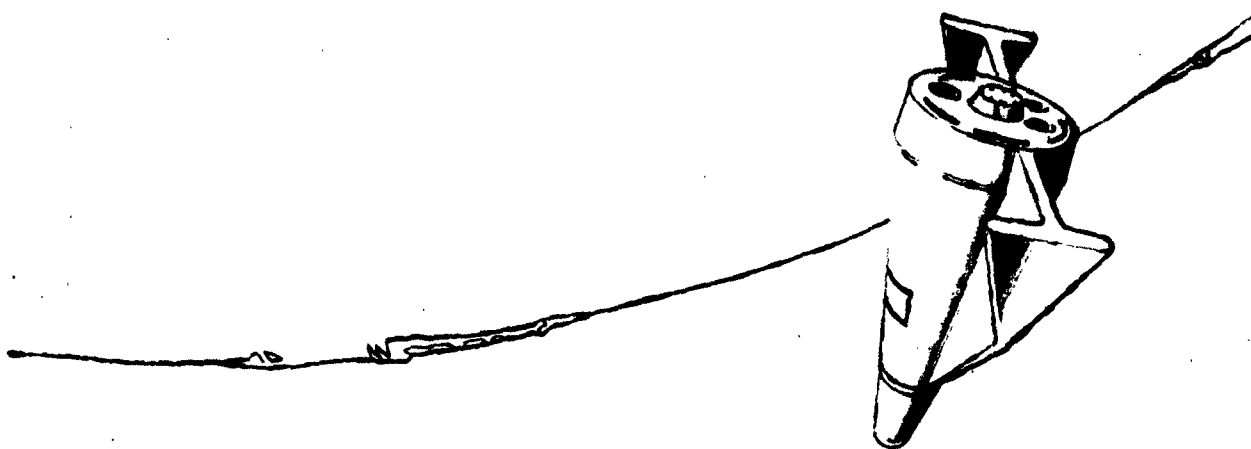
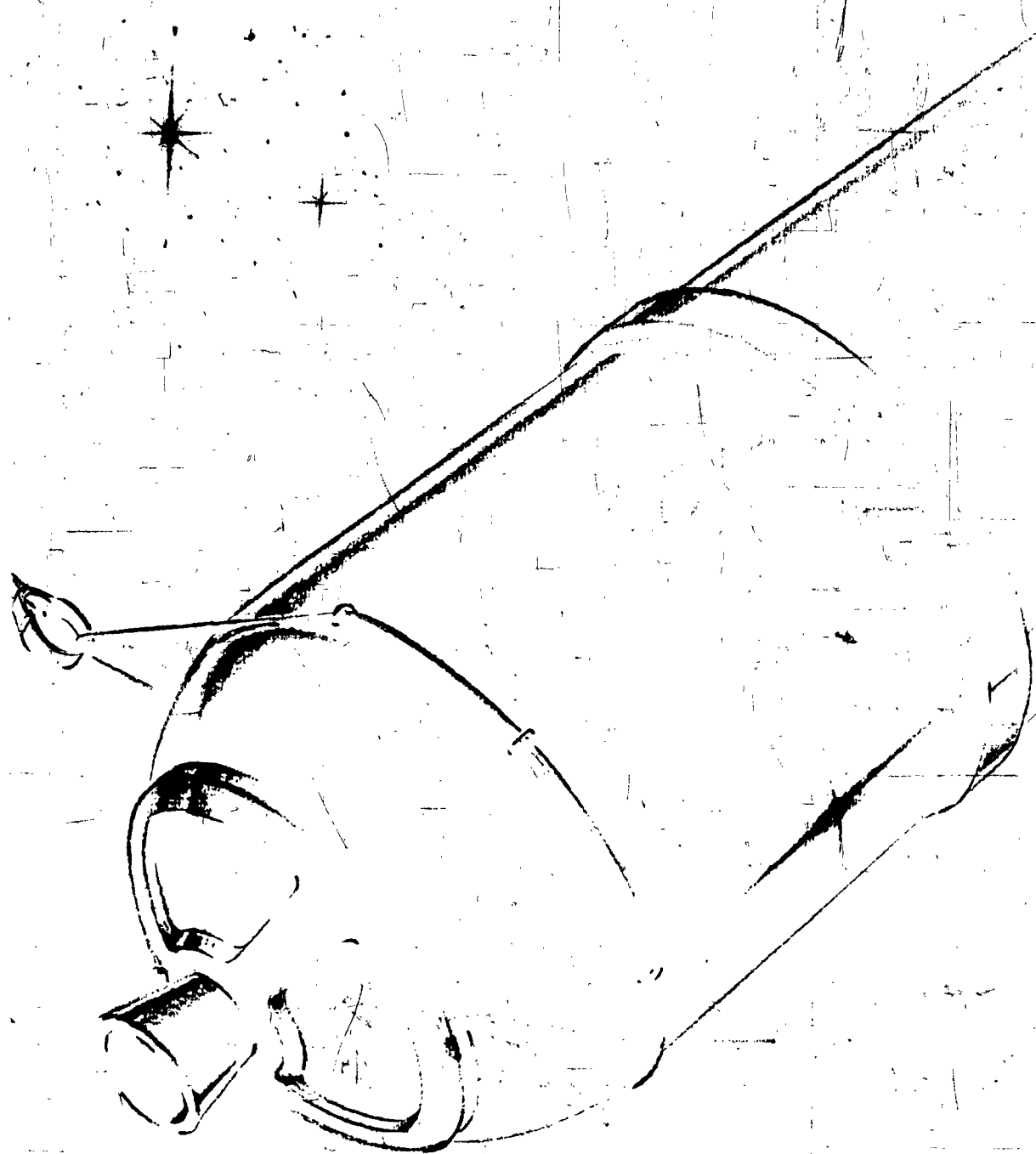


FIGURE 45
CONCEPT O-13
RENDEZVOUS BY SURFACE CONTACT

1





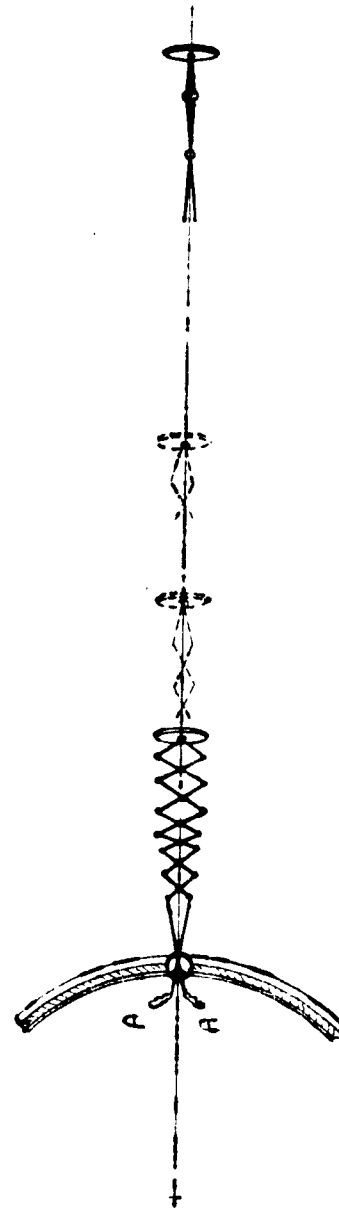
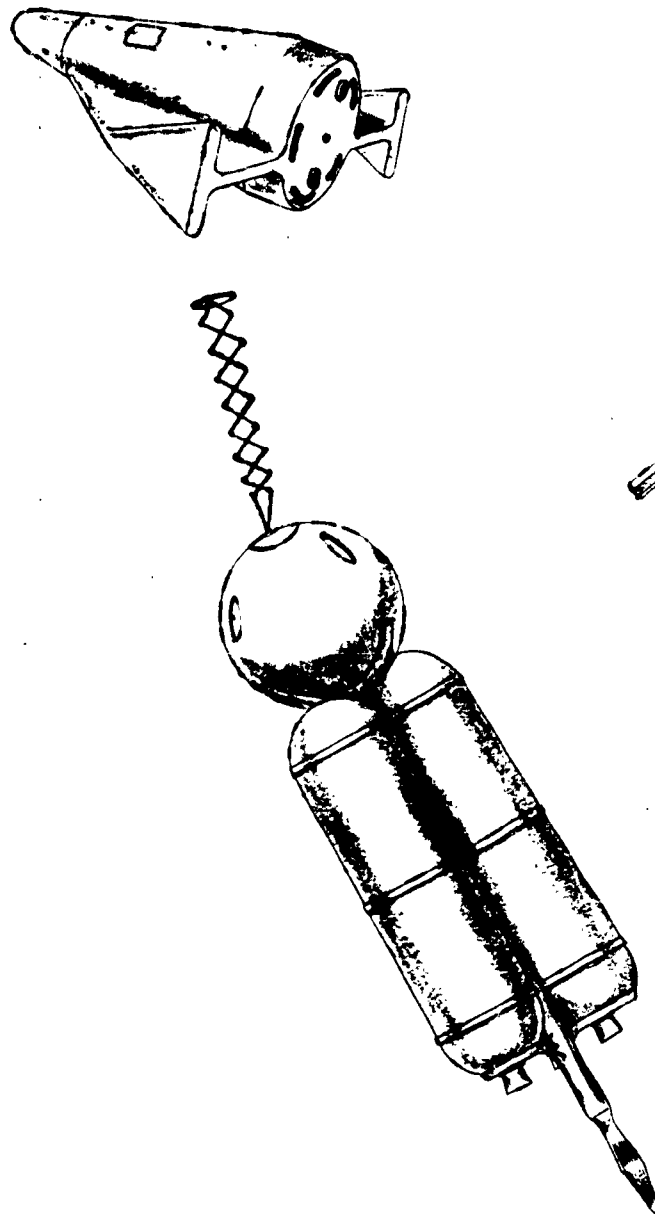


FIGURE 47
CONCEPT O-13
ATTACHMENT BY MECHANICAL PARALLELOGRAM GRAPPLER

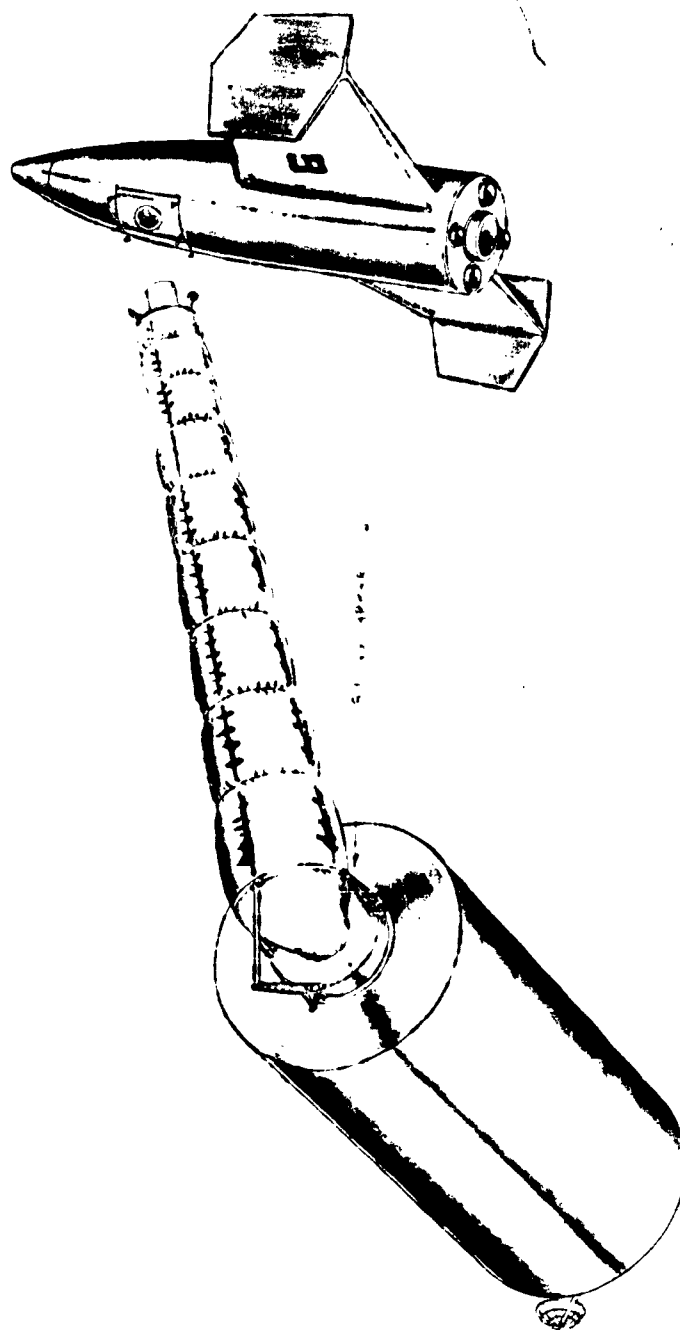
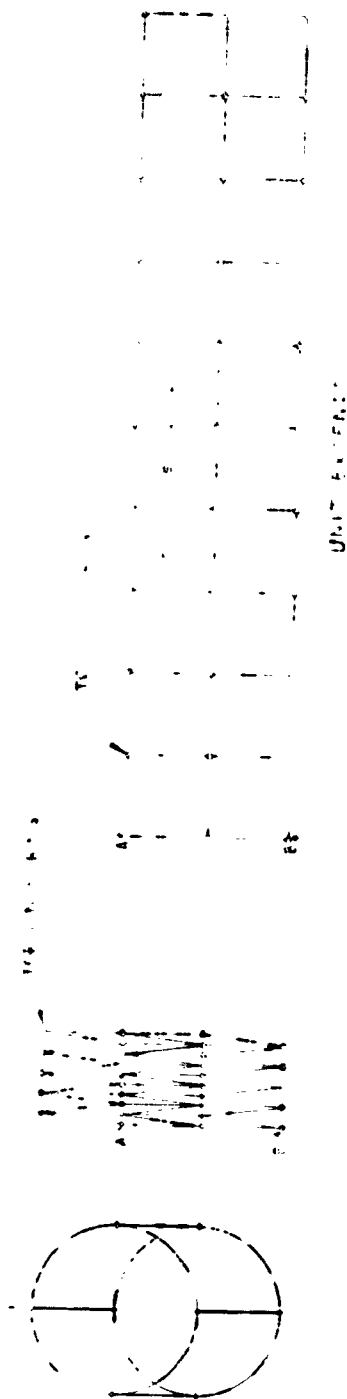


FIGURE 48
CONCEPT O-16
ATTACHMENT BY GAS-ACTUATED PARALLELOGRAM GRAPPLER

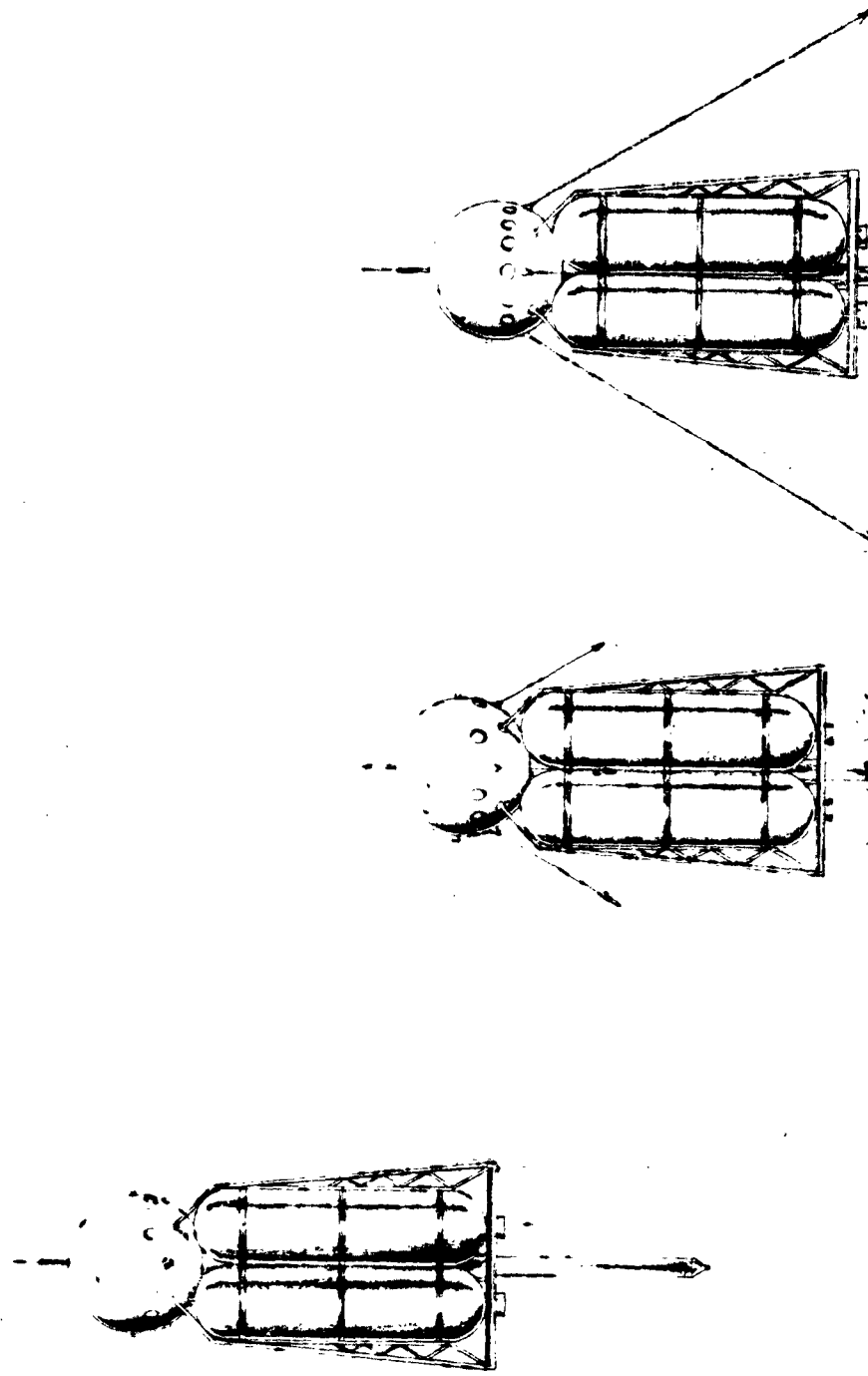
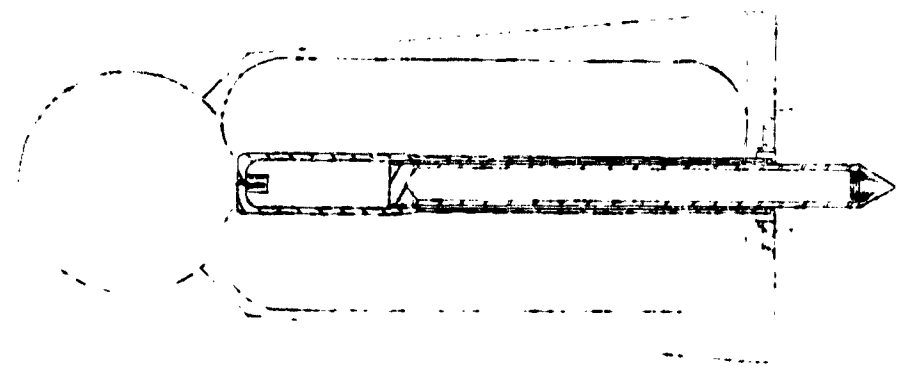
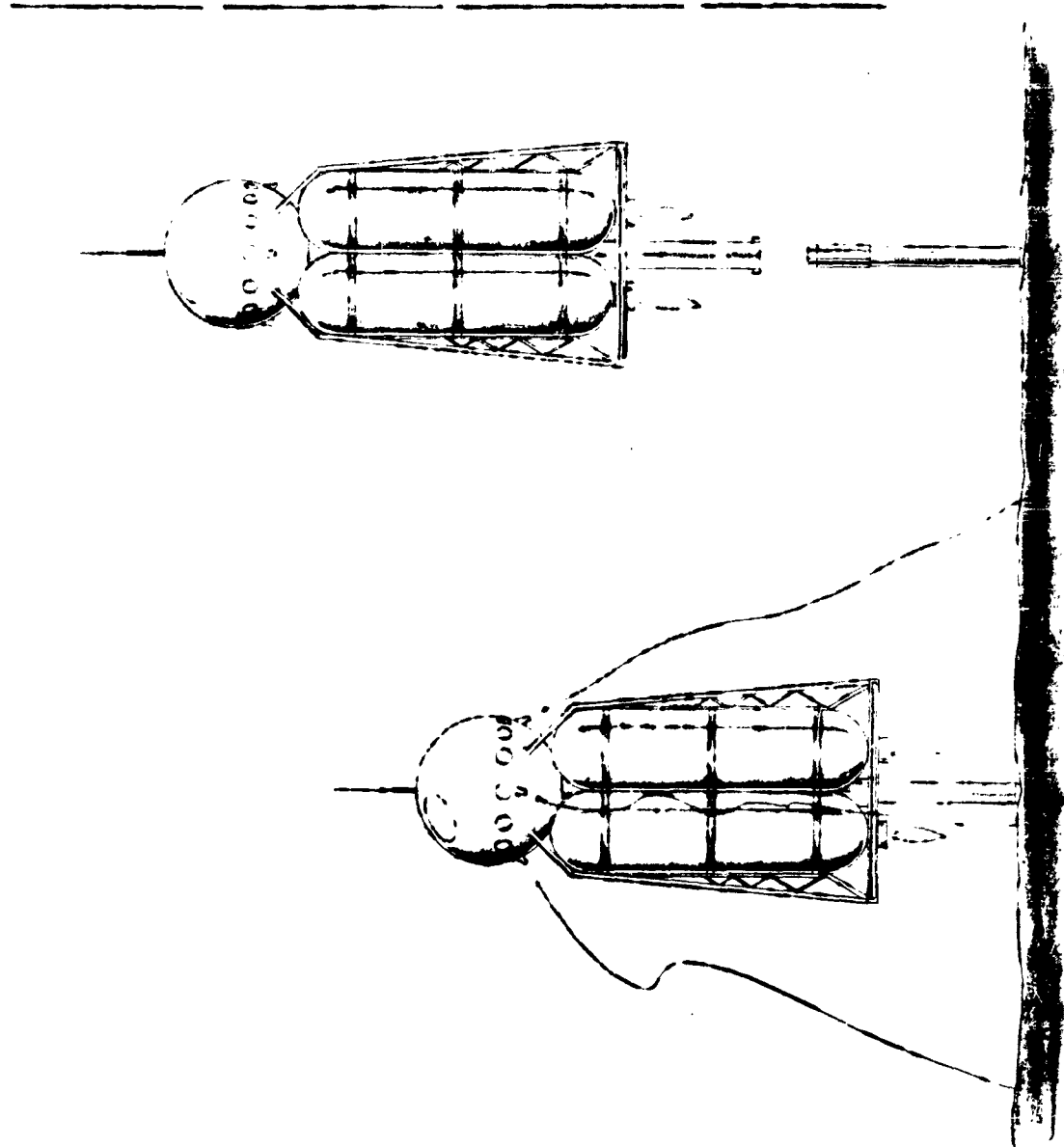


FIGURE 49
CONCEPT L-1
LUNAR ALIGNMENT - SINGLE OLEO STRUT WITH IMBEDMENT ANCHORS†



Basic Pogo Design



Pogo Fires and Lines Released

Pogo Gear Drops Out

FIGURE 50
CONCEPT L-2
LUNAR DEPARTURE ASSIST BY GAS-FIRED SQUIB[†]

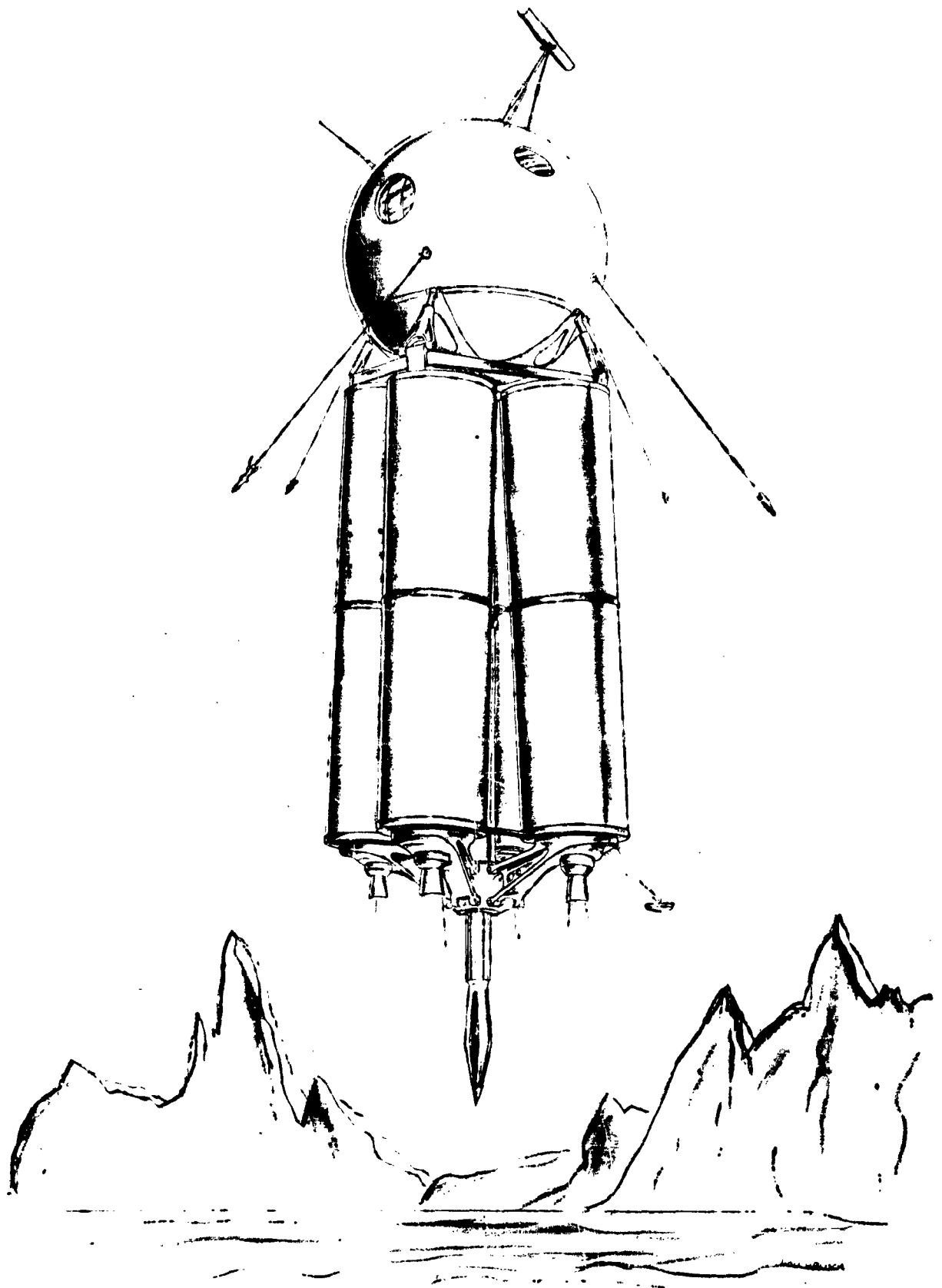


FIGURE 51
CONCEPT L-3
ALIGNMENT ON COLLAPSIBLE STRUT - PAYLOAD MOUNTED[†]
SEPARATELY FOR BANDPASS SHOCK ABSORPTION

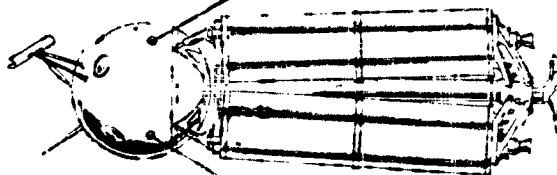
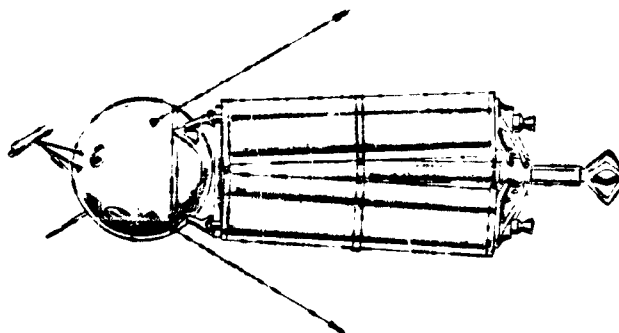


FIGURE 52
COLLAPSIBLE STRUT SEQUENCE FOR CONCEPT L-3[†]

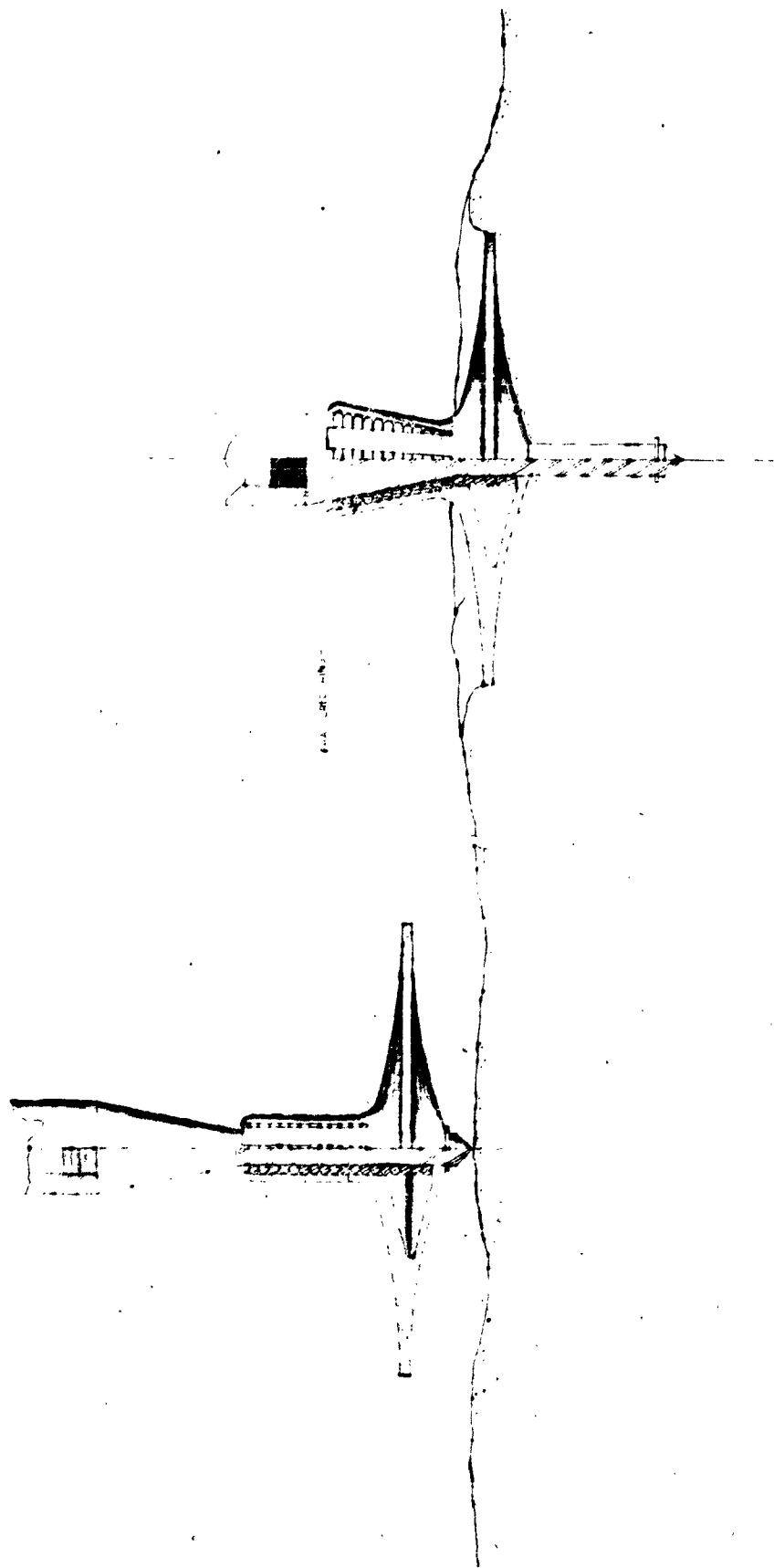


FIGURE 53
DESIGN CONCEPT OF COLLAPSIBLE STRUT FOR CONCEPT L-3[†]

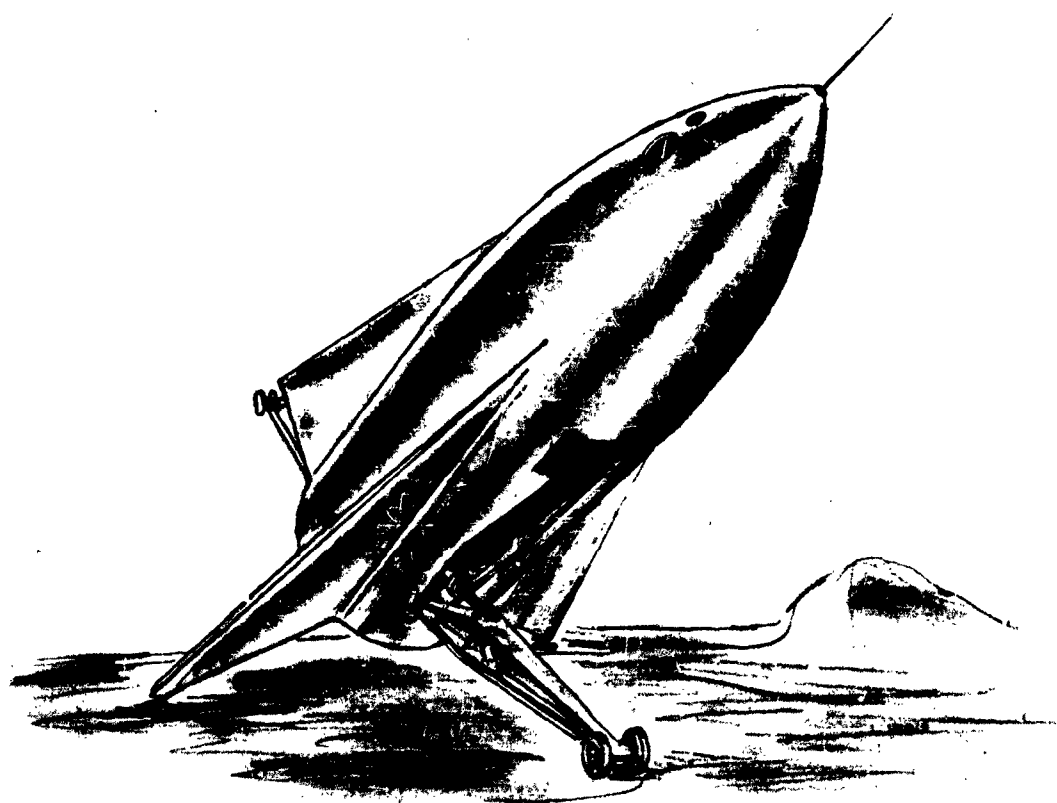
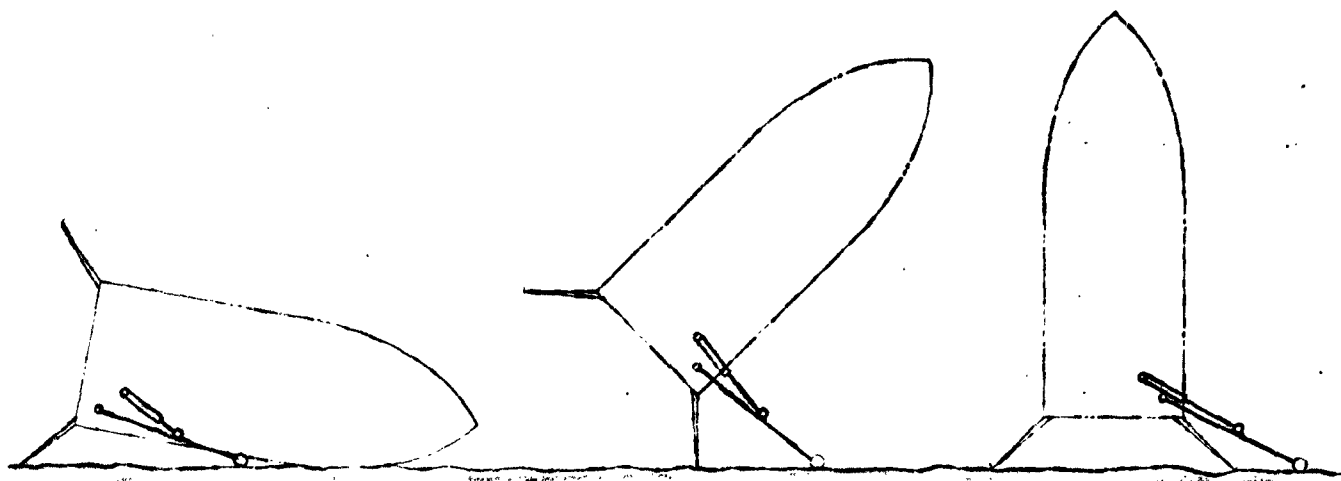
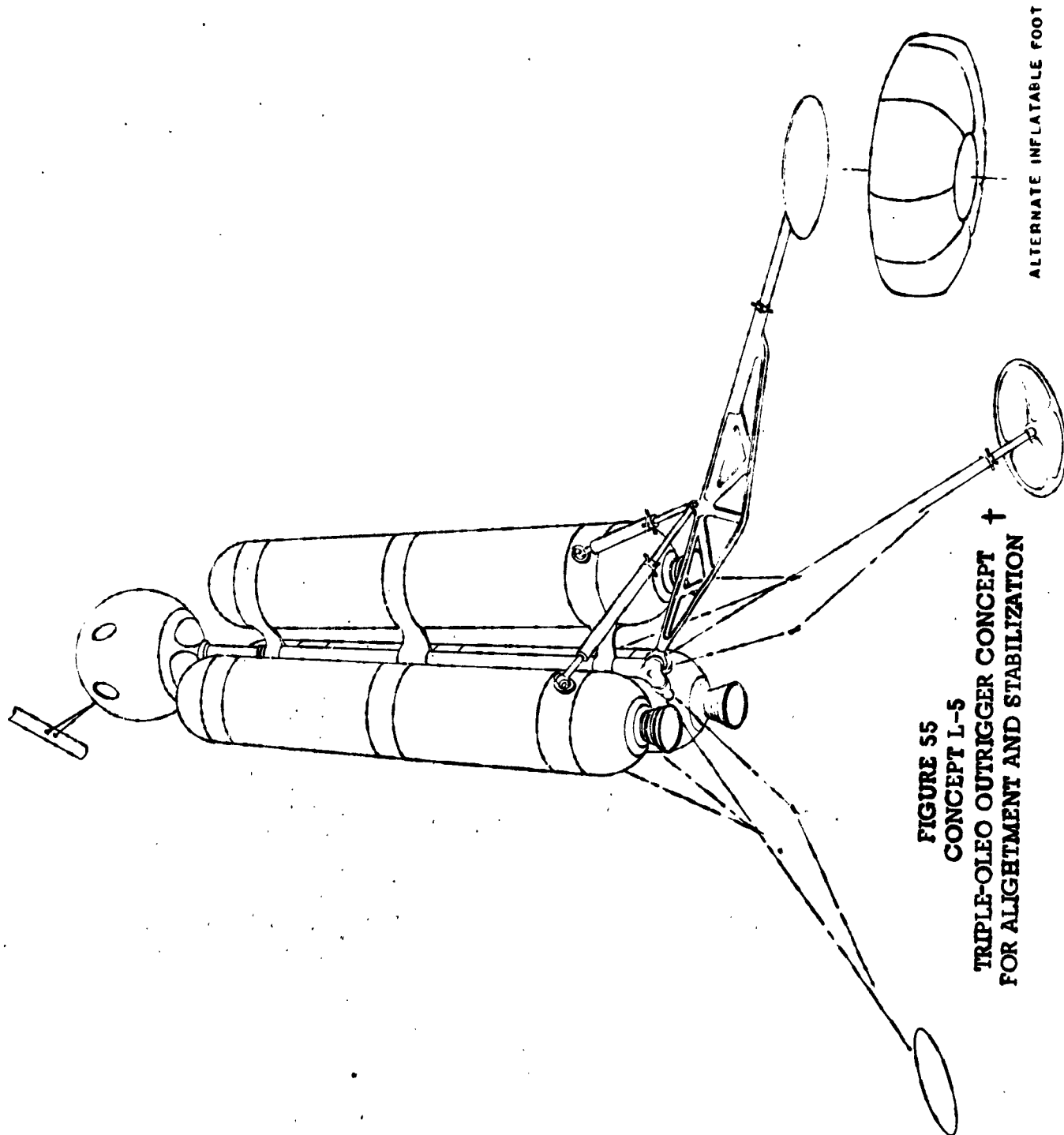
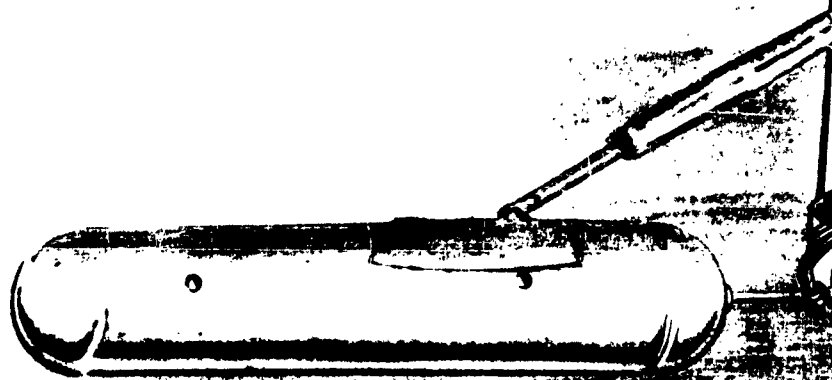


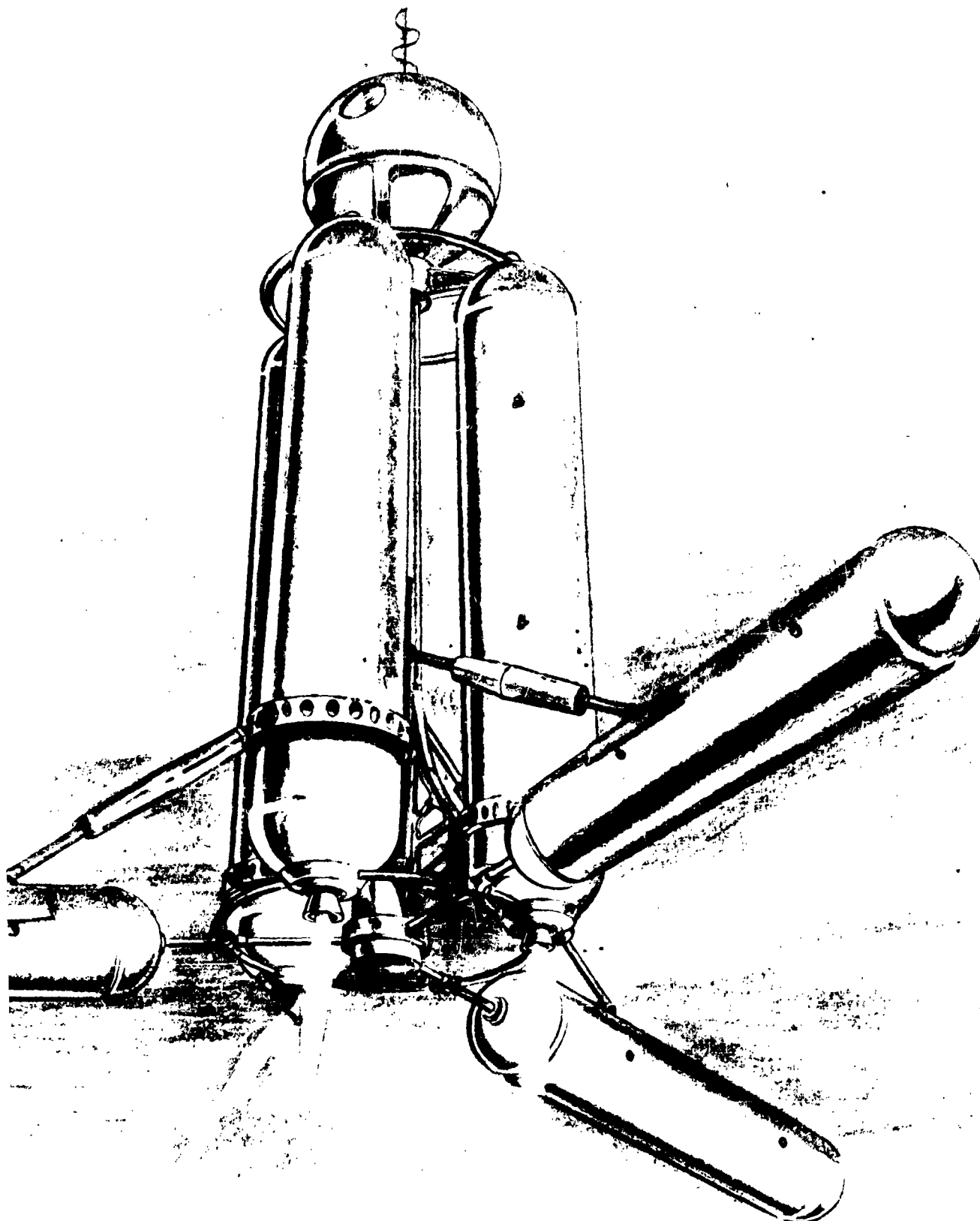
FIGURE 54
CONCEPT L-4
VEHICLE ERECTION ON LUNAR SURFACE
86





1





2

FIGURE 56
CONCEPT L-6
SECONDARY PROPELLANT TANKS SERVING AS ENERGY ABSORBERS

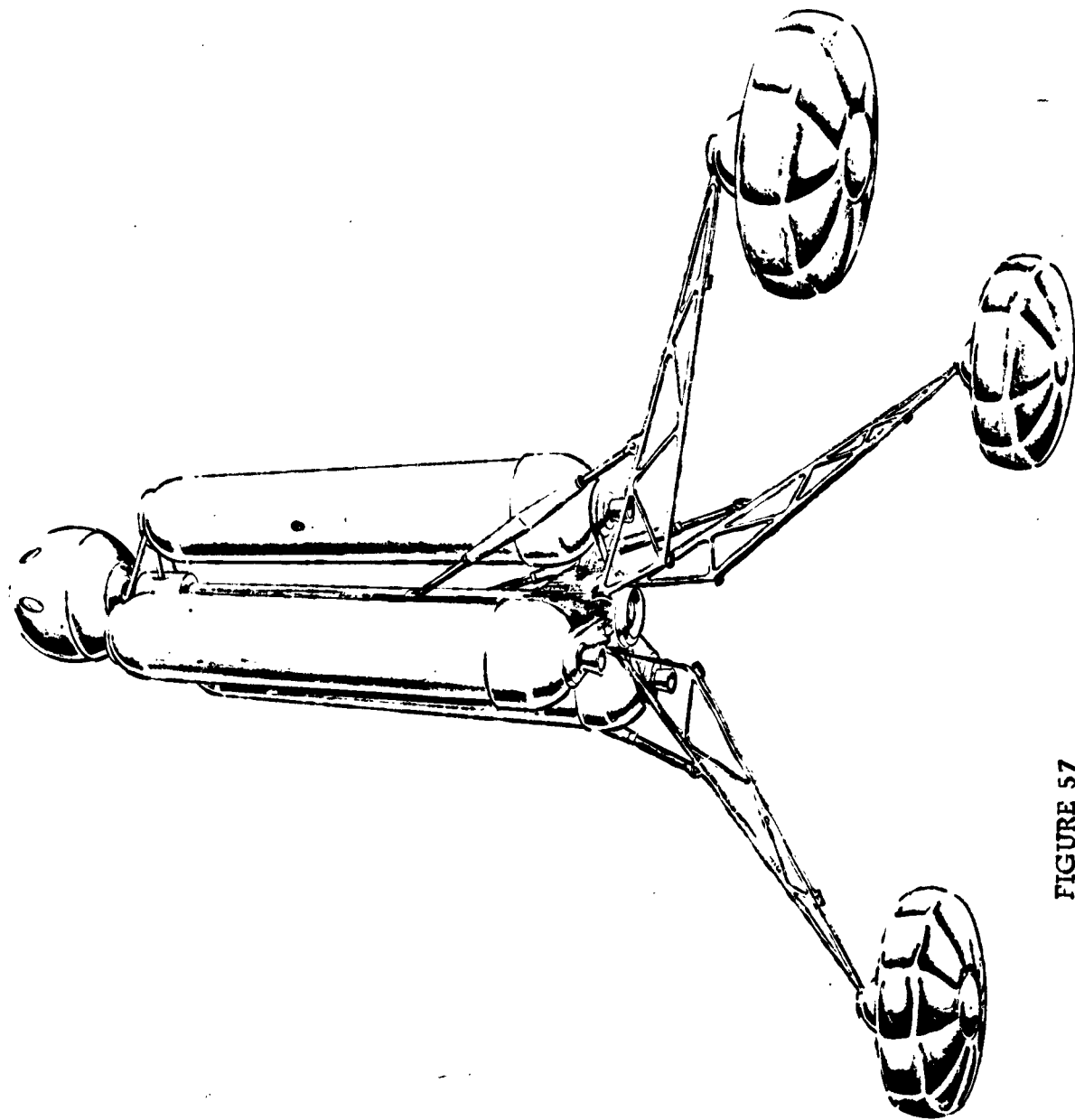
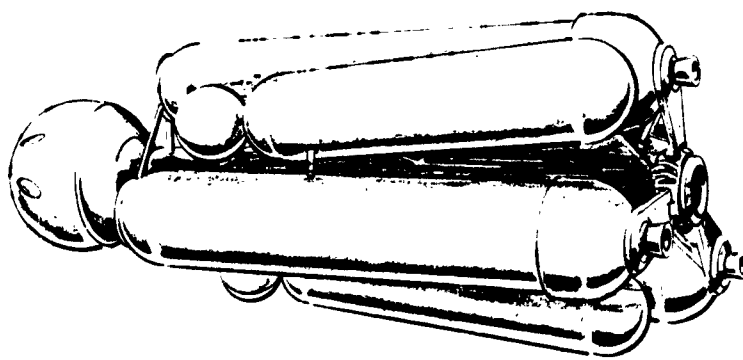


FIGURE 57
CONCEPT L-7
LARGE AREA INFLATABLE FEET FOR ACCOMMODATING SOFT LUNAR SURFACE †

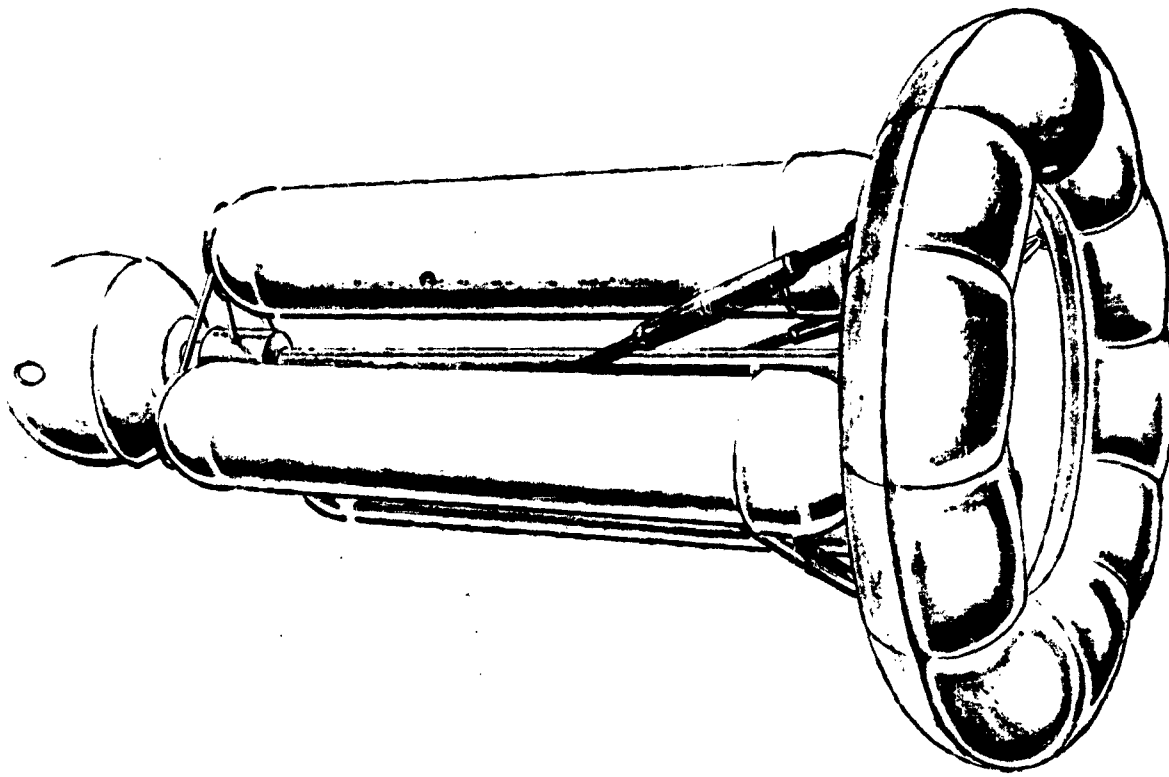
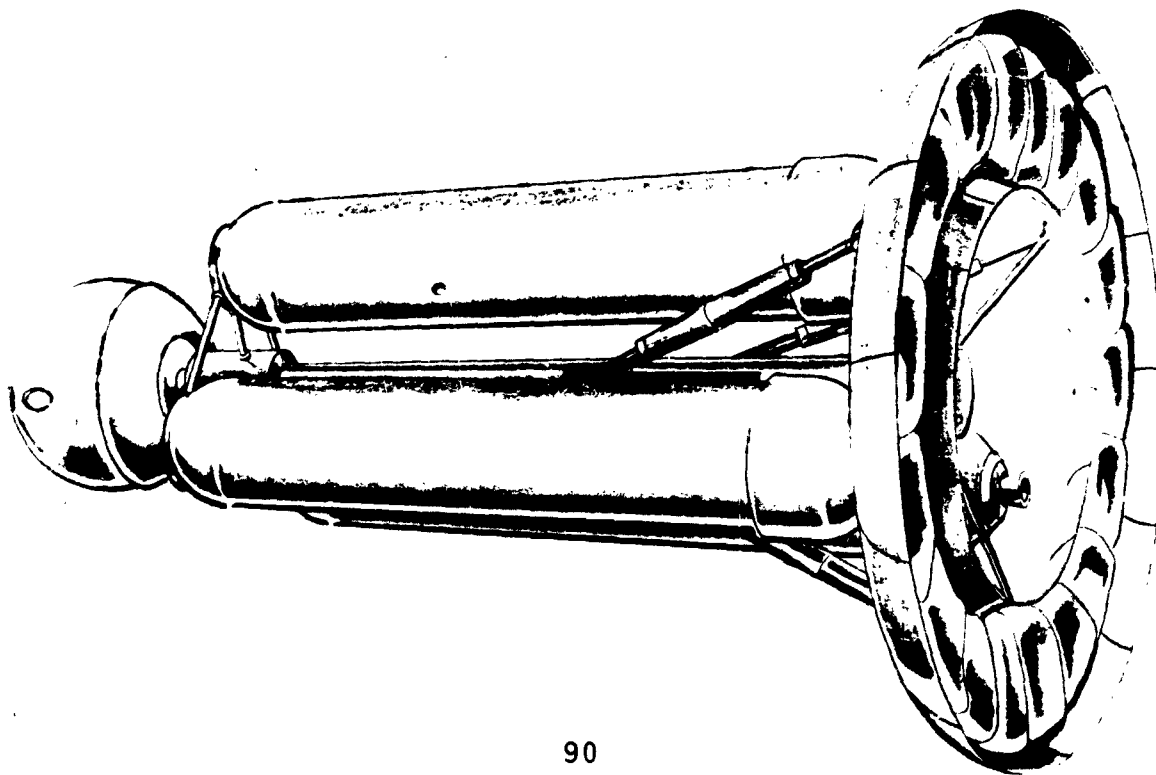


FIGURE 58
CONCEPT L-8
ALIGNMENT ON STABILIZING INFLATABLE TORUS BASE

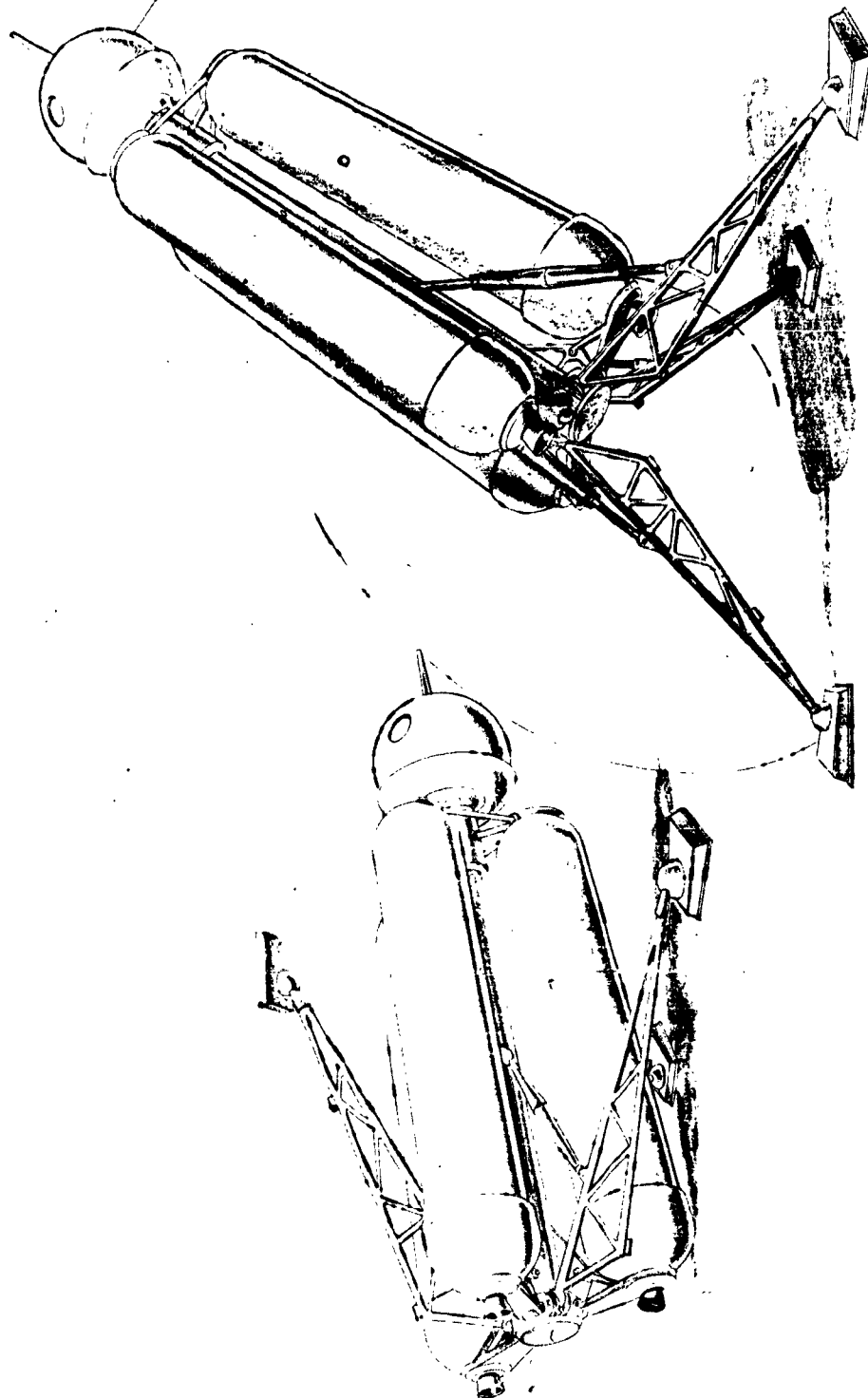


FIGURE 59
CONCEPT L-9
LUNAR ERECTION WITH TRI-OLEO OUTRIGGERS

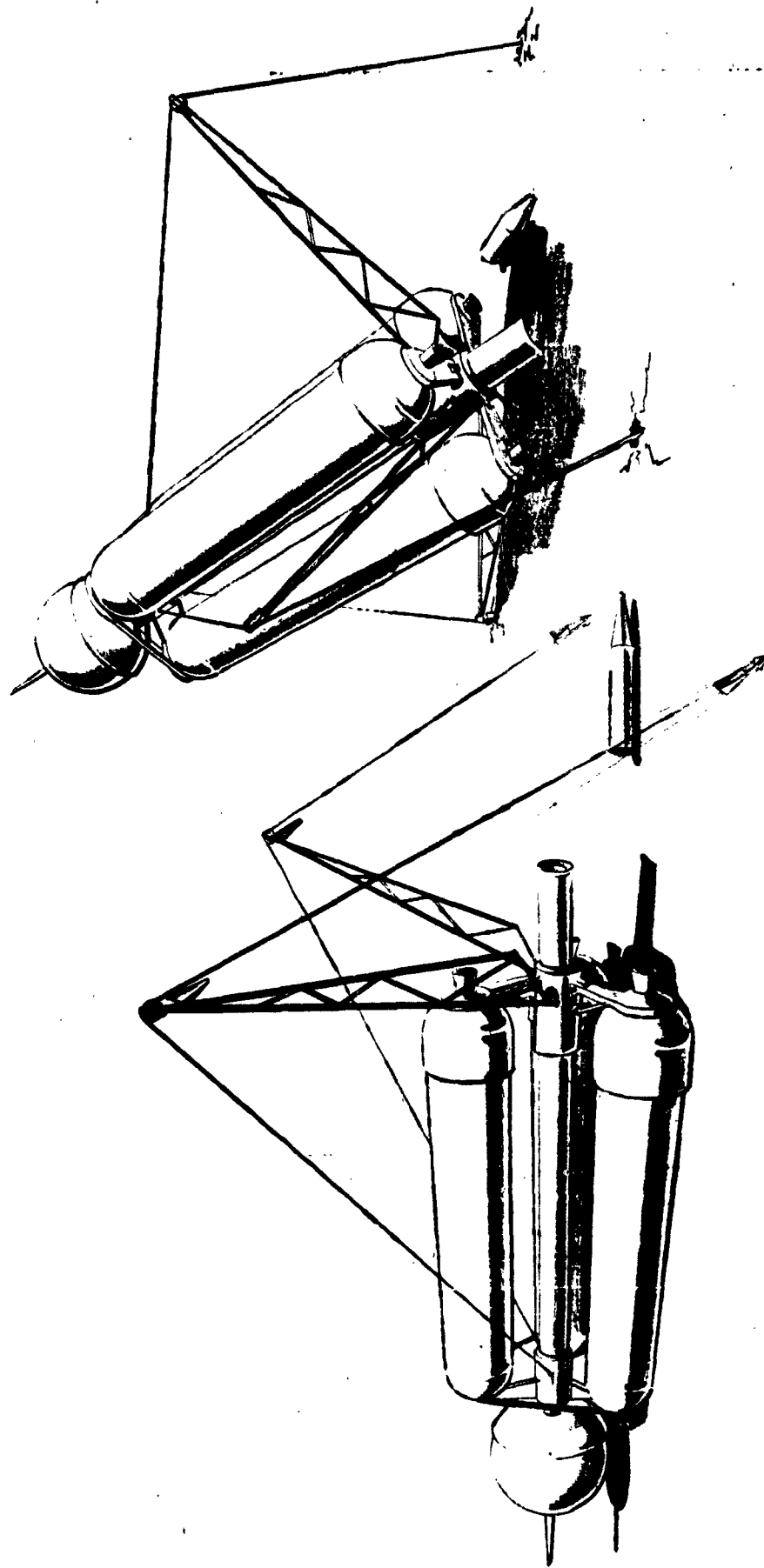


FIGURE 60
CONCEPT L-10
LUNAR ERECTION USING IMBEDMENT ANCHORS AND OUTRIGGERS

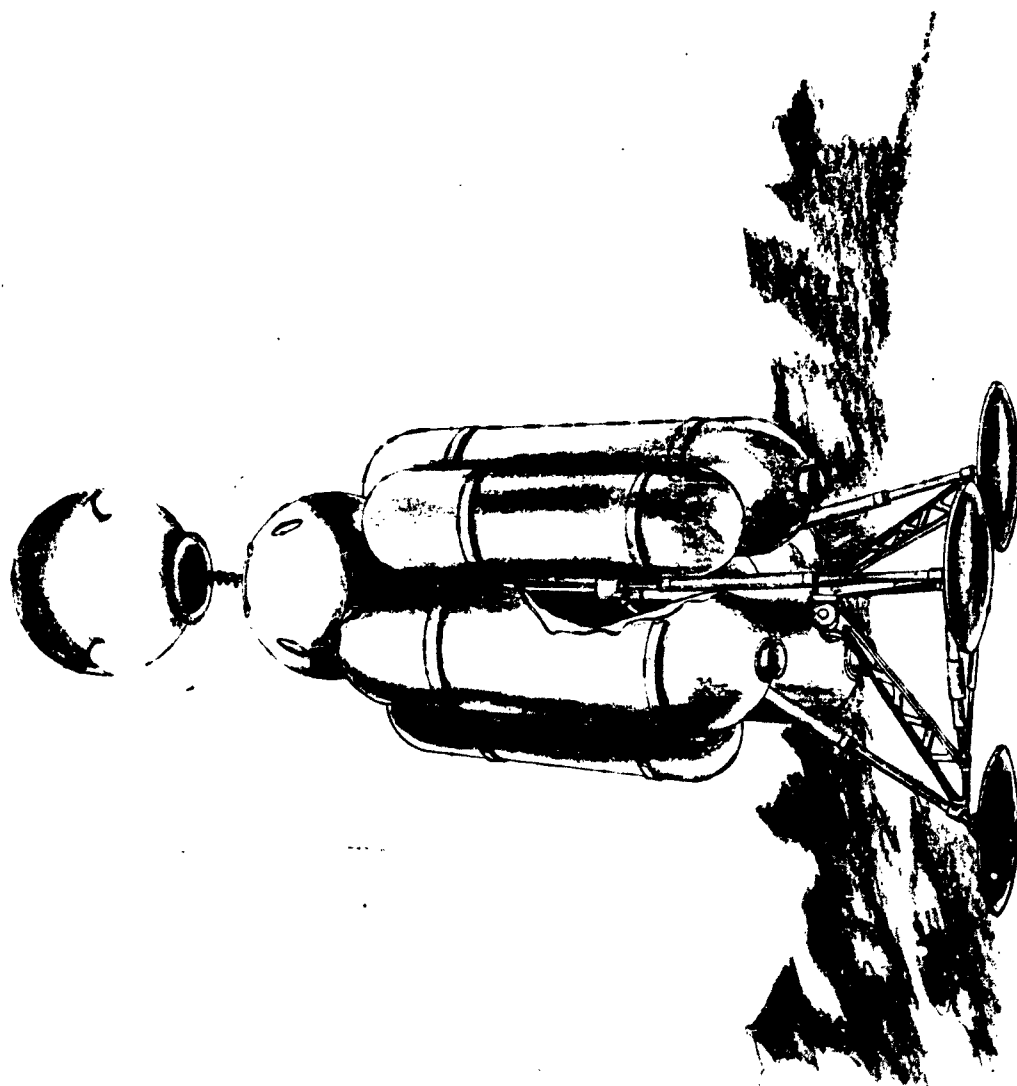
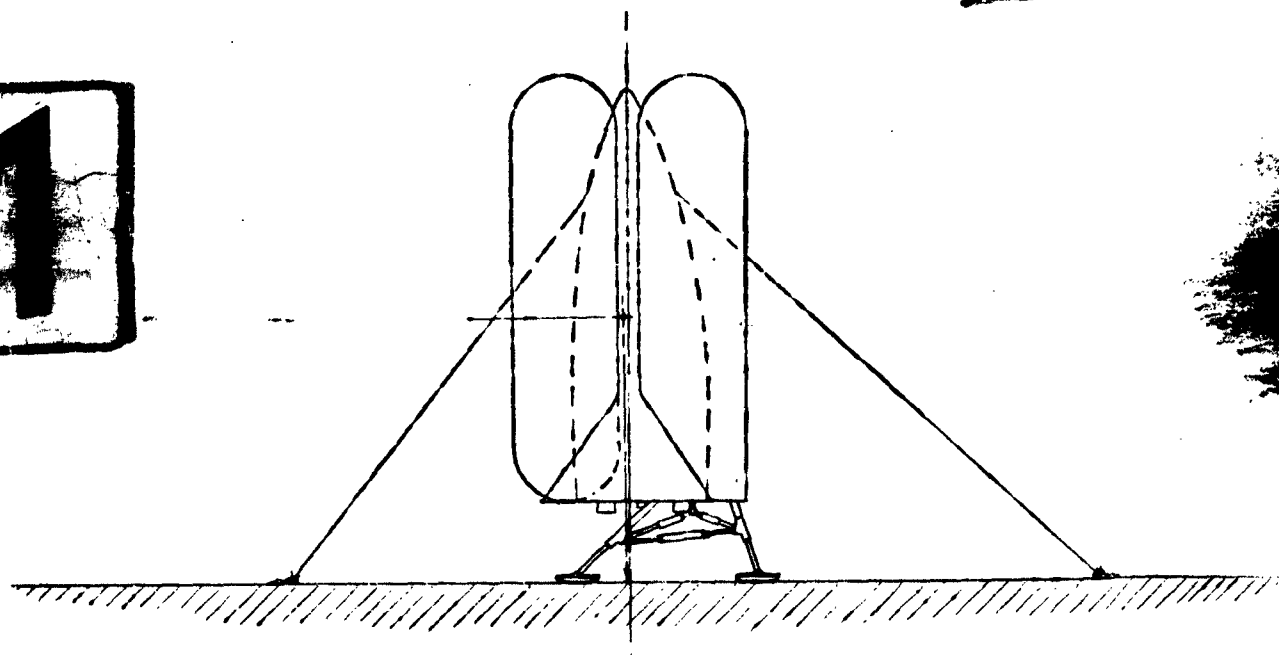
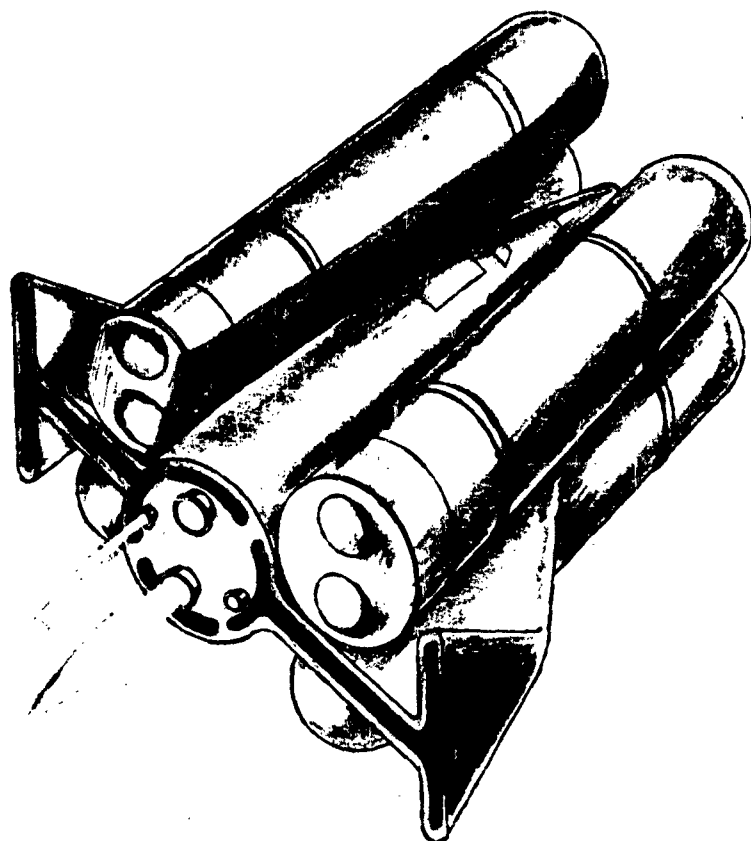


FIGURE 61
CONCEPT L-11
TRAIN ALIGNMENT - PAYLOAD SETTLED AT REDUCED IMPACT



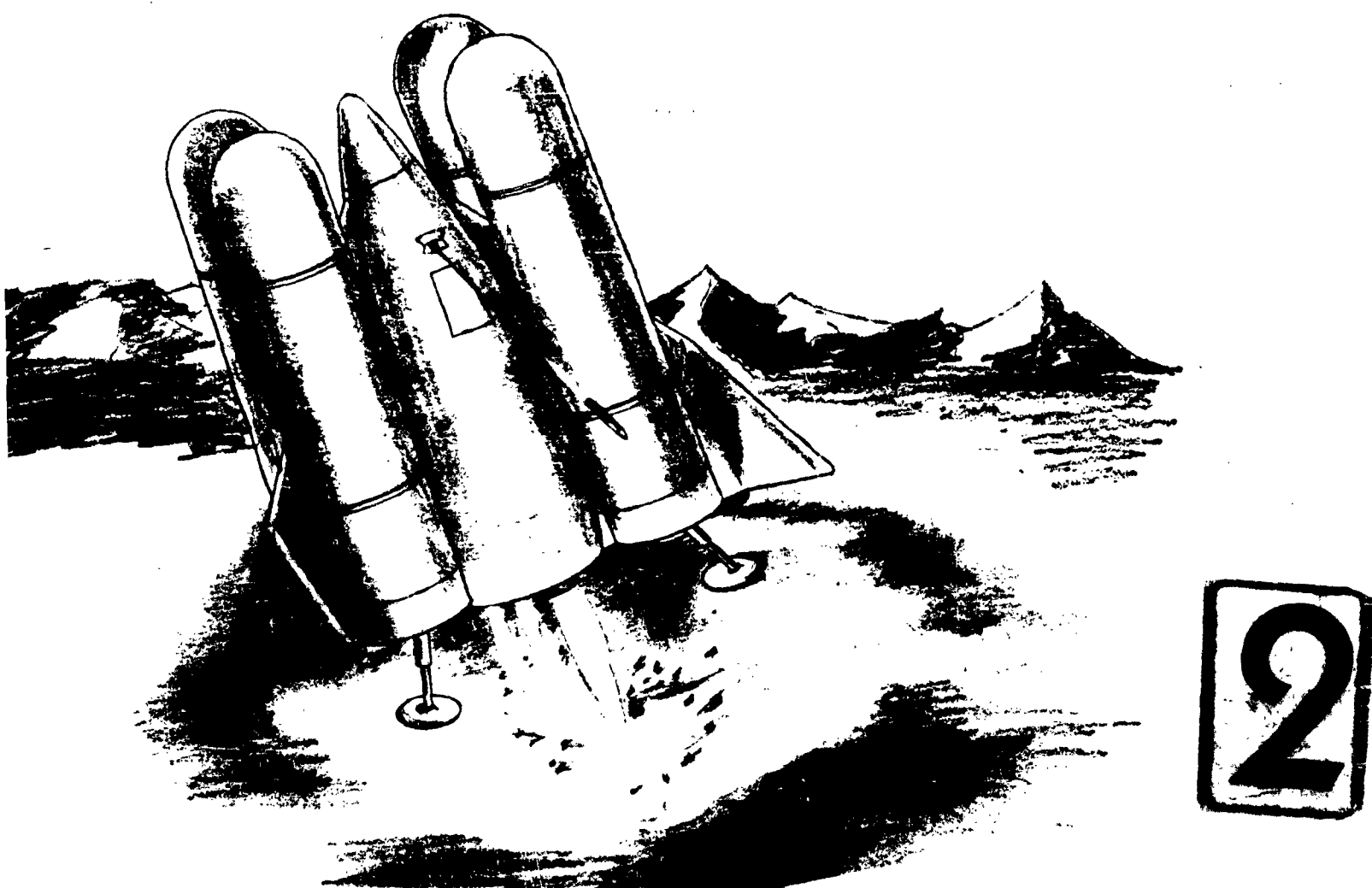


FIGURE 62
CONCEPT L-12
DOUBLE BIPOD STRUT SYSTEM FOR ALIGHTMENT WITH ANCHOR STABILIZATION

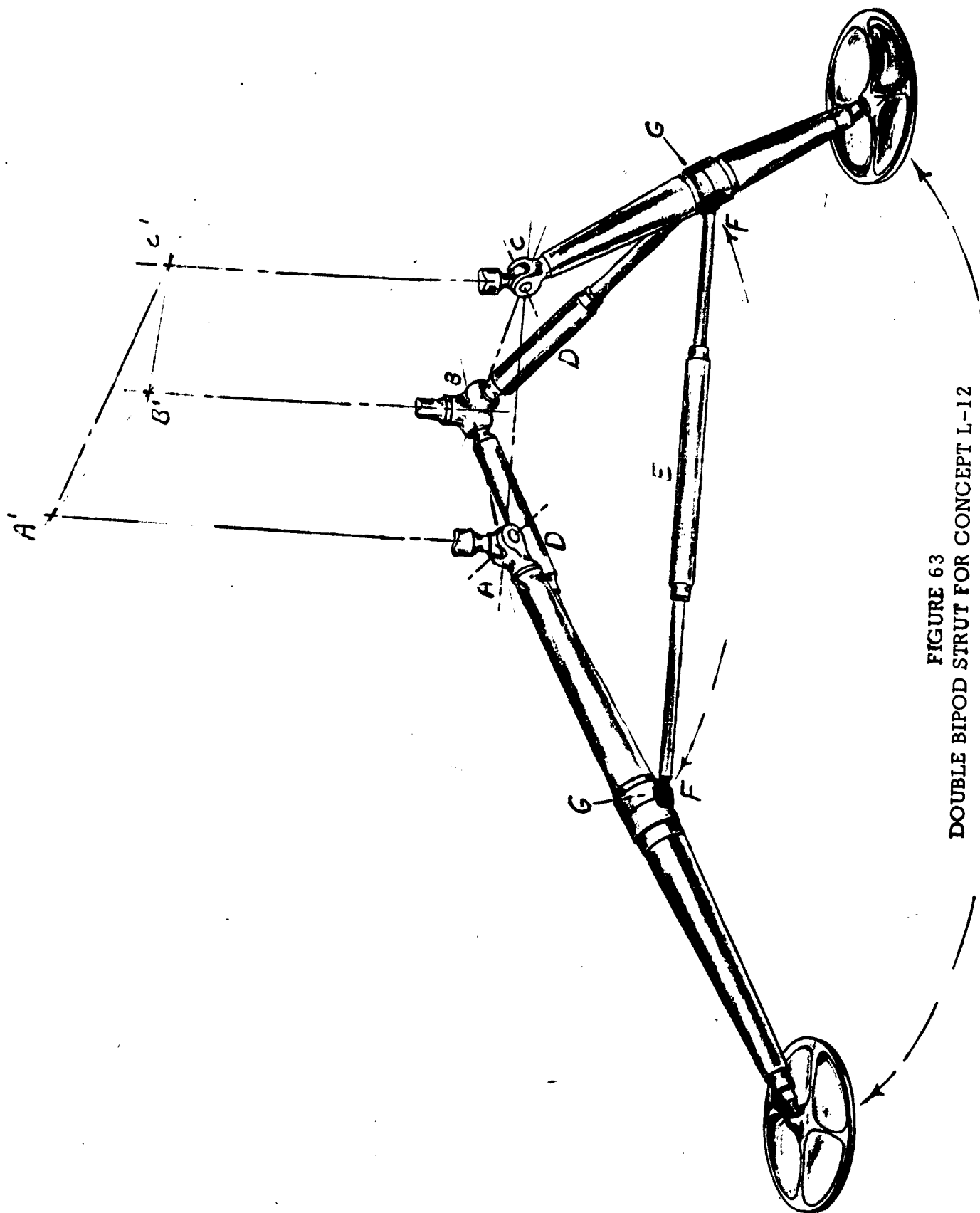


FIGURE 63
DOUBLE BIPOD STRUT FOR CONCEPT L-12

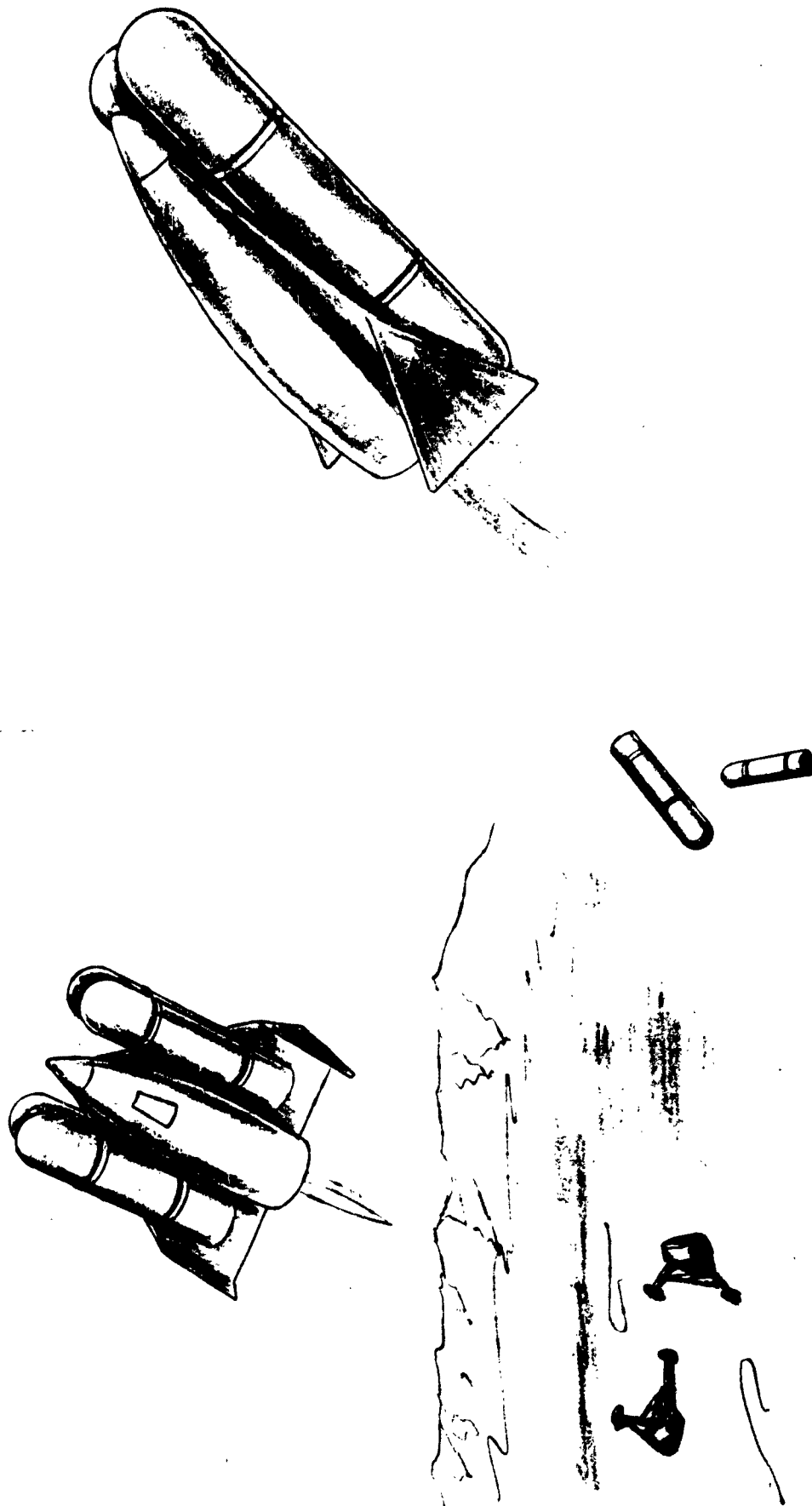


FIGURE 64
CONCEPT L-13
DEPARTURE FROM DOUBLE BIPOD STRUT PLATFORM

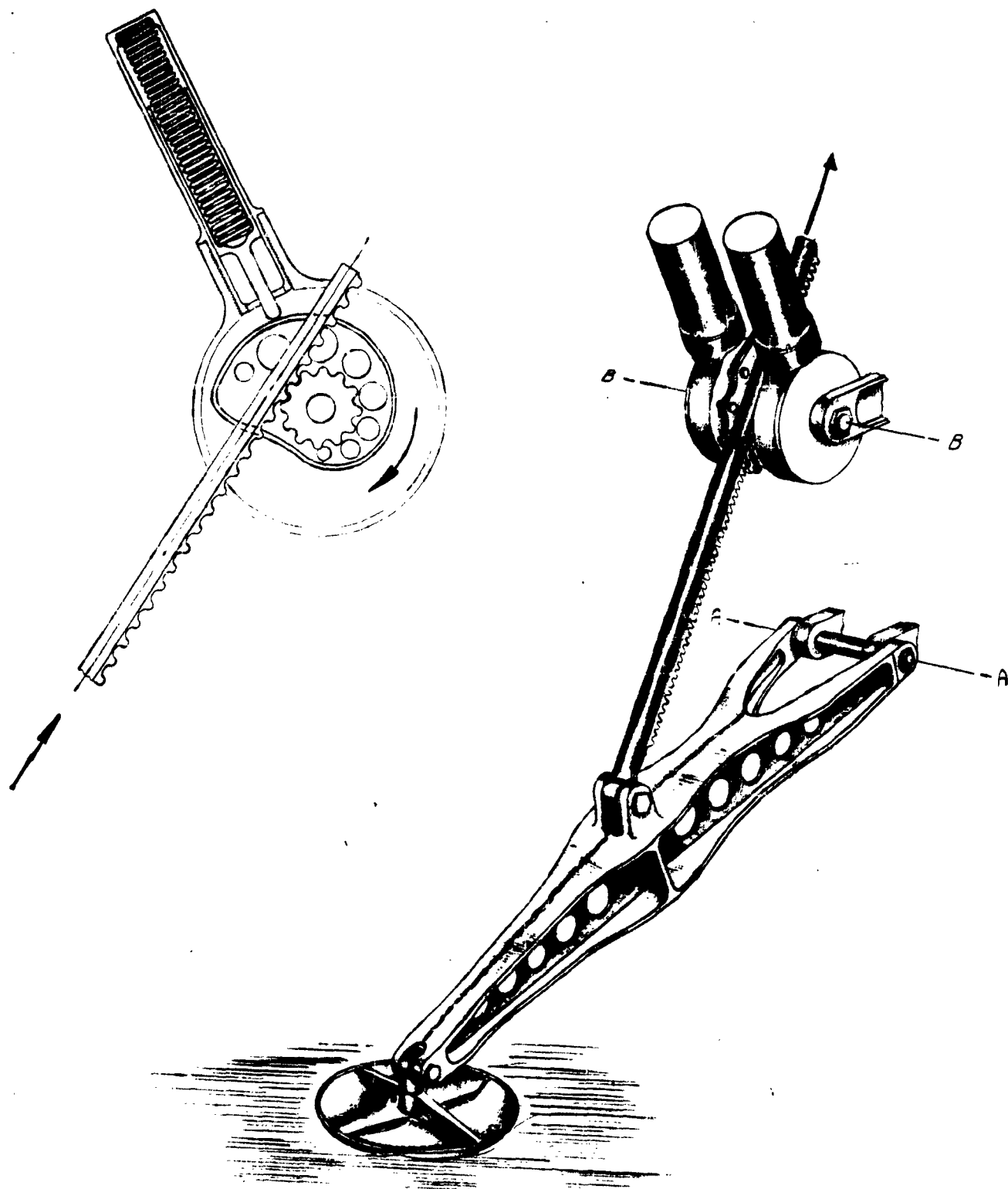


FIGURE 65
CONCEPT L-14
RACK AND PINION CYCLING SPRING FOR MECHANICAL SHOCK ABSORPTION

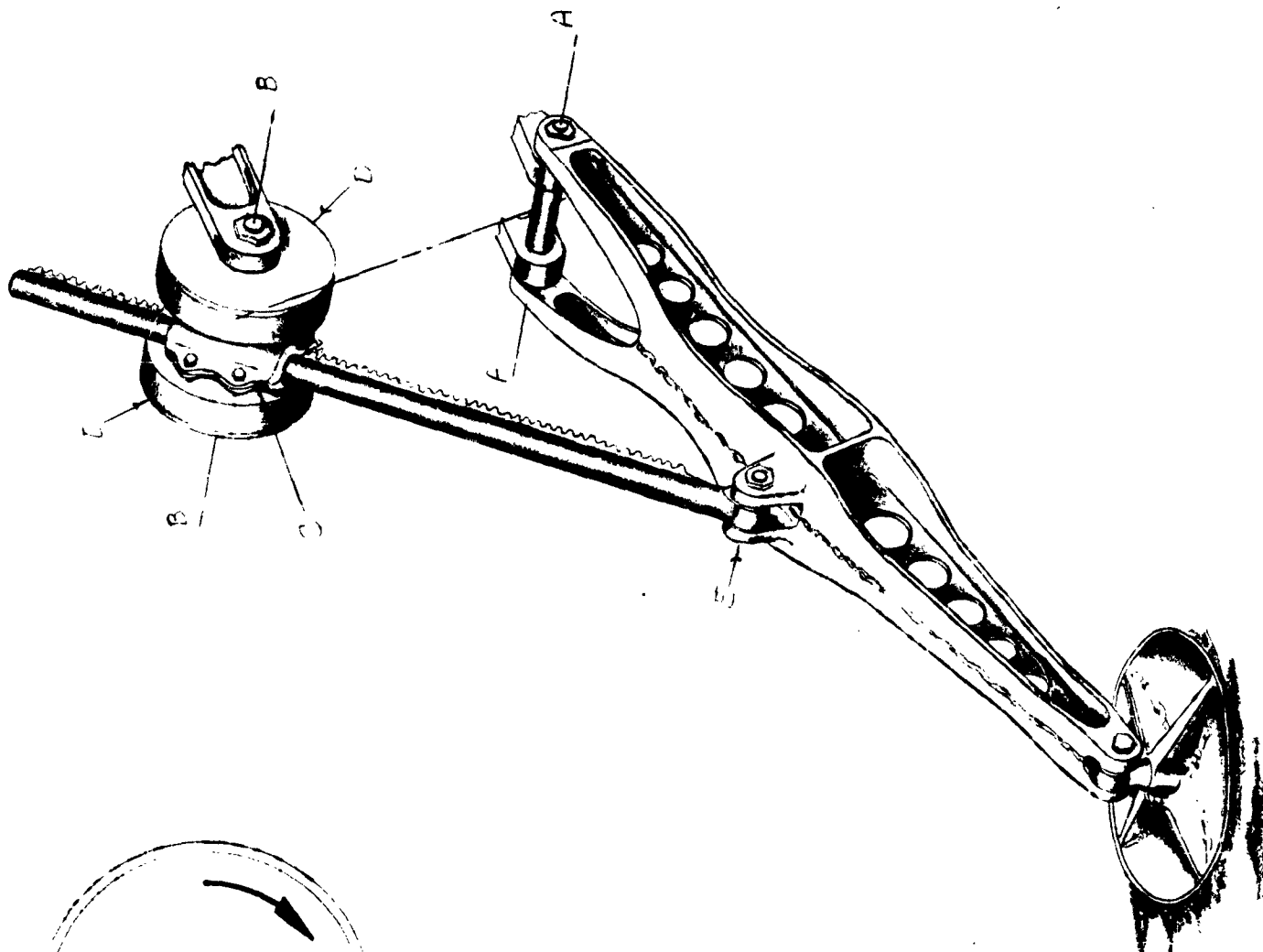
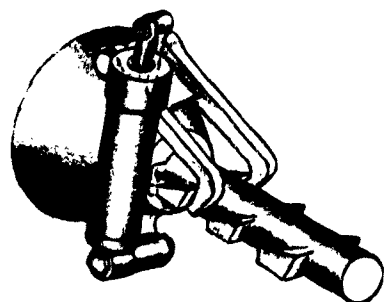
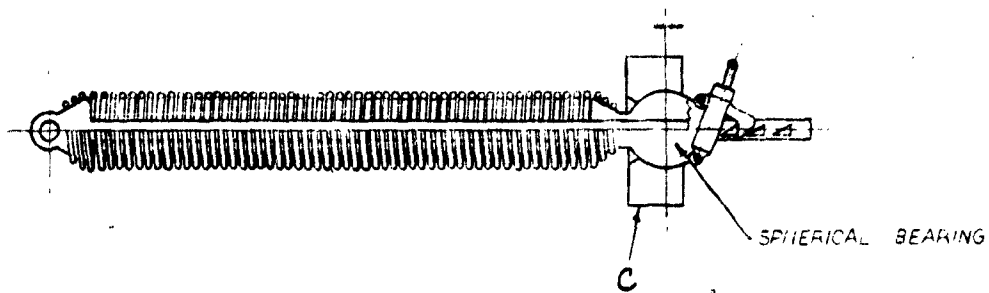


FIGURE 66
CONCEPT L-15
RACK AND PINION DISC BRAKE
FOR MECHANICAL SHOCK ABSORPTION



SPRING "NO BACK"

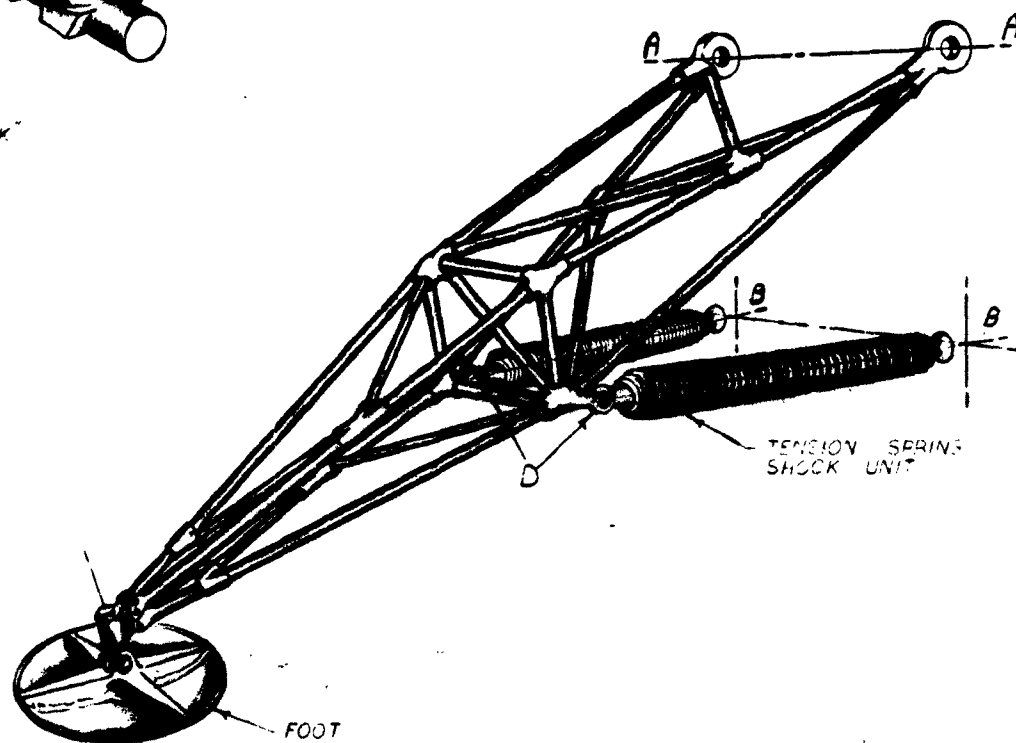
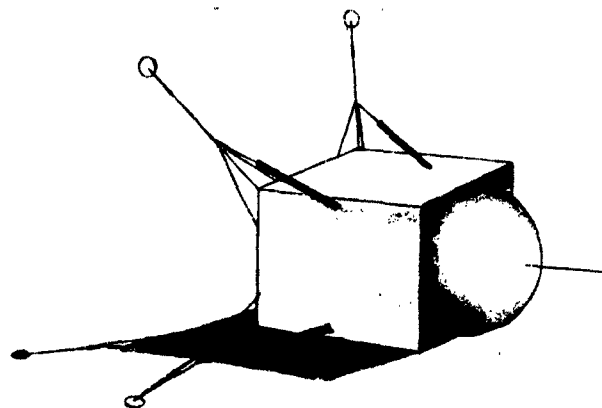
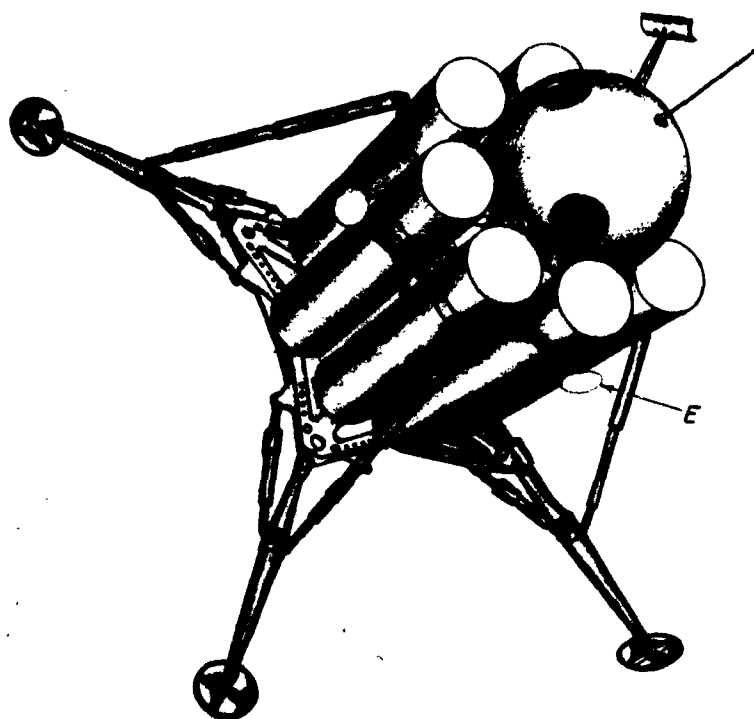
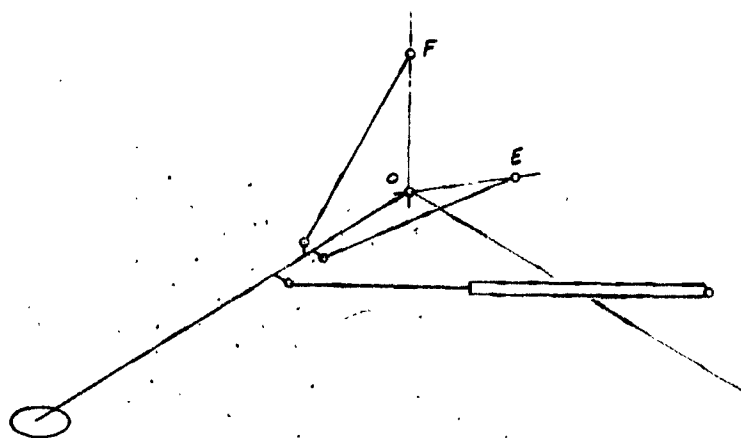


FIGURE 67
CONCEPT L-16
TENSION SPRING OUTRIGGER FOR MECHANICAL SHOCK ABSORPTION



H



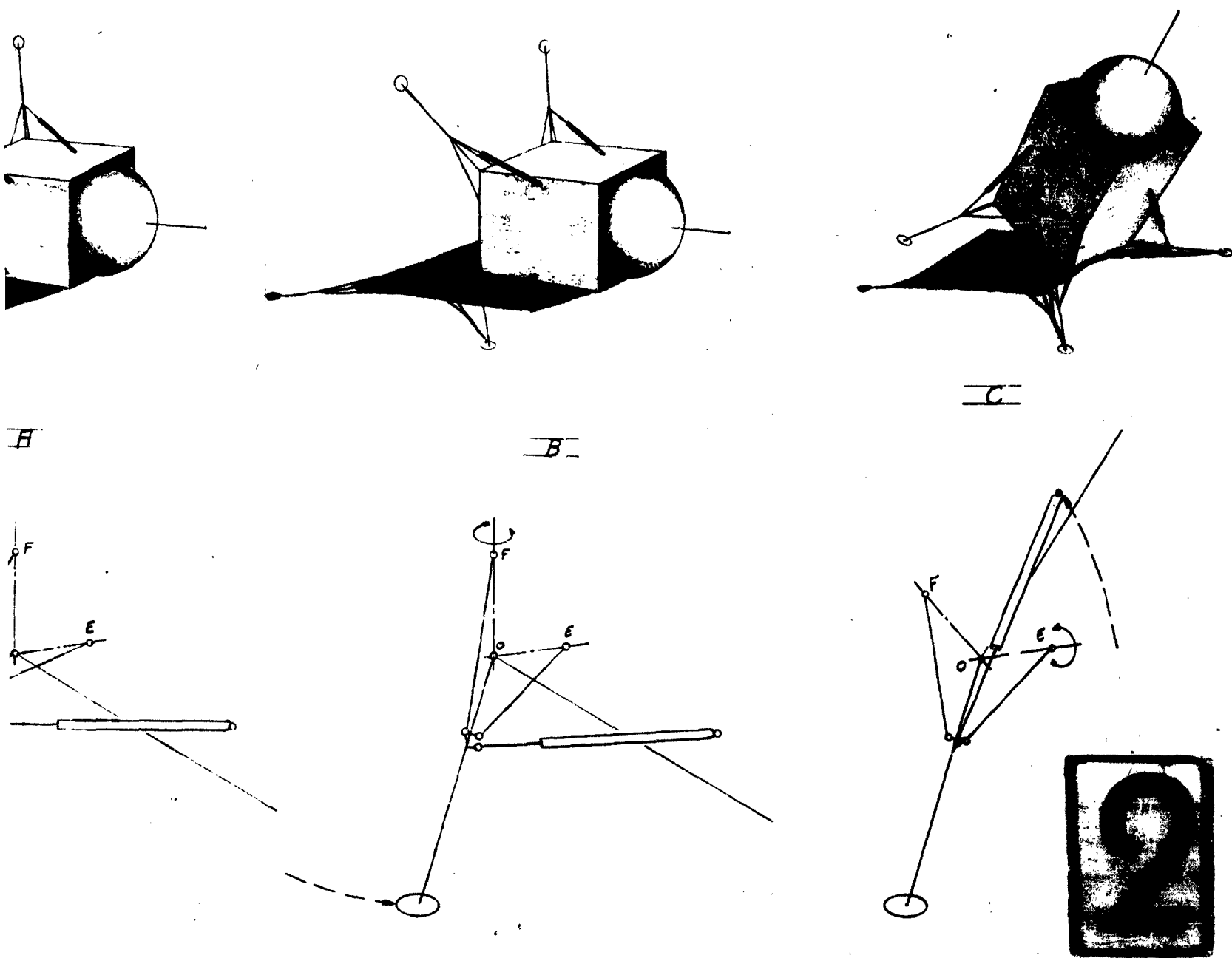


FIGURE 68
CONCEPT L-17
LUNAR ERECTION WITH VARIABLE PIVOT AXIS, 4-STRUT SYSTEM

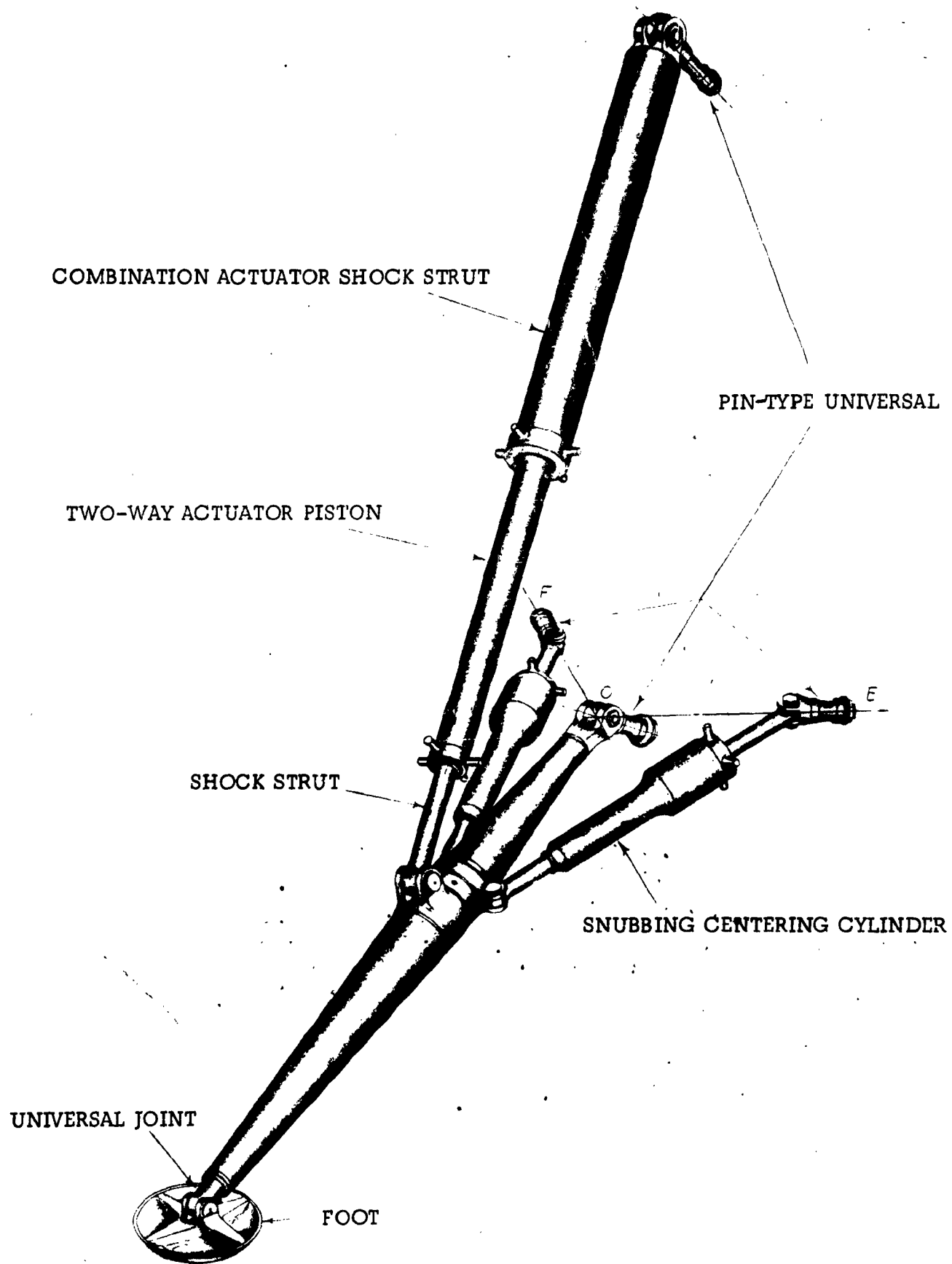


FIGURE 69
VARIABLE PIVOT AXIS SYSTEM FOR CONCEPT L-17

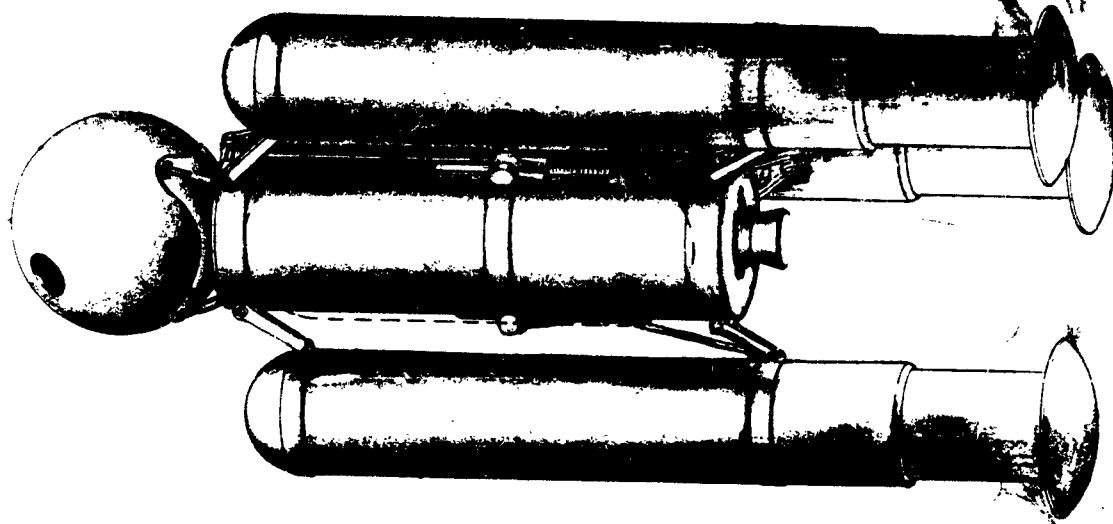
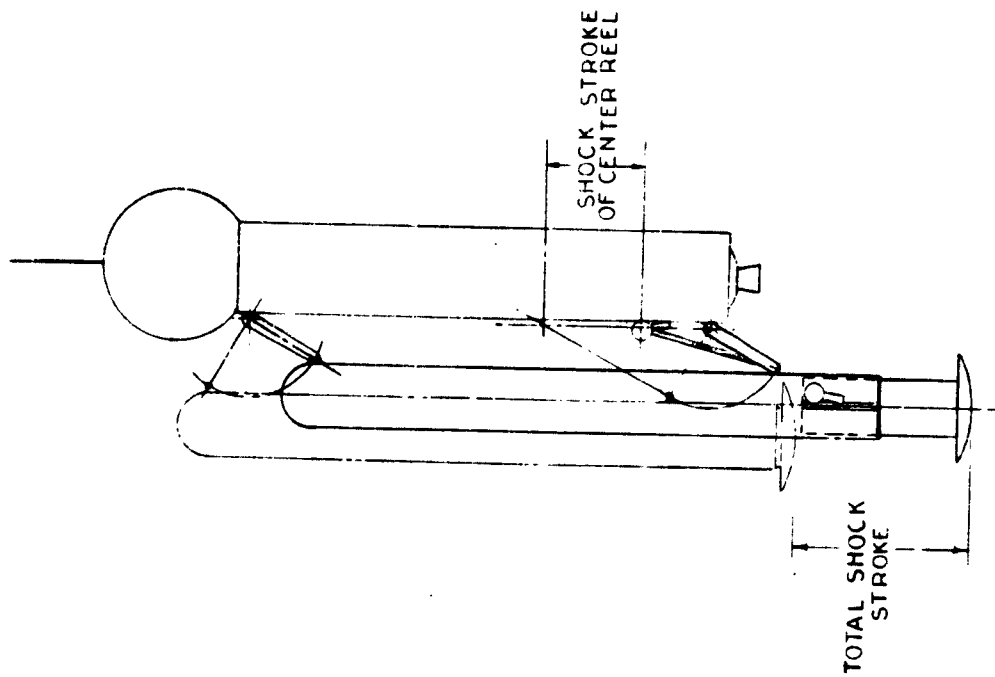


FIGURE 70
CONCEPT L-18
IMPACT ATTENUATION WITH REEL-OUT SHOCK ABSORBERS

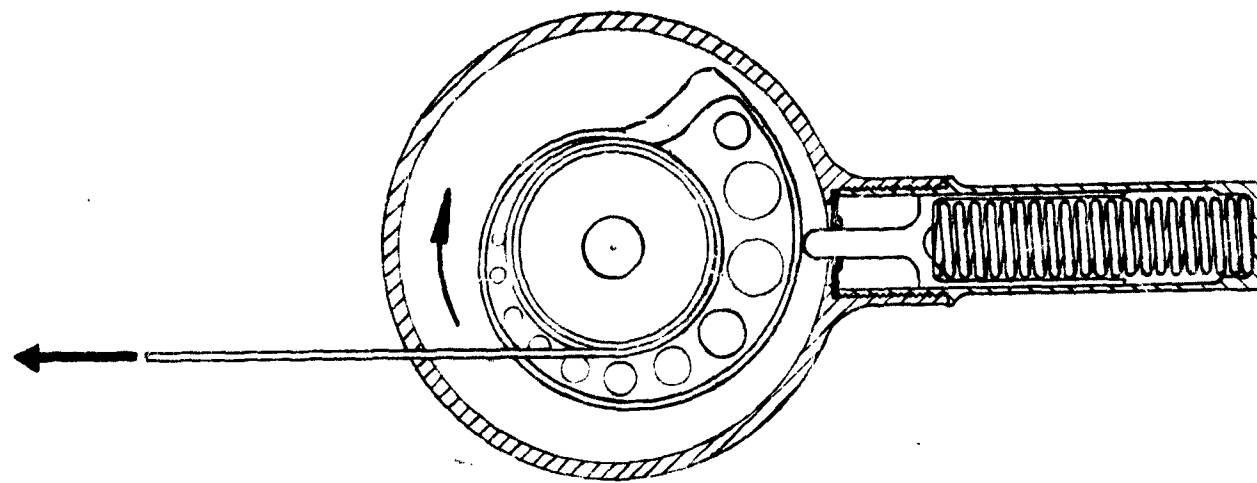
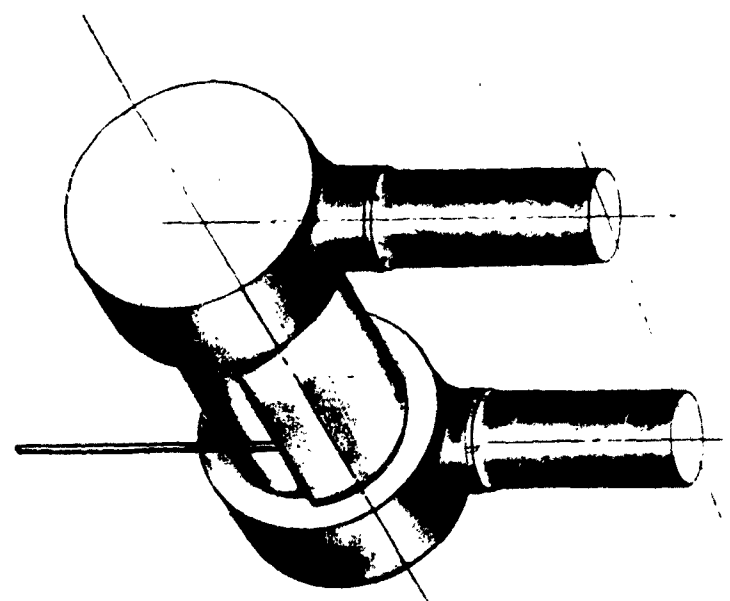


FIGURE 71
REEL-OUT SHOCK ABSORBER FOR CONCEPT L-18

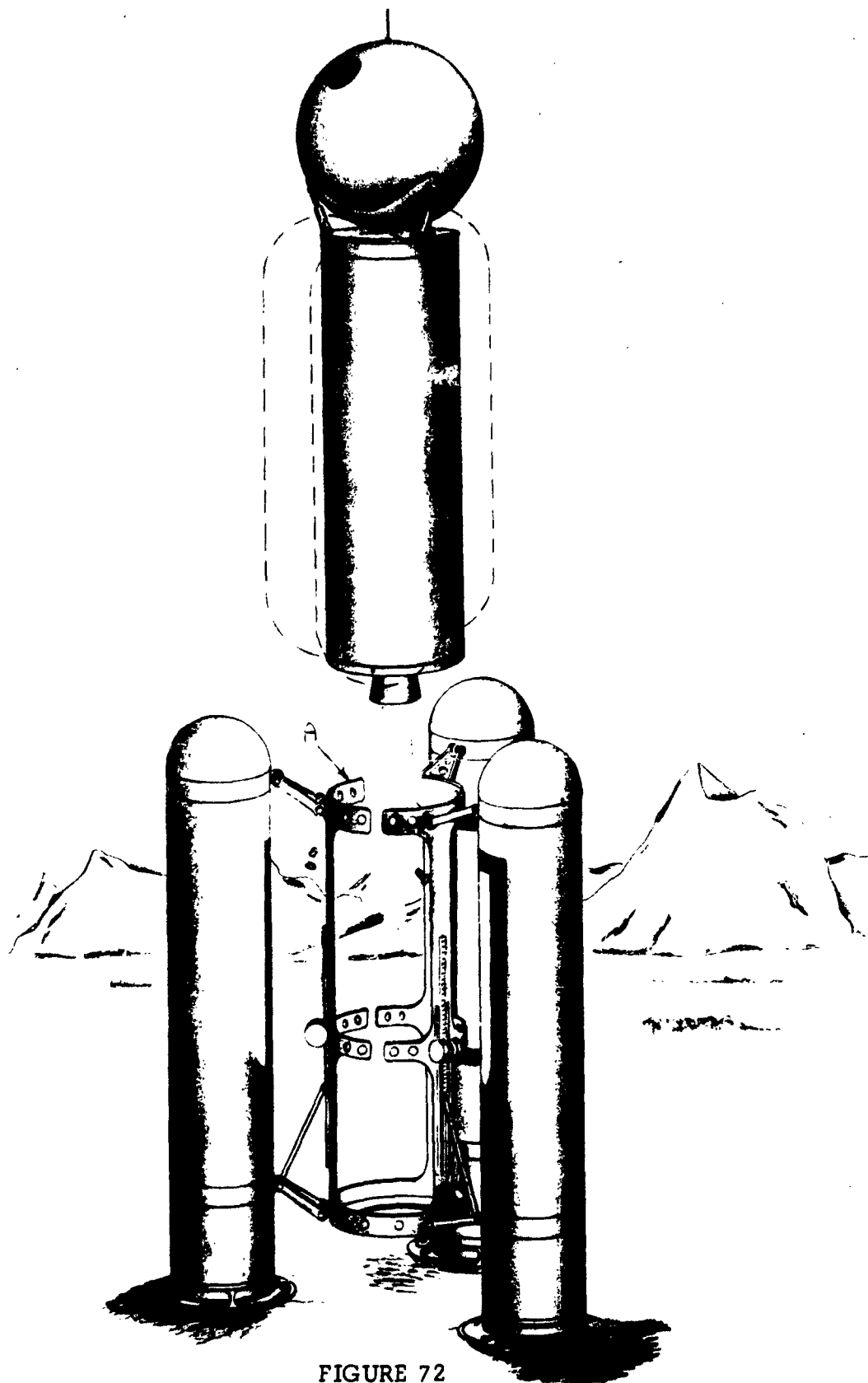
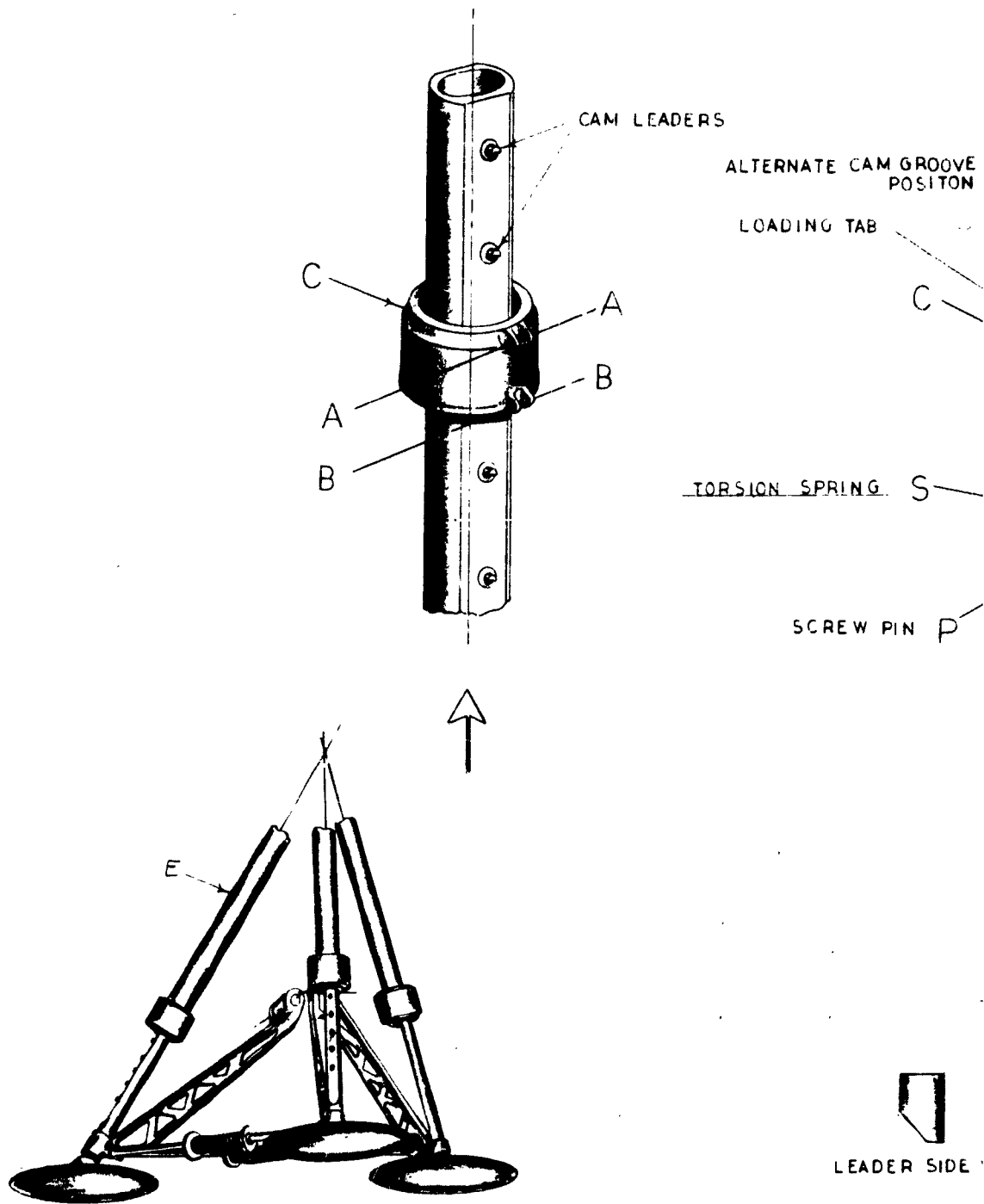
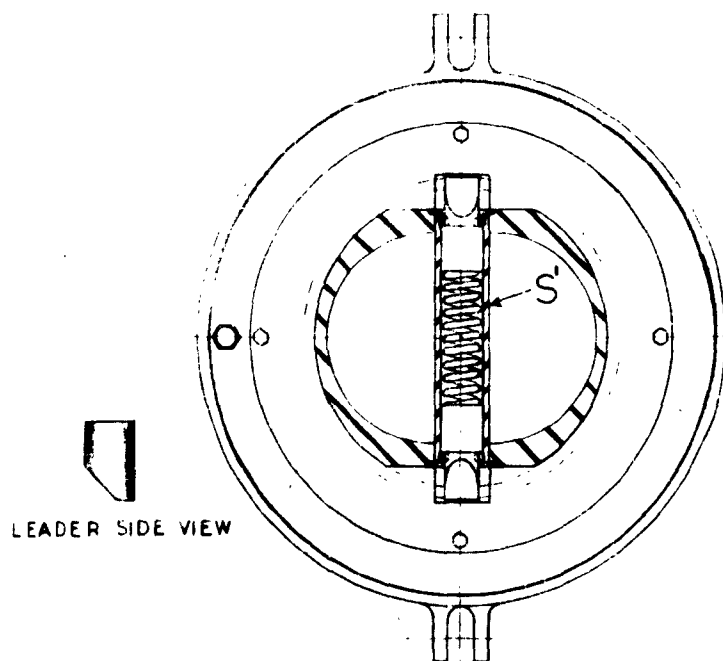
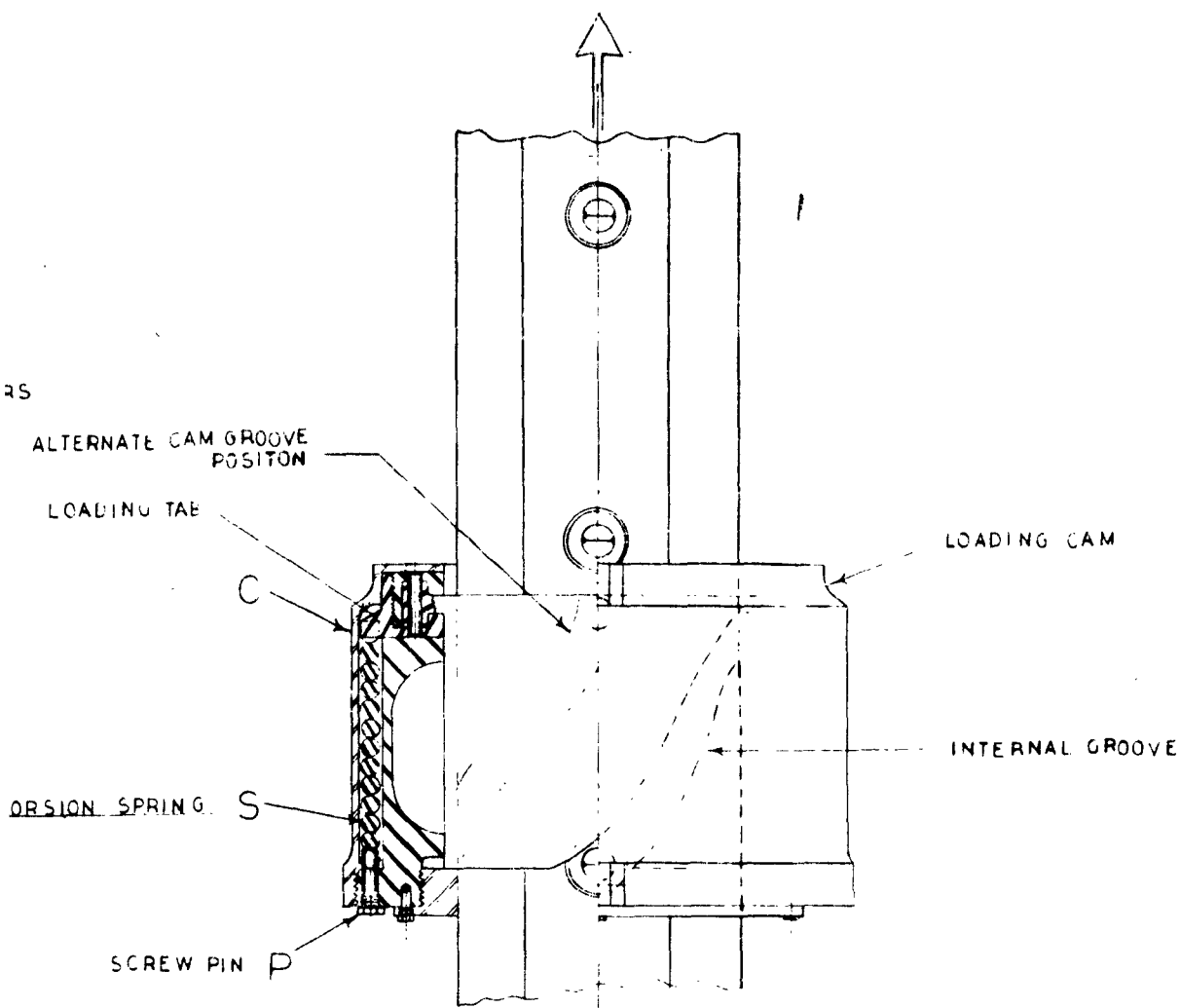


FIGURE 72
CONCEPT L-19
LUNAR DEPARTURE ASSIST FROM TANK PLATFORM†

1

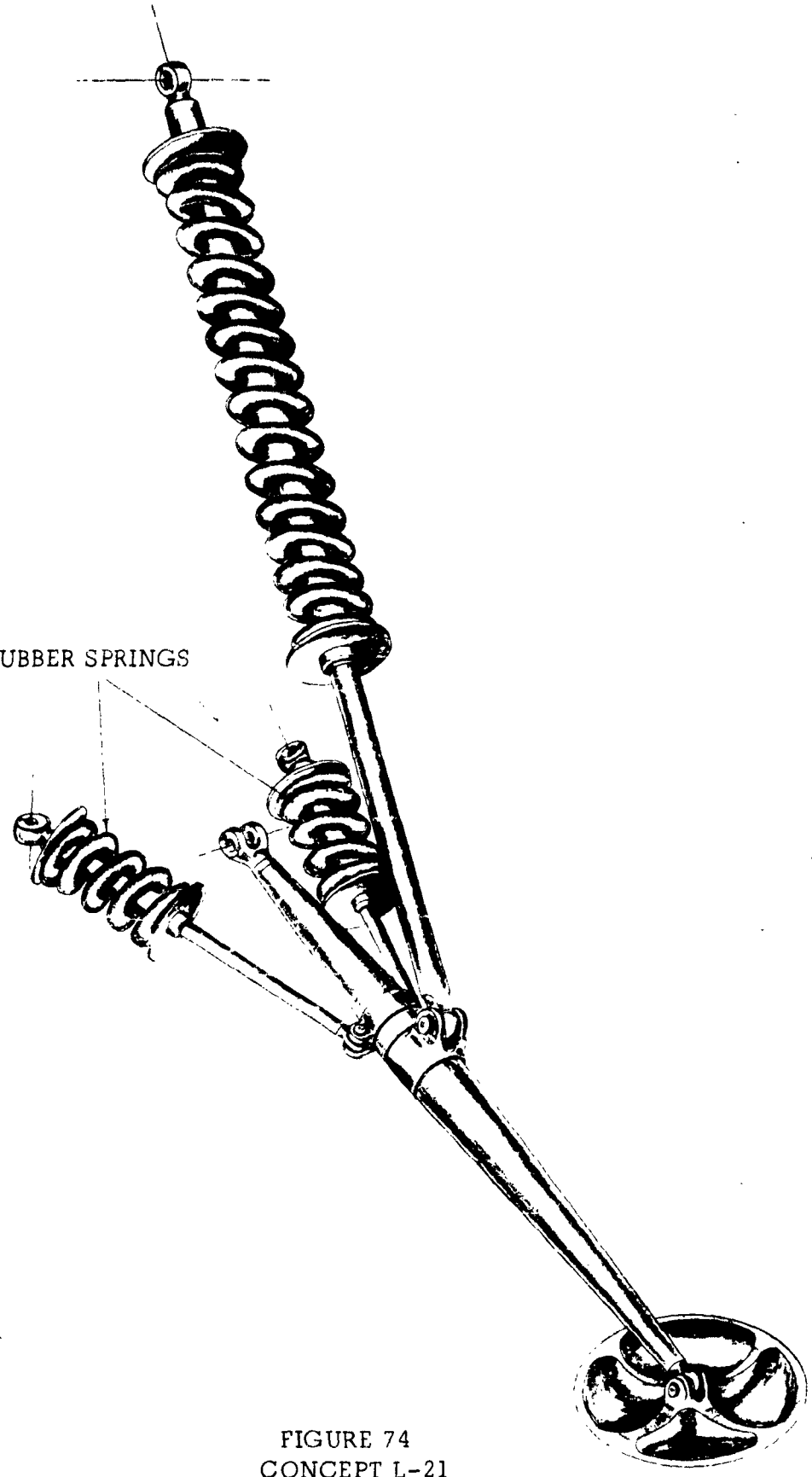


RS



2

FIGURE 73
CONCEPT L-20
TORSION SPRING SHOCK ABSORBER



SNUBBER SPRINGS

FIGURE 74
CONCEPT L-21
MECHANICAL COMPRESSION BUNGEE-OUTRIGGER ENERGY ABSORBER

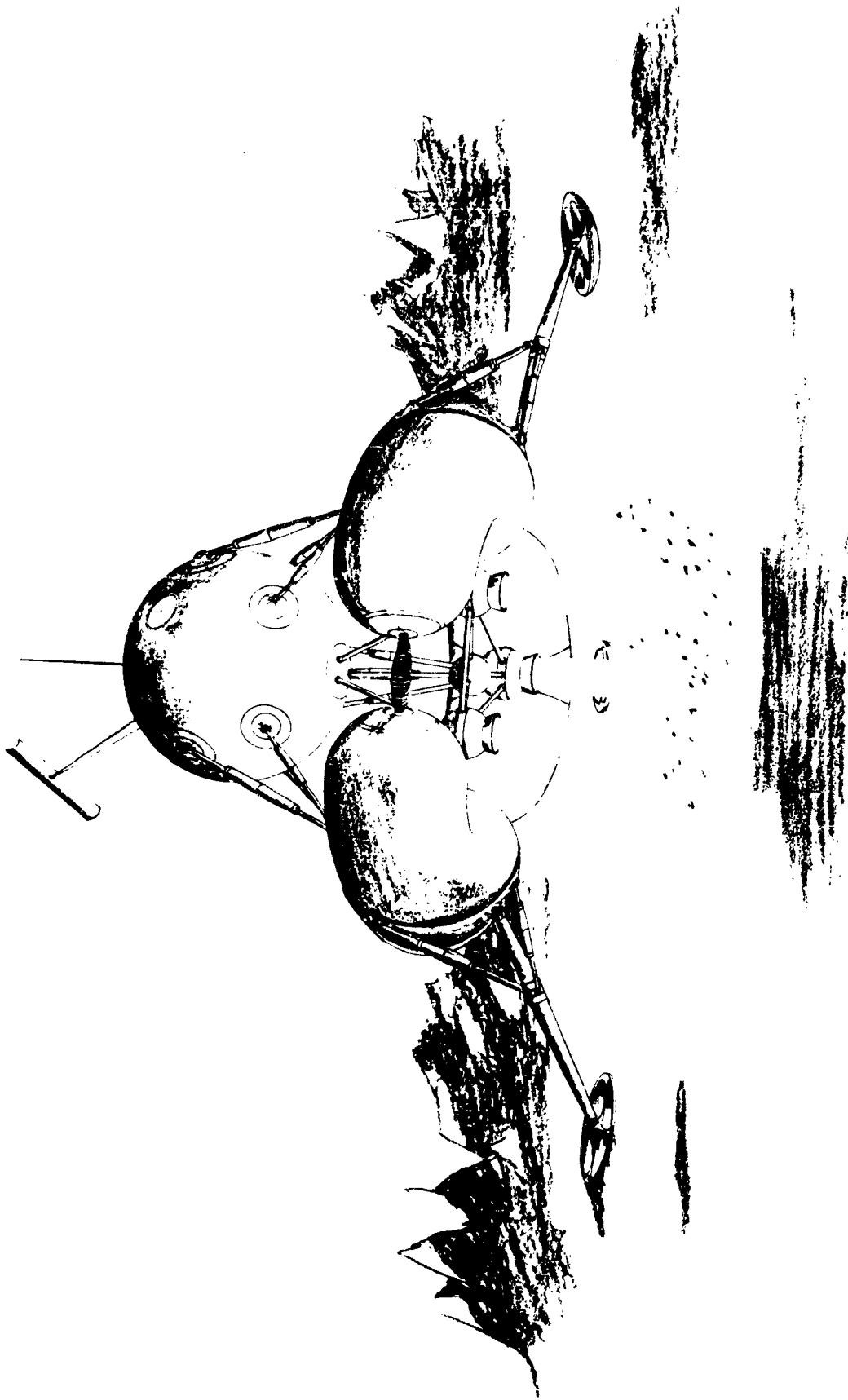


FIGURE 75
CONCEPT L-22
SHOCK ABSORPTION SYSTEM FOR LARGE HORIZONTAL VELOCITY COMPONENT
SEPARATELY MOUNTED PAYLOAD

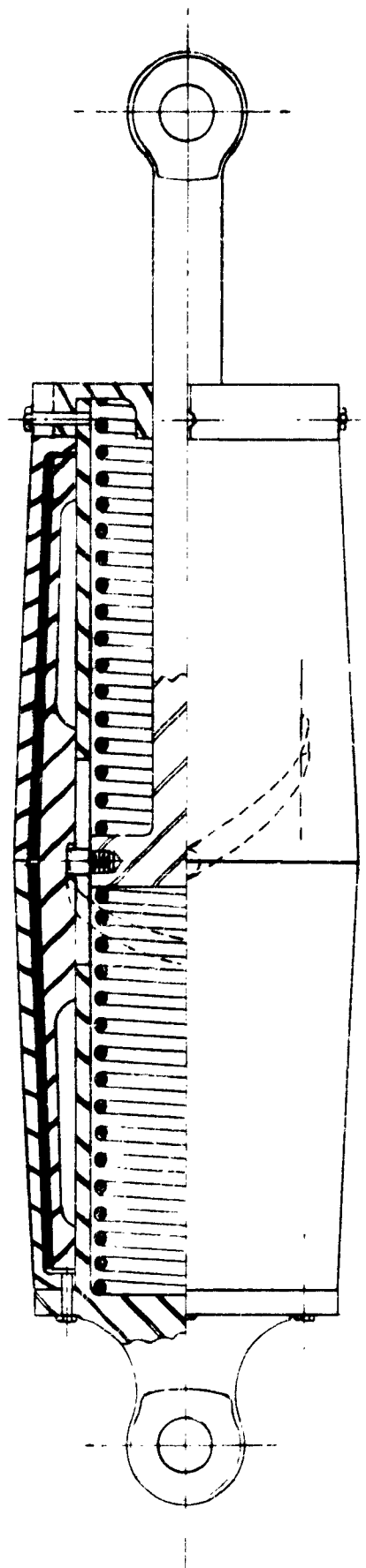


FIGURE 76
SELF-CENTERING SHOCK MITIGATION CYLINDER FOR CONCEPT L-22

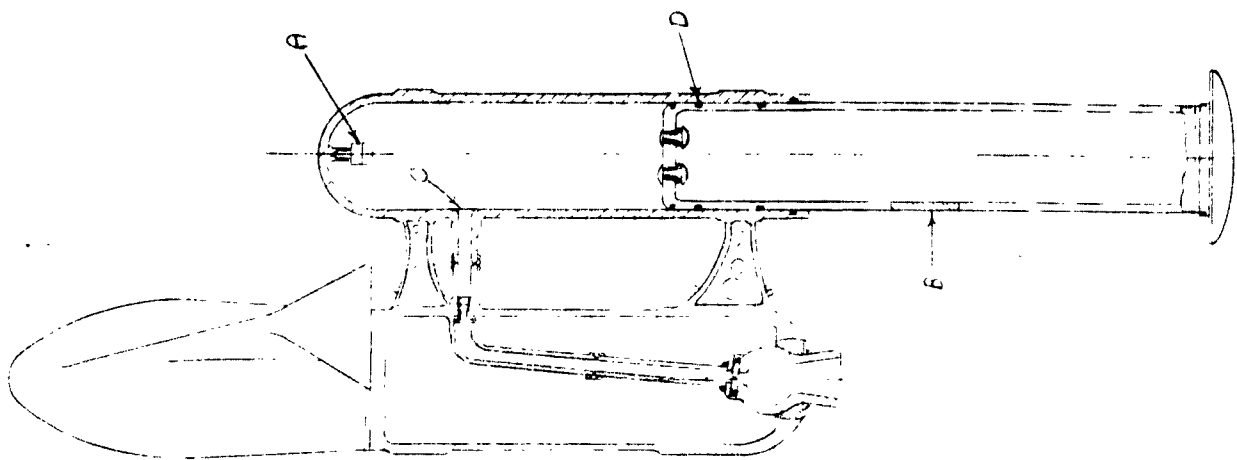
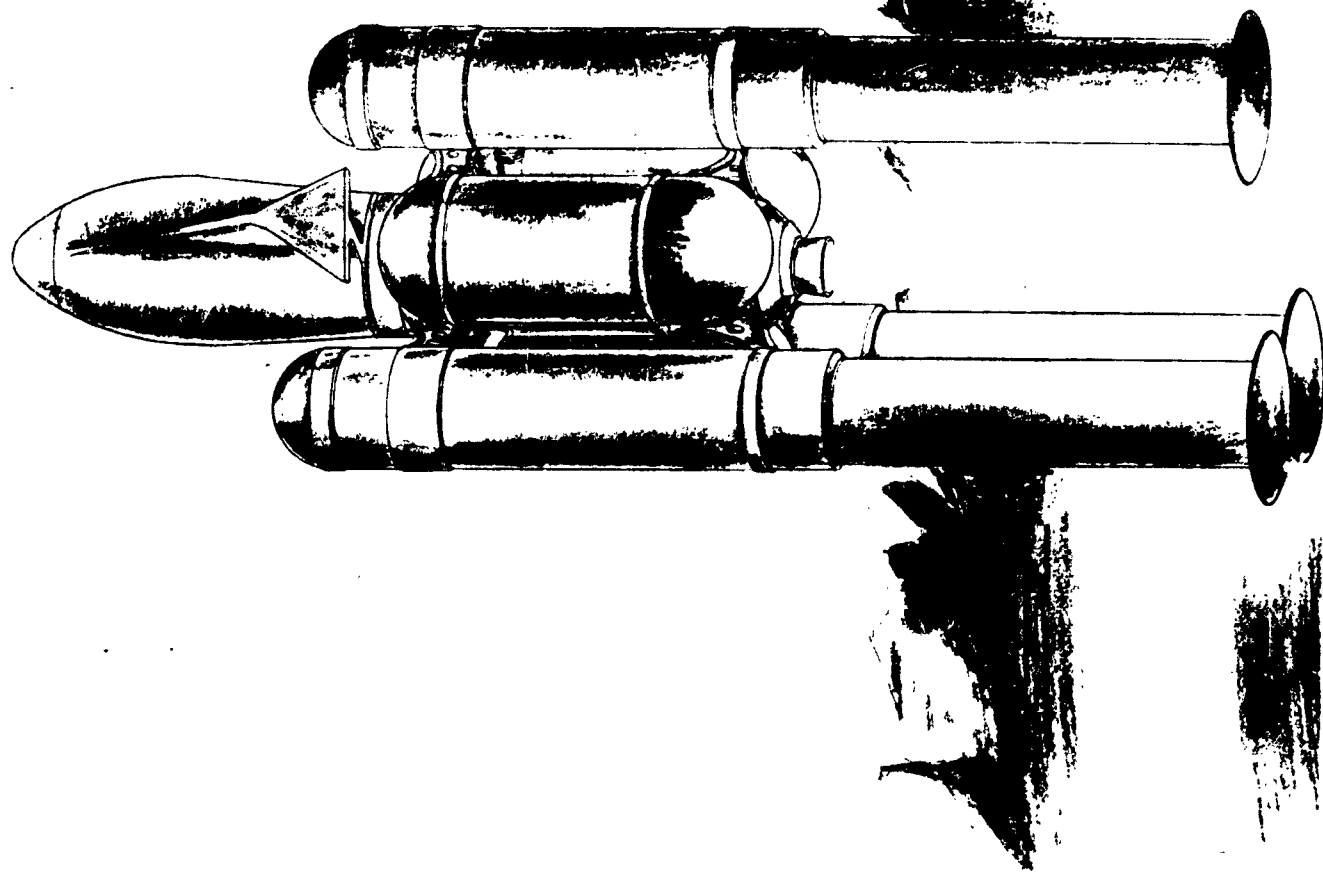


FIGURE 77

CONCEPT L-23

ENERGY ABSORBING SYSTEM USING PROPELLANT TANKS
AS VERTICAL TELESCOPING STRUTS

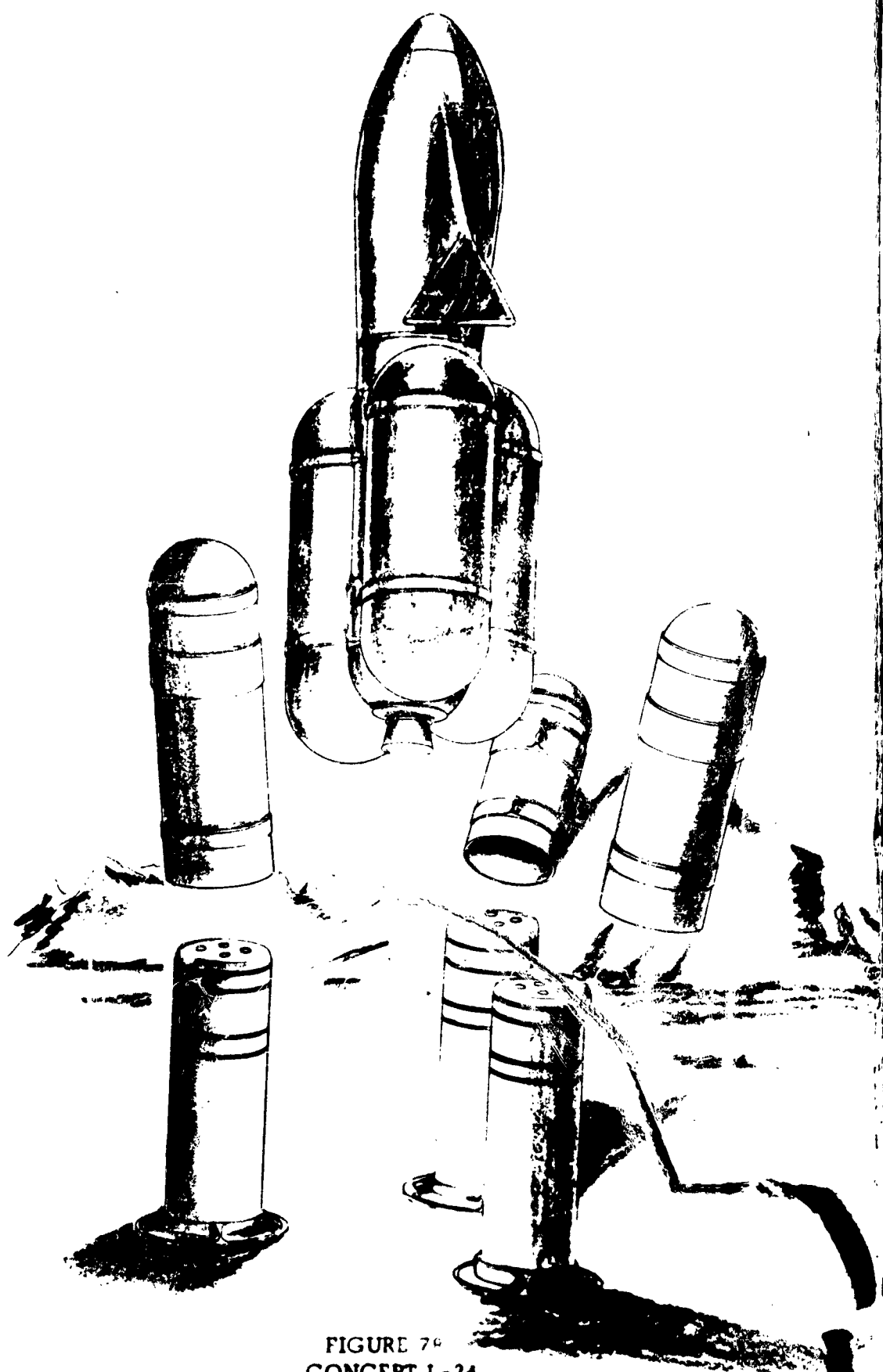


FIGURE 79
CONCEPT L-24
DEPARTURE ASSIST BY GAS-FIRED SQUIBS[†]
IN TELESCOPED TANKS (FOLLOWS L-23)